SPINT2 Suppresses Hippo Effector YAP and Limits Cellular Tolerance for Aneuploidy

SPINT2 Suppresses Hippo Effector YAP and Limits Cellular Tolerance for Aneuploidy

A dissertation presented

by

Huadi Zhang

to

The Division of Medical Sciences

in partial fulfillment of the requirements

for the degree of

Doctor of Philosophy

in the subject of

Biological and Biomedical Sciences

Harvard University

Cambridge, Massachusetts

August 2017

Dissertation Advisor: Professor David Pellman Huadi Zhang

SPINT2 Suppresses Hippo Effector YAP and Limits Cellular Tolerance for Aneuploidy

Abstract

Oncogenic transformation is often accompanied by chromosome instability, an increased rate of chromosome missegregation. The consequent gain or loss of chromosomes—termed aneuploidy—hinders the growth of most non-cancerous tissues, but is prevalent in tumors. During tumorigenesis, aneuploidy contributes to cellular heterogeneity and may promote downstream mutations, including chromosome rearrangements and oncogene amplification. Cellular mechanisms that safeguard against aneuploidy remain unclear.

The Hippo pathway is a tumor-suppressor mechanism with essential roles in regulating tissue homeostasis. YAP, the downstream effector inhibited by the Hippo pathway, is an oncogenic transcriptional cofactor that promotes proliferation and is frequently amplified in cancers. Upstream regulators of the Hippo pathway and YAP are partially understood.

SPINT2 is a transmembrane protein with extracellular serine protease inhibitor domains and is a negative regulator of various proteases including activators of growth factors. Epigenetic silencing of *SPINT2* by promoter hypermethylation is observed in cancers such as medulloblastoma, renal cell carcinoma, and acute myeloid leukemia. Notably, recent findings demonstrate that SPINT2 loss enables cells to tolerate multiple types of stress, including cytokinesis failure and DNA damage. Considering the distinct cellular machineries that respond to these stresses, it is conceivable that SPINT2 may regulate multiple signaling pathways.

In the present dissertation, I delineate SPINT2's role as a negative regulator of YAP. I demonstrate that SPINT2 limits YAP activity via protease-activated receptors. In addition, using

models of chromosome missegregation and aneuploidy, I establish that loss of SPINT2 confers heightened cellular tolerance for aneuploidy.

My findings highlight two intriguing hypotheses regarding cellular processes of cancer development. First, broad-spectrum membrane-anchored protease modulators such as SPINT2 may serve as "convergence points" where a multitude of extracellular signals are regulated for discrete downstream signaling events inside the cell. Second, the tolerance for aneuploidy may be a "built-in" component of oncogenic signaling such as YAP activation, as opposed to requiring separate cellular mechanisms. The aneuploid state of tumors, therefore, may be an integral output of intra- and extra-cellular oncogenic signaling, and may serve as a feedforward process that enhances further genomic instability during tumorigenesis.

Table of Contents

List of Figures and Tables

Dedication and Acknowledgements

I dedicate this dissertation to

my mother, Liya, and my father, Weihong.

I am forever empowered by the grit and strength they extracted from turmoil,

the curiosity and wisdom they crystalized from change, and

the unfazed passion they forged from faith and kindness.

谨以此论文献给

我的母亲利亚和我的父亲为虹

驱策我前行的是他们从动荡中提炼的刚毅与气力

从变迁中结晶的好学与智慧和

用信念与善良锻造的笃定热情

My graduate education has been a formative period thanks to the remarkable scholars, colleagues, friends, and family who have taught, mentored, and supported me.

I owe my rigorous scientific training to my dissertation advisor, Prof. David Pellman of Dana-Farber Cancer Institute and the Department of Cell Biology at Harvard Medical School. A brilliant physician-turned-cell biologist, David leads a research program with depth and breadth second to none, and has instilled in me a keen sensitivity not only to details, but also to the larger implications of data. David constantly pushes me to think beyond the next two, three, or five steps of my research, and motivates me to see my own work in a broader context. I am grateful for these moments of learning, and I am certain that they will propel me in my future endeavors.

My intellectual horizon has been irreversibly broadened by my work within the Secondary Field in Science, Technology, and Society. My advisors, Prof. Sheila Jasanoff of Harvard Kennedy School and Prof. David Jones of the Department of Global Health and Social Medicine at Harvard Medical School, have taught me to examine science from outside of the laboratory, and have inspired me to pursue my passion for innovations and technology-driven change.

My graduate work would not have come to this moment of completeness had it not been guided by the focused feedback from my Dissertation Advisory Committee: Prof. Alex Toker, my advisory committee chair, of Beth Israel Deaconess Medical Center and Harvard Medical School; Prof. Galit Lahav of the Department of Systems Biology at Harvard Medical School; and Prof. Danesh Moazed of the Department of Cell Biology at Harvard Medical School.

I am honored to have my work evaluated by my Dissertation Examiners: Prof. Alex Toker, examination chair; Prof. Suzanne Gaudet of Dana-Farber Cancer Institute and Harvard Medical School; Prof. Senthil Muthuswamy of Beth Israel Deaconess Medical Center and Harvard Medical School; and Prof. Xaralabos Varelas of Boston University School of Medicine.

My Harvard experience has been a beneficiary of the tireless stewardship of numerous university officials: Kate Hodgins, Daniel Gonzalez, Anne O'Shea, and Maria Bollinger of the Biological and Biomedical Sciences Program Office; Tatevik Holmgren and Lisa Rossini of the Division of Medical Sciences; and Heather Law and Laura Stark of the Office of Career Services.

I embarked on graduate scientific training because I wanted to become just like my undergraduate advisor, Prof. Nancy Pokrywka of Vassar College, a dedicated scientist and educator who showed me the wonders of biology and exemplified pedagogical craftsmanship.

I have developed as a scientist through the mentorship and friendship of many former and present Pellman Lab colleagues. I am indebted to Neil Ganem, a scientist extraordinaire, for his mentorship since my first-year rotation, which has grown into our collaboration. I thank Hubo Li for being a generous and trusted advisor, and a role model to emulate. Xiaolei Su and Benjamin Atkins were senior graduate students when I joined the lab, and were so encouraging and kind. I also learned tremendously from David Gordon and Hauke Cornils during our brief overlap.

I have done fun science in the company of an energetic crew of fellow college graduates: Arifa Ahsan, Hugo Arellano-Santoyo, Emily Jackson, Mitchell Leibowitz, and Shiwei Liu. Equally phenomenal are our post-doctoral fellows: Lin Deng, Mijung Kwon, Stamatis Papathanasiou, Alexander Spektor, Neil Umbreit, and Selwin Wu, who have taught me the art of science through their vast knowledge and incisive intuitions. Indispensable to my work is the support offered by Ema Stokasimov and Harriet Scott, our laboratory's managers.

My life in the lab has been especially enriched by these colleagues: Yosef Kaplan-Dor, with his unstoppable warmth and room-brightening spirit; Remigio Picone, with his whimsical artistry and creative perspectives; and I-Ju Lee, with her quick wit, sharp intellect, and never-ending big-heartedness. They will be truly missed.

Outside of my scholarly life, I have observed—sometimes with bewilderment—my own transformation into a better-rounded person thanks to my good fortune of meeting a group of extremely talented friends within the scientific community. I had such blasts tackling seemingly unconquerable challenges with Deep Agnani, Jarom Chung, Arun Pores Fernando, and Frederik Wirtz-Peitz. Jyoti Dev co-led a large student organization with me and never failed to inspire me with her effortless competency and level-headedness. These folks pushed me to grow and thrive.

My New England family has given me much love and joy. Kelsey and Mark epitomize creativity and ingenuity, and always nucleate fun; Annie and Brendan are the well-travelled, robust model adults that we strive to become one day; Steve, Julia, Marcus, and Sean teach me all kinds of cool stuff, science or otherwise. Their presence puts a big smile on my face every day.

A phone call away are my dear friends for more than ten years, Xinyi and Qingyi—my "siblings" who made the transpacific trip from our hometown of Wuhan, China, to the United States with me. We share the bond of not just age-old insider jokes, but also learning to own the life thousands of miles away from home. I am thankful for such great company in my journeys.

My extended family in Wuhan has thawed every blizzard-ridden Boston winter. The joie de vivre of my aunts, uncles, and cousins traverses the distance between us, and continues to motivate and ground me in my every endeavor.

I reserve the shiniest paragraph for my partner, Chris, who sees the world with the kindest eyes and shapes it with the sharpest drive, acutest intellect, and the most fabulous humor. My accomplishments are only half as good if I do not have this man to share them with. It seems that I have been wearing the "honeymoon goggles" for more than half a decade now.

And it feels amazing.

Chapter 1 : Introduction

Our pursuit for a greater understanding of cancer cells' inner workings has spanned more than 160 years. In 1855, Rudolf Virchow, a young physician at the University of Würzburg in Germany, established a theoretical framework to study biology in cellular terms. The cell theory, or *omnis cellula e cellula* (every cell from a pre-existing cell) as Virchow put it,[1] soon became popularized as a model to explain biological processes and to understand diseases, and marked a germinal moment when medicine—especially the modern concept of cancer—outgrew an era of "miasmas, neuroses, bad humors, and hysterias."[2,3]

At the turn of the 20th century, it became increasingly clear that cancer is characterized by uncontrolled cellular proliferation.[2,3] However, therapeutic options against cancer remained stagnant for another half-century. Solid tumors such as breast cancers were still removed with radical surgery or were essentially incinerated with radiation, practices developed in the 1890s. Patients with leukemia were considered "on their deathbeds" upon diagnosis.[2]

In 1948, Sidney Farber, a pathologist at Boston Children's Hospital in the United States, published a report that documented short-term remissions of childhood acute leukemias after treatment with aminopterin, an antifolate.[4] Aminopterin, the world's first chemotherapeutic agent,[2,5] was later found to inhibit cellular production of thymidylate and purine nucleotides, disrupting DNA and RNA synthesis.[5,6] The first chemotherapy-induced solid tumor regression was reported in 1956 by Min Chiu Li and Roy Hertz at the U.S. National Cancer Institute, in gestational choriocarcinoma treated with another antifolate, methotrexate.[7]

Fast forward 60 years, we now understand cancer as a collection of diseases characterized by anomalous cellular behaviors due to dynamic changes in the genome. Through a multi-step

process of cancer development—termed tumorigenesis or oncogenesis—cells accumulate genetic abnormalities in the regulatory circuits that control normal cellular proliferation and homeostasis, and transform into highly malignant derivatives.[8,9]

Research since the 1970s has set the foundation of our knowledge regarding two prominent categories of genetic alterations during tumorigenesis: the loss of tumor suppressor genes and the gain of oncogenes.[8] Tumor suppressor genes and proto-oncogenes (precursors of oncogenes) are often integral regulators of cellular proliferation and migration; misregulation of these genetic factors drives tumorigenesis by changing cells' intrinsic properties as well as their behaviors and functions in the microenvironment.[8,9]

Detailed investigations of both normal cellular physiology and cancer pathobiology have identified unique markers of cancer and have led to the development of targeted cancer drugs such as imatinib (targets BCR-ABL fusion oncoprotein in leukemias),[10-12] vemurafenib (targets mutant $BRAF^{V600E}$ in melanomas),[13-15] and pembrolizumab (inhibits PD-1 checkpoint).[16-18] The leap from aminopterin to these modern-day therapeutics highlights the impact of cancer cell biology research on the design and development of safe and effective cancer therapies.

Motivated by the complexities of tumorigenesis, my dissertation aims to expand our answers to the following questions. What genetic abnormalities drive cancer development? What cancer-specific phenotypes result from these abnormalities? I address these questions by characterizing a putative tumor suppressor gene, *SPINT2*, and a proto-oncogene, *ZEB2*. *SPINT2* is examined in the contexts of oncogenic signaling and tolerance for chromosome number changes in adherent human cell lines, and is the focus of Chapters 1–3. *ZEB2* is investigated in leukemia development, and is described and discussed in detail in Chapter 4. In Chapter 5, I synthesize the implications of my findings and lay out future research directions.

1.1 Extracellular Proteolysis in Development and Disease

1.1.1 Overview of extracellular proteases: regulation and signaling

1.1.2 Protease-activated receptors (PARs) and G protein signaling

1.1.3 Physiological functions of SPINT family protease inhibitors

1.2 Regulation of the Hippo Pathway by Protease-Activated Receptors (PARs)

1.2.1 The Hippo pathway in tissue homeostasis and cancer development

1.2.2 Regulation of the Hippo pathway by GPCRs

1.3 Aneuploidy: A Hallmark of Cancer

1.3.1 Causes and consequences of chromosome instability and aneuploidy

1.3.2 Cellular responses to aneuploidy

1.4 Conclusion and Research Goals

1.1 Extracellular Proteolysis in Development and Disease

1.1.1 Overview of extracellular proteases: regulation and signaling

Proteases are enzymes that mediate proteolysis—the hydrolysis and breakage of peptide bonds. Through proteolysis, proteases cleave their protein substrates into fragments, which may represent degraded, conformationally altered, or activated biological molecules.[19] Based on their enzymatic mechanisms, proteases are grouped into five catalytic classes: aspartic, cysteine, serine, and threonine proteases, named after the amino acid residue(s) at their active sites; and metalloproteases, which require metal cofactors for enzymatic activity.[20,21]

Extracellular proteolysis via proteases affords dynamic regulation of the extracellular environment,[22-26] which enables an organism to complete development,[22,23] defend against environmental insults,[24] and repair injuries.[25,26] Misregulation of extracellular proteolysis leads to pathological conditions such as developmental defects and cancer.[22-26] In humans, extracellular or transmembrane proteases comprise 22 aspartic proteases (e.g., pepsin A and cathepsin D); five cysteine proteases; 231 serine proteases (e.g., chymotrypsins, trypsins, and thrombin); six threonine proteases; and 141 metalloproteases (e.g., collagenases).[20,21]

Broadly speaking, extracellular proteases exert physiological functions via three types of mechanisms: 1) remodeling of the extracellular matrix; 2) indirect activation of cell-surface receptors via proteolytic activation of latent ligands; and 3) direct proteolytic activation of cell-surface receptors. These mechanisms are prevalent in metazoan physiology and disease.

The first functional mechanism of extracellular proteases, matrix remodeling, is best illustrated by mammalian development and wound repair. During murine embryo implantation, the developing blastocyst first “hatches” from the *zona pellucida* (ovum extracellular matrix) via matrix degradation by strypsin, a serine protease anchored on trophoblast membranes. This process

allows the blastocyst to be in direct contact with the endometrium (uterine epithelium).[27] Subsequently, the trophoblast secrets a suite of proteases including collagenase, stromelysin, and plasminogen activator to help the embryo implant into the uterine wall.[28,29]

During injuries that disrupt vasculature, our hemostatic machinery mounts a coagulation response to prevent excessive blood loss.[30] Coagulation is initiated by the exposure of blood to tissue factor, a transmembrane receptor expressed in extravascular tissues.[31] Tissue factor binds its circulating ligand, Factor VII (FVII) and converts it into the active serine protease FVIIa. Tissue factor/FVIIa then triggers a downstream protease cascade that leads to thrombin-mediated proteolytic conversion of the soluble fibrinogen to the insoluble fibrin, forming a blood clot.[31,32]

The healing of the wound, on the other hand, requires the orchestration of matrix metalloproteases (MMPs). In the epithelium, MMPs are usually expressed at basal levels and are suppressed by membrane-anchored protease inhibitors; upon injury, MMPs are rapidly induced by growth factors or cytokines.[33] During the initial stages of skin injury, MMP2 is first induced to degrade fibrin blood clots. Subsequently, a subset of epithelial MMPs (e.g., MMP1, 8, 9, and 13) clears the existing extracellular matrix to allow for fibroblast-mediated matrix renewal and remodeling. Finally, wound-edge MMPs such as MMP3 and MMP10 facilitate keratinocyte migration for wound closure, and promote re-epithelialization of the wound site.[33,34]

The second extracellular proteolytic mechanism—indirect activation of cell-surface receptors—is exemplified by the dorsoventral patterning of *Drosophila* embryos, a process mediated by a sequentially-activating extracellular proteolytic cascade involving serine proteases Nudel, GD, Snake, and Easter.[35] Specifically, Nudel, GD, and Snake are uniformly expressed in the embryonic cavity. Snake cleaves and activates ventrally restricted Easter, which in turn cleaves and activates Spätzle, a Toll/NF-κB signaling ligand that initiates ventral morphogenesis.[36,37]

Remarkably, the conserved NF-κB pathway is repurposed for mammalian pathogen defense, and is activated by proteolytically processed interleukin-1 cytokines to modulate innate immunity and inflammation.[38,39]

The third functional mode of extracellular proteases, direct proteolytic activation of cell-surface receptors, canonically involves protease-activated receptors (PARs). PARs exert self-activation upon extracellular cleavage of their N-terminus peptides.[40,41] PAR3 and PAR4, for example, are known to mediate thrombin-induced platelet activation during murine vascular injury.[42] PARs are described in detail in the next section (1.1.2).

Given their crucial roles in organismal growth, defense, and repair, it is unsurprising that extracellular proteases also modulate pathological processes. Indeed, misregulated proteolysis outside of the cell membrane promotes a wide range of diseases. In Alzheimer's disease, BACE1 (β secretase-1; a membrane-bound aspartic protease) contributes to the generation of toxic amyloid plaques when its proteolytic cleavage of the amyloid precursor protein is uncoordinated with other secretases.[43,44] Hemophilia A, an X-linked bleeding disorder, is caused by the deficiency of serine protease cofactor FVIII.[45] In tumorigenesis, the signaling and matrix remodeling properties of extracellular proteases, especially metalloproteases, are widely misappropriated to promote cancer cell survival and metastasis.[46-48] For instance, members of the a-disintegrin-and-metalloproteinase (ADAM) family are linked to tumor survival due to their roles in epidermal growth factor (EGF) signaling. ADAM10 promotes EGF transactivation and release,[49] and ADAM17 proteolytically activates ligands of EGF receptor.[50] In addition, proteolytic cleavage and activation of latent forms of transforming growth factor β (TGFβ) by MMP2, MMP9, and MMP14 has been implicated in stroma-mediated tumor invasion and metastasis.[49]

The plethora of disorders with misregulated extracellular proteolysis highlights the importance of the physiological control of extracellular proteases, oftentimes exerted by secreted or transmembrane protease inhibitors. For example, Serpin-27A, a secreted inhibitor of serine proteases, regulates *Drosophila* embryonic dorsoventral patterning; loss of this protein leads to ventralization of the entire embryo.[51] In murine physiology, membrane-bound serine protease inhibitor Spint1 is required for colorectal tissue homeostasis. Mice with intestinal epithelium-specific loss of Spint1 exhibit defective intestinal tissue architecture and function.[52] SPINT family protease inhibitors are further discussed in Section 1.1.3.

Genetically encoded protease inhibitors tend to have broad-spectrum and redundant inhibitory effects. For example, human tissue inhibitors of metalloprotease 1–4 (TIMP1 to TIMP4) constitute a family of proteins that competitively inhibit all 23 known human MMPs.[53,54] TIMP1's inhibitory range is restricted by its low affinity toward membrane MMPs such as MMP14, MMP16, and MMP24. On the other hand, TIMP3 has additional inhibitory effects on the ADAM family proteases.[53] The variety of combinatorial functions by protease-protease inhibitor interactions is likely the result of tissue-specific expression of distinct subsets of enzymes and inhibitors.[55]

Inhibition of disease-promoting proteases is a plausible avenue for clinical intervention. For example, naturally occurring protease inhibitors have been harnessed for disease treatment. TFPI1 (tissue factor pathway inhibitor 1; a Kunitz-type serine protease inhibitor) has been engineered for improved inhibitory specificity against plasma kallikrein, and has been approved for treatment of hereditary angioedema.[54] In addition, synthetic small-molecule inhibitors of cathepsin K, a cysteine protease, are under active development for their inhibitory effects on tumor osteolytic metastases.[48,56]

Therefore, detailed characterization of the functions of proteases and protease inhibitors in specific tissues and physiological contexts not only enhances of our understanding of protease-related disease biology, but may also inform downstream drug design and development.

1.1.2 Protease-activated receptors (PARs) and G protein signaling

Protease-activated receptors (PARs) are a class of G protein-coupled receptors (GPCRs) and comprise four members: PAR1 (encoded by the *F2R* gene), PAR2 (*F2RL1*), PAR3 (*F2RL2*), and PAR4 (*F2RL3*).[40] PARs play crucial roles in embryonic development,[57] hemostasis,[58] and cancer progression.[59-62]

PAR activation occurs through irreversible proteolysis. Proteases bind to and cleave the extracellular N-terminus of a PAR and unmasks a new N-terminus peptide that serves as the ligand to trigger intracellular signaling.[40,41] Ligand activation of PARs induces conformational changes of their intracellular domains, which in turn promote GTP binding to the G_α subunits of coupled heterotrimeric G proteins. GTP-bound G_α, along with associated G_β/G_γ subunits, elicit diverse cellular responses.[40] The activating proteases, ligand peptides, coupled G_α subunits, and signal termination mechanisms of PARs are summarized in Table 1-1.[40]

G proteins (GTP-binding proteins) are molecular switches that modulate intracellular signaling. Heterotrimeric G proteins respond to GPCR activation and play crucial roles in regulating cellular behaviors.[63] G protein heterotrimers are composed of three subunits, G_α, G_β, and G_γ. G_α and G_γ are usually attached to the inner surface of the plasma membrane, allowing for interactions between a G protein and the cytoplasmic domains of receptors.[64] G_α, a GTPase, hydrolyzes GTP to GDP. In its GDP-bound state, G_α maintains association with G_β/G_γ, representing an inactive G protein complex. Upon stimulation of GPCRs, GTP replaces GDP and

binds G_α, and causes the dissociation of G_α from G_β/G_γ. The dissociated GTP-G_α can interact with a wide range of target proteins to trigger downstream signaling. Upon GTP hydrolysis to GDP, G_α re-associates with G_β/G_γ and reverts to the inactive state.[63,64] Therefore, the cycling of G_α between its inactive GDP-bound and active GTP-bound states is the mediator of the "switching" function of G proteins.[63] The G_β/G_γ subunit, on the other hand, can also directly modulate cellular processes such as ion channels.[65]

Table 1-1. PARs: activating proteases, ligand peptides, G_α, and signal termination.

	Activating proteases	**Ligand peptide**	**Coupled G_α**	**Termination**
PAR1	Thrombin; Trypsin; Plasmin; Tissue Factor-FVIIa-FXa; APC-EPCR; MMP1; Granzymes	SFLLRN	$G_{q/11}$ $G_{12/13}$ $G_{i/o}$	Phosphorylation; β-arrestins; Internalization; Degradation
PAR2	Trypsin; Tryptase; Tissue Factor-FVIIa; Tissue Factor-FVIIa-FXa; Matriptase; Bacterial gingipains; Kallikreins; Granzymes	SLIGKV	$G_{q/11}$ $G_{12/13}$ $G_{i/o}$	Phosphorylation; β-arrestins
PAR3	Thrombin	TFRGAP	$G_{q/11}$	Unknown
PAR4	Thrombin; Trypsin; Plasmin; Tissue Factor-FVIIa-FXa; Cathepsin G; Bacterial gingipains; Kallikreins; MASP-1	GYGQV	$G_{q/11}$ $G_{12/13}$	Internalization

Adapted from Soh et al. (2010)[40]

The type of G_α subunit largely determines G protein specificity in downstream signaling.[64] There are four main classes of G_α based on amino acid sequence and functional similarities: $G_{q/11}$, $G_{12/13}$, $G_{i/o}$, and G_s. In general, the $G_{q/11}$ family G proteins activate phospholipase C (PLC), and the $G_{12/13}$ family is linked to the regulation of small GTPases such as Rho. $G_{i/o}$ and G_s are named for

their prominent effects on adenylyl cyclase (AC) and AC-mediated cellular cAMP production: $G_{i/o}$ inhibits, and G_s stimulates, AC.[66]

Human G_α subunits are encoded by 16 genes. *GNAQ*, *GNA11*, *GNA14*, and *GNA15* encode $G_{q/11}$ family subunits; *GNA12* and *GNA13* constitute the $G_{12/13}$ family ; $G_{i/o}$ are gene products of *GNAI1*, *GNAI2*, *GNAI3*, *GNAO1*, *GNAT1*, *GNAT2*, *GNAT3*, and *GNAZ*; G_s subunits are products of *GNAL* and *GNAS*.[67] While context specificity exists between genes within each family, it is believed that they exhibit significant functional redundancy.[68]

PAR-mediated G protein signaling has been well characterized in hemostasis and vascular biology. For example, it has been shown that PAR1 and PAR3 are necessary for thrombin-mediated murine platelet activation.[58] G_q-deficient mice produce platelets that fail to aggregate or release ATP—hallmarks of platelet activation—following treatment with pharmacological platelet activators; these mice also exhibit lengthened bleeding times post-injury.[69] On the other hand, G_{13} is required for platelet shape change following thrombin stimulation. In platelets depleted of G_{13}, thrombin no longer induces RhoA-mediated myosin light chain phosphorylation, suggesting that G_{13} activates a RhoA- and Rho kinase (ROCK)-dependent pathway in platelet shape change and activation.[70] These findings are consistent with $G_{q/11}$ and $G_{12/13}$ coupling to PAR3 and PAR4 (Table 1-1),[40] as well as the known roles of PLC-mediated intracellular Ca^{2+} release[71] and Rho GTPase-mediated cytoskeleton reorganization[72] during platelet activation.

The roles of PARs during cancer development are increasingly uncovered. Booden et al. (2004)[73] showed that PAR1 knock-down in invasive human breast carcinoma cell lines attenuated invasive phenotypes. Further, the authors showed that the cell-surface half-life of activated PAR1 following thrombin treatment was more than 10-fold longer in invasive carcinoma cells compared to non-transformed breast epithelial cells; this was due to reduced endocytosis of cell-surface

PAR1. These findings strongly suggested that persistent PAR1 activation contributed to tumors' invasive phenotypes.[73] Additionally, Caruso and colleagues (2006)[60] demonstrated that PAR2 activation promoted the growth of gastric cancer cell lines in an EGF receptor-dependent manner.

Nevertheless, potential oncogenic pathways mediated by PARs and their associated G proteins are only partially understood and require further investigation.

1.1.3 Physiological functions of SPINT family protease inhibitors

Extracellular proteases are tightly regulated by membrane or extracellular protease inhibitors.[54] Recent analysis of vertebrate genomes have identified a large number of trypsin-like membrane serine proteases.[20,21,74] These proteases are commonly inhibited by three classes of protease inhibitors: serpin-, Kazal-, and Kunitz-type protease inhibitors. Serpin-type protease inhibitors have been extensively studied for their roles in coagulation and fibrinolysis; Kazal and Kunitz protease inhibitors are less understood.[74-76]

Serine protease inhibitor, Kunitz-type (SPINT) proteins are a class of broad-spectrum membrane-bound protease inhibitors that regulate a wide range of cellular and physiological processes such as development and tissue homeostasis.[52,77-81] Kunitz-type domains are common in nature and act as both serine protease inhibitors and toxins in animal venoms. They consist of 50–70 amino acids and adopt a conserved structure with two antiparallel β-sheets, in addition to helical regions stabilized by disulfide bridges.[82]

SPINT protease inhibitors are encoded by two genes, *SPINT1* and *SPINT2*. In humans, *SPINT1* is located on chromosome 15q15.1 and encodes a 529-amino acid protein (~57 kDa); SPINT2 is mapped to chromosome 19q13.1 and encodes a 252-amino acid protein (~28 kDa).[83] Both SPINT1 and SPINT2 may possess slightly shortened protein isoforms due to alternative

splicing[84-86] and may be modified by glycosylation.[87,88] Starting from the N-terminus, SPINT2 is composed of two Kunitz domains followed by a single-span C-terminus transmembrane domain, and lacks an N-terminus domain of unknown function found in SPINT1. In the first Kunitz domain, SPINT1 and SPINT2 share 56% amino acid sequence identity; in the second Kunitz domain, they share 39% identity in amino acid sequences.[89]

Murine Spint1 and Spint2 play important roles in placental development. Szabo and colleagues (2007 and 2009)[80,90] showed that the development of murine placenta required matriptase inhibition by both Spint1 and Spint2. Matriptase is a serine protease encoded by the *St14* gene. Specifically, Spint1 loss led to disorganized laminin deposition and altered expression of E-cadherin and β-catenin in chorionic trophoblasts, and caused matriptase-dependent disruption of placental epithelial integrity.[90] Spint2 depletion resulted in a similar disruption of placental development.[80] Additionally, *Spint2* knock-out induced significant defects in embryonic neural tube closure, a defect partially rescued by matriptase depletion.

Notably, murine *Spint1* and *Spint2* exhibit nonallelic non-complementation for embryonic lethality, highlighting their delicate dosage balance during development.[80] *Spint1*, *Spint2*, and *St14* are expected to segregate independently since they are located on separate chromosomes. However, in a cross between $Spint1^{+/-};Spint2^{+/+};St14^{+/-}$ and $Spint1^{+/+};Spint2^{+/-};St14^{+/+}$ mice, Szabo et al. (2009)[80] did not identify a single offspring with the $Spint2^{+/-};Spint1^{+/-};St14^{+/+}$ genotype among a litter of 76. On the other hand, heterozygous loss of matriptase permitted term development of $Spint1^{+/-};Spint2^{+/-}$ mice—$Spint1^{+/-};Spint2^{+/-};St14^{+/-}$ offspring were found at the expected frequency. These findings suggest that matriptase requires sufficient combined inhibitory activity of *Spint1* and *Spint2* during development.[80]

Despite their functional redundancy during development, *SPINT1* and *SPINT2* are expressed in a highly divergent fashion in adult mammalian tissues. In a comprehensive panel of adult human tissues, transcriptome analysis shows that *SPINT1* and *SPINT2* are abundantly co-expressed only in colon (transverse), esophageal mucosa, minor salivary gland, skin, and vaginal tissues. *SPINT2*, on the other hand, is uniquely expressed at high abundance in aorta, bladder, kidney cortex, lung, pituitary, prostate, stomach, testicle, and thyroid tissues.[91]

Given SPINT1 and SPINT2's integral roles during the developmental process, it is unsurprising that their misregulation has been implicated in human cancers. For instance, an increased ratio between *ST14* and *SPINT1* mRNAs was observed in colorectal cancer and advanced ovarian cancer.[92,93] In addition, *SPINT2* is silenced by promoter hypermethylation in a wide range of cancers including medulloblastoma, melanoma, acute myeloid leukemia, and esophageal, gastric, liver, and renal cancers.[94-100]

Nevertheless, these correlative observations do not fully explain how SPINTs regulate pro-tumorigenic cellular behaviors such as proliferation or migration. Further exploration is required to understand SPINTs' impact on cellular physiology.

1.2 Regulation of the Hippo Pathway by Protease-Activated Receptors (PARs)

1.2.1 The Hippo pathway in tissue homeostasis and cancer development

The Hippo pathway has emerged as a central signaling cascade that controls tissue homeostasis and cell proliferation, and suppresses tumorigenesis.[101-104]

In 1995, reports by Justice et al. and Xu et al. showed that in *Drosophila*, deletion of the gene *Warts* resulted in overgrowth of multiple tissues.[105,106] These findings were subsequently corroborated by studies that defined a *Drosophila* signaling network involving Hippo,[107-111]

Salvador,[112,113] Warts, and Mats[114] proteins, revealing a pathway whose perturbations led to dramatic tissue overgrowth unseen in previously defined developmental pathways. In 2005, Yorkie, a transcriptional cofactor, was identified as the downstream effector of the Hippo pathway.[115] Expectedly, *Yorkie* gene mutations lead to tissue undergrowth while its overexpression phenocopied *Warts* loss.[115]

The Hippo pathway is evolutionarily conserved. In mammals, MST1 and MST2 are homologous to *Drosophila* Hippo and represent the upstream kinases; LATS1 and LATS2 (Warts) are intermediary kinases; SAV1 (Salvador) and MOB1A/B (Mats) are regulatory scaffold proteins; and YAP and TAZ are the downstream effectors (Yorkie).[102]

MST1/2 and LATS1/2 constitute the core kinase cassette of the Hippo pathway.[101-103] MST1 and MST2 bind to SAV1 to form active enzymes that phosphorylate and activate LATS1 and LATS2 kinases, as well as LATS regulatory subunits MOB1A and MOB1B. The activated LATS-MOB1 complexes phosphorylate YAP and TAZ. Phosphorylated YAP and TAZ lose transcriptional functions through their cytoplasmic sequestration or proteasomal degradation.[103] In humans, YAP and TAZ are respectively encoded by the paralogous genes *YAP1* and *TAZ*. In their un- or under-phosphorylated state, YAP/TAZ localize to the nucleus and interact with key DNA-binding partners such as the TEAD family transcription factors to mediate gene expression.[102,103] Among an extensive transcriptional program mediated by YAP/TAZ, *CTGF* (connective tissue growth factor) and *CYR61* (cysteine rich angiogenic inducer 61) are prominent markers of YAP/TAZ activity.[102,103]

LATS1/2 phosphorylate YAP at five serine/threonine residues and TAZ at four such sites. Among them, the best characterized are YAP serine 127 (S127; equivalent to S89 in TAZ) and S397 (also termed S381 due to alternative isoforms;[116,117] equivalent to TAZ S311)[103,117] YAP

S127 phosphorylation generates a 14-3-3 binding site and lead to YAP cytoplasmic sequestration. 14-3-3 proteins are regulatory chaperones that mediate intracellular signaling by modulating ligand localization or activity.[118] YAP S397 phosphorylation, on the other hand, creates a phosphodegron and lead to ubiquitination and proteasomal degradation of YAP. Despite the phospho-S397 degron, YAP is relatively stable in the cell and is mainly regulated by nuclear-cytoplasmic localization. By contrast, TAZ has a short half-life (<2 h) and is predominantly regulated via degradation, possibly due to an extra N-terminus phosphodegron.[102,103]

The Hippo pathway has well-documented roles in tissue homeostasis and regeneration. In *Drosophila*, Yorkie is required for stem cell-mediated tissue repair following acute injuries in the intestine.[119] In the murine liver, Yap is transiently activated upon injury to promote progenitor cell proliferation and repress hepatocyte proliferation; depletion of Yap inhibits injury-induced hepatocyte and bile duct proliferation.[120,121]

On the cellular level, the canonical Hippo axis (MST-LATS-YAP) suppresses YAP/TAZ activity via molecular signals of cell polarity and epithelial architecture. For example, Scribble (SCRIB), a basolateral membrane-localized cell polarity determinant, interacts with both MST1/2 and LATS1/2 and promotes LATS1/2 activation; loss of SCRIB leads to increased YAP activity.[122] Similarly, neurofibromin 2 (NF2), a membrane-cytoskeleton scaffolding protein, recruits LATS1/2 to the plasma membrane and promotes their phosphorylation through MST1/2, suppressing YAP/TAZ activity.[123,124]

Interestingly, MST kinases are not always necessary for LATS-YAP signaling, but LATS1/2 appear to be the primary kinases that regulate YAP/TAZ. Illustratively, a recent report by Meng and colleagues (2015)[125] demonstrated LATS1/2, but not MST1/2, double knock-out in HEK-293A cells abolished YAP S127 phosphorylation. Furthermore, YAP/TAZ activity has been

shown to be modulated by additional kinases such as ABL[126] and CDK1[127] through direct phosphorylation, as well as microRNAs including miR-141 and miR-200a.[104]

LATS1/2 and YAP/TAZ can be further regulated by a variety of mechanical and biochemical signals including cell-cell contact, cytoskeletal organization, extracellular matrix rigidity, and cellular metabolic status.[103,128]

In mammalian cells, increased cell-cell contact and disruptions to the actin cytoskeleton lead to LATS activation followed by phosphorylation and cytoplasmic retention of YAP/TAZ, resulting in limited cell proliferation.[129-132] In addition, YAP and TAZ mediate cellular behaviors in response changes in extracellular matrix rigidity: a rigid matrix promotes YAP/TAZ nuclear localization and transcriptional activity in adherent human cells.[133] YAP and TAZ have also been reported to respond to cellular energy stress. AMP-activated protein kinase (AMPK), a central kinase induced by serum or glucose starvation, inactivates YAP/TAZ through LATS-mediated phosphorylation.[134,135]

Misregulation of Hippo pathway components is frequently implicated in tumorigenesis. For example, in non-transformed human mammary epithelial cells, YAP overexpression induces phenotypes associated with oncogenic transformation, including epithelial-mesenchymal transition, anchorage-independent growth, and attenuated apoptosis.[136] In mice, depletion of Nf2, Mst1/2, Lats1, Sav1, or Mob1a/b results in a wide array of cancers including acute lymphoblastic leukemia, hepatocellular carcinoma, osteosarcoma, and ovarian carcinoma.[101] Yap overexpression leads to murine carcinomas in liver and skin.[101] In human cancers, *LATS2* is frequently deleted in malignant mesothelioma, an aggressive cancer associated with asbestos exposure.[137] Additionally, *YAP1* is part of a chromosome 11 amplicon (11q22) observed in human glioblastomas, squamous-

cell carcinomas, and tumors of pancreas, lung, ovary, and cervix.[136] A syntenic amplicon has been documented in murine models of breast and liver cancers.[138,139]

Taken together, these findings highlight the tumor-suppressing functions of the Hippo pathway, and suggest that mechanisms that activate YAP/TAZ may play crucial roles during oncogenic transformation.

1.2.2 Regulation of the Hippo pathway by GPCRs

Recent evidence has demonstrated that GPCRs directly regulate the Hippo pathway.[102] It has been well-established that YAP/TAZ are regulated by GPCRs coupled with $G_{q/11}$, $G_{12/13}$, and G_s. Stimulation of $G_{q/11}$ by angiotensin II (via receptor AT1R)[140] and estrogen (via receptor GPER)[141] leads to YAP/TAZ activation. Similarly, when activated by ligands such as thrombin, lysophosphatidic acid (LPA), and sphingosine 1-phosphophate (S1P), $G_{12/13}$-coupled receptors repress phosphorylation of YAP.[142,143] Additionally, epinephrine, an activator of G_s-coupled receptors, leads to dose-dependent YAP phosphorylation and inactivation.[142]

Correspondingly, the well-known downstream effectors of G_α have been linked to YAP/TAZ regulation. Phospholipase Cβ (PLCβ), a major downstream effector of $G_{q/11}$ signals, is required for GPER (G protein-coupled estrogen receptor)-mediated TAZ dephosphorylation and nuclear localization in ZR-75-30 human metastatic breast cancer cells.[141] *Botulinum* toxin C3, a specific inhibitor of Rho GTPases (often activated by $G_{12/13}$), abolishes LPA/S1P-induced YAP/TAZ dephosphorylation in HEK-293A cells.[142] Protein kinase A (PKA), a main effector of G_s-AC signaling, has been shown to induce YAP phosphorylation via LATS kinases.[144]

Notably, Mo and colleagues (2012)[143] reported that stimulation of PAR1 and PAR2 by activating proteases or peptide analogs resulted in YAP/TAZ activation. Specifically, treatment of

human cell lines HEK-293A, HUVEC, and MDA-MB-231 with thrombin, TRAP6 (PAR1 peptide agonist), and SLIGRL (PAR2 peptide agonist) strongly reduced YAP phosphorylation. Furthermore, the authors showed that TRAP6-induced YAP/TAZ activation was dependent on $G_{12/13}$ and downstream Rho GTPases.[143] Interestingly, TRAP6 did not appear to alter MST1/2 kinase activity, but rather inhibited LATS1. These findings illustrate a PAR1-$G_{12/13}$-Rho-LATS pathway in YAP/TAZ regulation, highlight the broader role of PARs in regulating the Hippo pathway, and motivate detailed characterization of upstream and downstream factors that modulate PAR-mediated regulation of Hippo signaling.

1.3 Aneuploidy: A Hallmark of Cancer

1.3.1 Causes and consequences of chromosome instability and aneuploidy

In 1914, zoologist Theodor Boveri proposed that an abnormal chromosome constitution, while detrimental to normal cellular physiology, might promote cancer development.[145] The abnormal chromosome constitution observed by Boveri is now referred to as aneuploidy—the numerical deviation from multiples of a haploid chromosome complement.

Indeed, aneuploidy is a frequent consequence of genome instability, a hallmark of cancer.[9] Specifically, genome instability can manifest as an increased incidence of chromosome missegregation, termed chromosome instability, leading to aneuploidy in tumors.[146] Genome instability is considered an enabling characteristic during tumorigenesis due to its role in promoting mutations and genetic heterogeneity, which allows cells to acquire additional tumor phenotypes.[9,147] In humans, most types (~90%) of solid tumors and half of hematopoietic cancers exhibit whole-chromosome aneuploidies.[148-151] For example, 34% of Ewing sarcomas harbor extra copies of chromosome 8, and 50% of melanomas sustain recurrent loss of chromosome 3.[146]

Boveri's initial proposition regarding the seemingly paradoxical roles of aneuploidy in normal physiology and cancer was followed by a century-long inquiry into the causes and consequences of chromosome gains or losses. Nevertheless, we have only begun to understand the cellular responses to aneuploidy.[146-148,152]

Chromosome segregation errors that lead to aneuploidy can occur through four mechanisms. First, defects in the spindle assembly checkpoint (SAC) contribute to increased chromosome missegregation. SAC is the primary cellular mechanism that prevents erroneous partitioning of chromosomes during mitosis in eukaryotes.[152] It ensures the high fidelity of chromosome missegregation by suppressing the onset of mitotic anaphase until all chromosomes are properly bi-oriented (sister chromatids are attached to opposite spindle poles) in the mitotic spindle.[147,152] Perturbations to the SAC pathway, therefore, result in attenuated cell cycle delay when chromosomes are improperly attached, and lead to aneuploidy.

Second, aneuploidy can be driven by improper kinetochore-microtubule attachments such as merotely or syntely. Merotely refers to single kinetochores being attached to microtubules emanated from multiple spindle poles.[146,152] Syntely, on the other hand, results from the attachment of both sister kinetochores to the same mitotic pole.[147,153] Merotelic and syntelic attachments lead to segregation defects such as lagging chromosomes, and result in subsequent incorrect partitioning of chromosomes into the daughter cells.[147] Interestingly, cells harboring extra centrosomes, commonly observed in cancers,[146] tend to form merotelic attachments that lead to chromosome instability.[153]

Third, spindle multipolarity has been proposed to be a mechanism that generates aneuploidy.[146,152] Upon centrosome amplification, cells may form mitotic spindles that contain more than two poles due to the presence of additional microtubule organizing centers.

Theoretically, therefore, when the multiple spindle poles attempt to partition the cell during the mitotic program, the duplicated chromosome complement will be distributed into more than two daughter cells that are significantly aneuploid.[146,152] However, it has been shown that these daughter cells are usually inviable, presumably due to the drastic loss of genomic content.[153]

Lastly, defects in sister chromatid cohesion may also contribute to chromosome missegregation.[146,147,152] For example, it has been shown that loss of factors that promote sister chromatid cohesion, such as cohesin-SA2 and BAF180, induces chromosome instability and the consequent aneuploidy in mammalian cells.[154,155] Several mechanisms have been proposed to explain the association between the loss of cohesion regulators and aneuploidy: premature separation of sister chromatids, weakened telomeric cohesion, and cohesion-independent regulation of centrioles.[156] Nevertheless, the mechanisms by which cohesion factors modulate chromosome missegregation remain unclear.

1.3.2 Cellular responses to aneuploidy

In stark contrast to the prevalence of aneuploidy in cancers, non-cancerous tissues rarely tolerate aneuploidy.[146,148] In humans, whole-chromosome aneuploidy is among the most common causes of miscarriage and developmental defects.[157] Down syndrome, or somatic trisomy 21, is the only autosomal aneuploidy that permits survival until adulthood, and is associated with developmental delays.[148] In various organisms such as budding and fission yeasts, *Drosophila*, *C. elegans*, mice, and humans, aneuploid cells exhibit severely delayed proliferation and decreased cellular fitness.[148] Interestingly, some somatic tissues have heightened tolerance for aneuploidy. For example, mammalian neurons exhibit low levels of mosaic aneuploidy, while hepatocytes have a wide range of karyotypes including aneuploidy and polyploidy.[148,158-161] It has been proposed

that somatic aneuploidy in certain tissues may promote genetic diversity.[148] However, mechanisms conferring cellular tolerance for aneuploidy and functional consequences of somatic aneuploidy remain poorly understood.

Aneuploidy is defined by a deviation in the quantity of chromosomal DNA from wild-type, euploid cells. However, DNA per se does not appear to confer a proliferative disadvantage: yeast strains engineered to carry large human artificial chromosomes, presumed to have virtually no protein-coding functions, do not exhibit reduced fitness.[162] While gains or losses of genes associated with specific aneuploidies may exert potent effects on cellular fitness, the general effect of aneuploidy-associated proliferative disadvantage is best explained by gene dosage.[148] In other words, proteomic imbalances resulting from aneuploid genomes exert antiproliferative effects.

Two broad lines of evidence lend support to this model. First, the fitness disadvantage associated with each aneuploidy strongly correlates with the number of protein-coding genes with altered dosage. It has been shown that cells from Down syndrome patients,[163,164] as well as aneuploid cells in other organisms,[162,165] generally scale their transcriptomes and proteomes corresponding to their specific aneuploidy.[166,167] Notably, the trisomic chromosome in Down syndrome, chromosome 21, is among human chromosomes encoding the fewest proteins.[148] Furthermore, as reported by Torres and colleagues (2007),[162] in aneuploid cells derived from haploid budding yeast, the G_1 cell cycle delay is more severe in cells that have gained larger chromosomes or those with more copies of the same chromosome.[162] These findings strongly suggest that in the scenario of chromosome gains, the extra quantities of gene products directly impose a fitness cost.

Second, it has become increasingly clear that aneuploidy is associated with proteotoxic stress. In healthy cells, chaperone-mediated pathways facilitate the correct folding of proteins; the

autophagy machinery and the ubiquitin-proteasome system ensure proper degradation and disposal of misfolded proteins.[168] Aneuploidy causes defects in both protein folding and protein degradation machineries. Oromendia et al. (2012)[169] observed that disomies in haploid budding yeast cells increased protein aggregate formation and decreased Hsp90-mediated protein folding capacity. Similarly, Donnelly et al. (2014)[170] found that chromosomally stable trisomic and tetrasomic HCT-116 human colorectal carcinoma cells were sensitive to HSP90 inhibition, and exhibited delayed protein refolding following heat shock. More recently, Santaguida and colleagues (2015)[171] showed that autophagosomal cargoes such as protein aggregates accumulated in, and were not effectively degraded by, lysosomes in aneuploid human retinal pigment epithelial (RPE-1) cells. Taken together, these findings illustrate that aneuploidy is a highly taxing condition on cellular mechanisms responsible for protein quality control.

If aneuploidy comes with such a high fitness cost, why is it frequently observed in cancers? It has been shown that aneuploidy may be a byproduct of oncogenic transformation. For instance, loss of the RB tumor suppressor promotes merotelic attachments in RPE-1 cells and leads to chromosome missegregation and aneuploidy.[172] Nevertheless, aneuploidy has also been reported to play an active role in cancer development. In Kras-addicted murine lung adenocarcinomas, chromosome missegregation facilitates tumor relapse following Kras withdrawal.[173]

Earlier this year, Sheltzer and colleagues (2017)[174] reported that trisomic murine embryonic fibroblasts (MEFs) and HCT-116 human colorectal cancer cells generally exhibited prolonged doubling time compared to diploid counterparts. Furthermore, this fitness disparity persisted upon induction of oncogenic signals such as p53 loss or the expression of SV40 large T antigen (LTa) and $Hras^{V12}$.[174] These results suggest that such oncogenic cues are not sufficient to

allow whole-chromosome aneuploid cells to overcome their proliferative disadvantage during the initial stages of oncogenic transformation.

Nevertheless, the authors also observed that some oncogene-transduced trisomy MEF lines gradually shortened their doubling time during serial passaging *in vitro*.[174] For example, several independent LTa-expressing trisomy-19 MEF lines exhibited improved growth phenotypes over time, and was found to have gained extra copies of chromosome 12 in the process. Still more intriguing, tumor cells derived from subcutaneously transplanted trisomy MEFs (with p53 inhibition and $Hras^{V12}$ expression) possessed similar proliferative and colony-forming potential, and increased karyotype variation, compared to tumors derived from otherwise isogenic diploid counterparts.[174] For instance, segmental and structural chromosome alterations appeared to be more common in trisomy-derived, as opposed to diploid-derived, tumors. This observation is consistent with prior findings that DNA replication and repair are defective in aneuploid cells.[175,176] Collectively, these findings highlight a potentially double-sided role of aneuploidy during tumorigenesis: while whole-chromosome aneuploidy causes an initial reduction in fitness, it may confer long-term advantage through karyotype heterogeneity. However, mechanisms that permit aneuploidy in tumor cells—and may subsequently enable potential karyotype evolution—have remained elusive.

The differential tolerance for aneuploidy in cancers and normal somatic tissues represents a key distinction between cancerous and non-transformed cells. Hence, how cells respond to aneuploidy is of therapeutic interest:[146,148] it is conceivable that inhibition of cellular aneuploidy tolerance can potentially suppress cancer cell survival and proliferation while leaving normal cells unaffected. Therefore, a deeper knowledge of the mechanisms that confer cellular tolerance for aneuploidy informs such a therapeutic strategy and elucidates a key aspect of tumor biology.

1.4 Conclusion and Research Goals

Tumorigenesis is a complex process that "rewires" and takes advantage of cellular mechanisms that are necessary for normal physiological functions such as development, wound healing, and tissue homeostasis. How extracellular signals are relayed to induce cancer cell phenotypes via intracellular events remains a partially answered question; detailed understanding of cancer's unique characteristics—such as loss of tumor suppressors and acquisition of aneuploidy tolerance—provides insights on cancer cells' vulnerabilities.

My main research project aims to characterize functions of SPINT2, a serine protease inhibitor and a putative tumor suppressor, and to understand the relationship between oncogenic signaling and aneuploidy. Specifically, I aim to:

I. Characterize SPINT2's role in regulating the Hippo pathway effector YAP (Chapter 2).
    a. Identify mechanisms that mediate SPINT2-YAP regulation.
    b. Determine whether SPINT2 loss promotes oncogenic transformation.

II. Characterize SPINT2's effect on cellular tolerance for aneuploidy (Chapter 3).
    a. Identify mechanisms by which SPINT2 regulates aneuploidy tolerance.
    b. Determine the relationship between SPINT2 loss and aneuploidy in human cancers.

This work sheds light on SPINT2's functions in connecting the extracellular environment to intracellular responses such as gene expression and aneuploidy tolerance, and deepens our understanding of tumorigenesis and cancer cell phenotypes.

Chapter 2 : Suppression of the Hippo Pathway Effector YAP by SPINT2 via Protease-Activated Receptors (PARs) and Associated G Proteins

---

Summary

Using imaging, biochemical, and genomic techniques, I characterize SPINT2's function as a negative regulator of the Hippo effector YAP. I demonstrate that this regulation is achieved by SPINT2's inhibition of PAR1, PAR2, and their coupled G proteins through a candidate-based RNA interference (RNAi) screen. I further explore SPINT2's role as a putative tumor suppressor, and how my findings relate to our understanding of tumor microenvironment and tumorigenesis.

2.1 Introduction

SPINT2 encodes a serine protease inhibitor that is known to function as a negative regulator of hepatocyte growth factor (HGF) signaling,[86] and is commonly silenced by epigenetic mechanisms in a wide range of tumors including leukemia, medulloblastoma, renal and gastric cancers, and metastatic melanoma.[94-100] During development, murine Spint2 has been shown to regulate protease-mediated morphogenesis of neural tube development.[80] Recent studies in human cancer cell lines have linked SPINT2 suppression to invasive and motile phenotypes.[100,177] While regarded as a putative tumor suppressor, SPINT2's roles in tumorigenesis have not been thoroughly characterized. In 2014, our group reported that SPINT2 depletion, in a fashion similar to knock-down of Hippo pathway kinase LATS2, allowed cells to circumvent the G_1 cell cycle arrest caused by cytokinesis failure.[178] This finding prompted us to explore whether SPINT2 may regulate the Hippo pathway.

The Hippo pathway is a kinase cascade known for its essential role in organ size control and tissue homeostasis,[117] and is commonly perturbed in cancers.[103,179] Most upstream are the MST1 and MST2 kinases, which are regulated by a variety of extracellular signals such as substrate adhesion, cell-cell contact, and cell polarity. MST1/2 phosphorylate and activate kinases LATS1 and LATS2, which can in turn phosphorylate YAP and its paralog TAZ, transcription coregulators that carry out the output of Hippo signaling.[103,117] When phosphorylated by LATS1/2, YAP and TAZ are inactivated through cytoplasmic sequestration or proteasomal degradation.[103] In their unphosphorylated forms, YAP and TAZ localize to the nucleus and primarily bind to TEAD-family transcription factors to induce the gene expression of secreted factors such as *CTGF* (connective tissue growth factor), *CYR61* (cysteine rich angiogenic inducer 61), and *EDN1*

(endothelin 1).[103,117] The localization, phosphorylation, and transcriptional activity of YAP/TAZ, therefore, represent a robust readout of Hippo pathway status.

Recently, alternative upstream stimuli regulating the Hippo pathway have been identified. For example, G protein-coupled receptors (GPCRs) also serve as upstream regulators of LATS1/2, and consequently, YAP/TAZ.[142] While ligands that regulate YAP/TAZ through GPCRs are gradually uncovered,[142] the upstream—and extracellular—mechanisms that regulate the Hippo pathway in normal tissues and cancers remain incompletely understood.

Protease-activated receptors (PARs) are a class of GPCRs recently shown to regulate the Hippo pathway.[143] PARs are activated by proteolytic cleavage of their own N-termini. Activation of PAR1 by thrombin (a known activator) or ligand-mimetic peptides inhibits LATS1/2 phosphorylation and activates YAP via $G_{12/13}$. In addition, peptide activation of PAR2 results in YAP dephosphorylation.[143]

In this chapter, I demonstrate that SPINT2 dampens YAP activity via inhibition of PAR1 and PAR2, likely through $G_{i/o}$. I show that PAR1 and PAR2 are both required for SPINT2-YAP signaling, and that SPINT2 directly regulates the proteolytic cleavage of PAR1 and PAR2. My findings shed light on SPINT2's functions as a putative tumor suppressor, and establish SPINT2 as a regulator of potentially oncogenic PAR and YAP signaling.

2.2 Results

2.2.1 SPINT2 depletion results in YAP activation

When dephosphorylated, YAP and TAZ are translocated into the nucleus and mainly interact with TEAD family transcription factors to regulate gene expression.[103] To determine the activity of YAP/TAZ, I assayed for YAP/TAZ nuclear localization, YAP phosphorylation status, as well as YAP target gene expression.

Immunofluorescence staining using a YAP/TAZ dual-specific antibody revealed that following transient (48–72 h) depletion of SPINT2 by small interfering RNA (siRNA), YAP/TAZ predominantly localized to the nuclei of hTERT-immortalized, non-transformed human retinal pigment epithelial (RPE-1) cells, similar to the effect of LATS1 and LATS2 double knock-down (Figure 2-1A). Four independent siRNAs resulted in efficient, albeit varying degrees of, *SPINT2* knock-down (Figure 2-1B–C), as measured by immunoblots and quantitative PCR (qPCR).

Average fluorescence intensities of YAP/TAZ staining within the nuclear and cytoplasmic compartments of each cell were acquired using confocal microscopy and quantified, and the distribution of nuclear:cytoplasmic intensity (N:C) ratio was plotted in Figure 2-2A. Cells with N:C ratio greater than 1.0 were defined as exhibiting nuclear localization of YAP/TAZ. Strikingly, SPINT2 depletion resulted in statistically significant increases in the proportion of cells with nuclear YAP/TAZ (Figure 2-2B).

It is worth noting that the effects of SPINT2 knock-down on YAP/TAZ nuclear localization appears to correlate with the degree of SPINT2 protein and mRNA depletion by each siRNA, suggesting that the phenotypes I observed were indeed a direct consequence of the intended RNAi suppression of *SPINT2*.

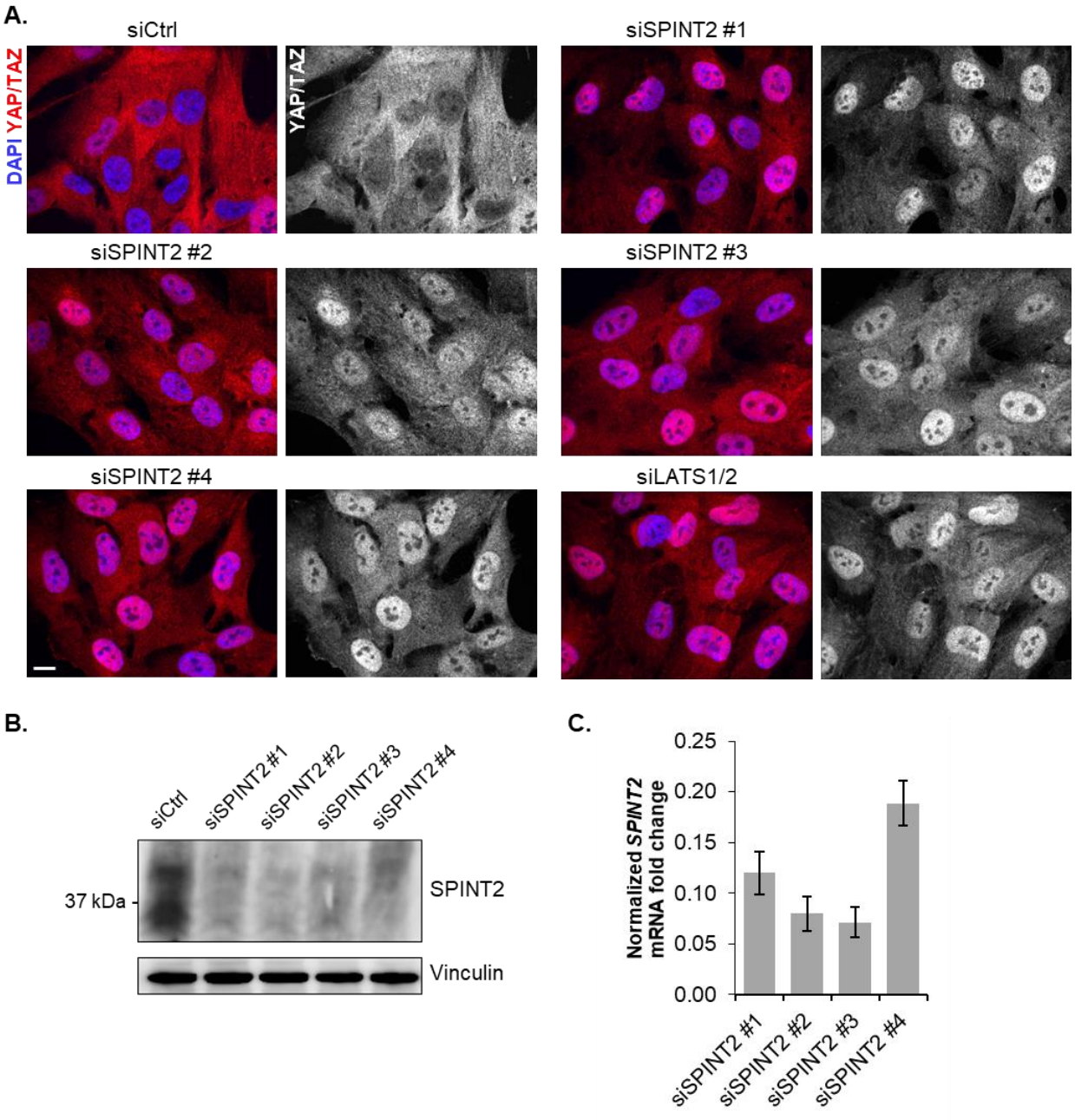

Figure 2-1. SPINT2 depletion leads to nuclear localization of YAP/TAZ in RPE-1 cells.

A. Immunofluorescence staining of YAP/TAZ in RPE-1 cells. Magnification, 60X; scale bar, 10 μm. **B**. Immunoblot of cell lysates following *SPINT2* depletion by siRNAs. **C**. qPCR of *SPINT2* mRNA following siRNA treatment. Error bars, standard deviation (SD); n=3.

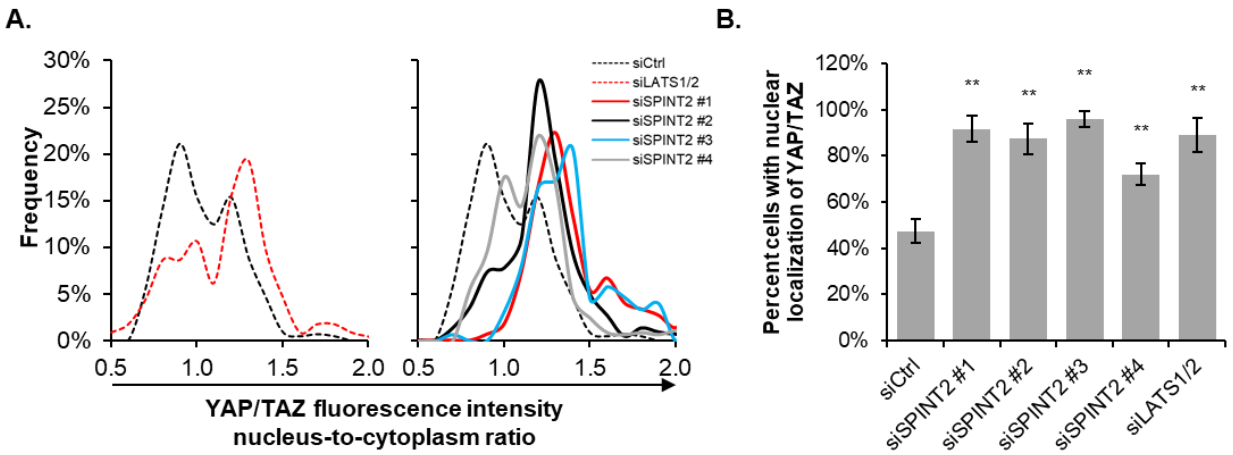

Figure 2-2. Quantification of YAP/TAZ nuclear localization in RPE-1 cells following SPINT2 depletion.

A. Histograms of YAP/TAZ fluorescence intensity N:C ratio following SPINT2 knock-down. 400 cells were quantified in each sample. **B**. Average frequencies of cells with nuclear YAP/TAZ following SPINT2 depletion. Error bars, SD (n=3). **, $p<0.01$, *t*-test.

To confirm the generality of SPINT2's effects on YAP/TAZ, I performed similar immunofluorescence experiments in the HCT-116 human colorectal carcinoma cell line. Compared to RPE-1 cells, HCT-116 cells represent a distinct tissue origin and transformation status. I utilized the most effective siRNA against *SPINT2*, siSPINT2 #3 (Figure 2-1C, Figure 2-2). Notably, HCT-116 cells appeared to exhibit similar phenotypes in terms of YAP/TAZ localization as RPE-1 cells following SPINT2 depletion (Figure 2-3). However, due to the morphology of HCT-116 cells (extremely small cytoplasmic volumes relative to nuclei), it was experimentally challenging to obtain accurate quantification of fluorescence intensities of the nuclear and cytoplasmic compartments.

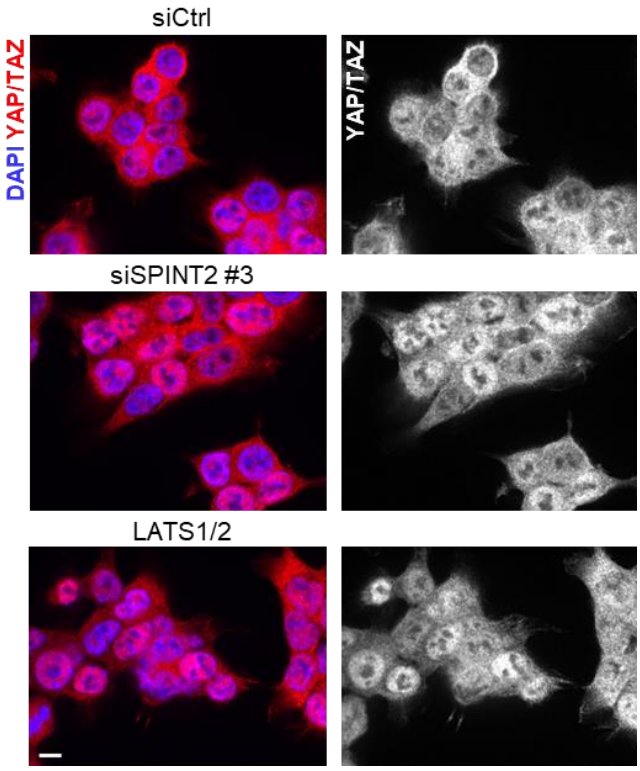

Figure 2-3. SPINT2 depletion induces nuclear localization of YAP/TAZ in HCT-116 cells. Immunofluorescence staining of YAP/TAZ in HCT-116. Magnification, 60X; scale bar, 10 μm.

Next, I sought to verify whether the increase in nuclear localization of YAP/TAZ following SPINT2 depletion led to upregulation of YAP target genes, the ultimate output when the Hippo signaling pathway switches off.[103,142] To this end, I performed qPCR measurements of well-characterized YAP targets: *CTGF*, *CYR61*, and *EDN1*,[141,142,178,180] and detected upregulation of these genes following SPINT2 depletion in both RPE-1 (Figure 2-4A) and HCT-116 cells (Figure 2-4B). To complement these results, I performed a gain-of-function experiment by transfecting HCT-116 cells with low and high amounts of CMV promoter-driven *SPINT2* cDNA, and saw an inverse correlation between mRNAs of YAP target genes and *SPINT2* (Figure 2-4B).

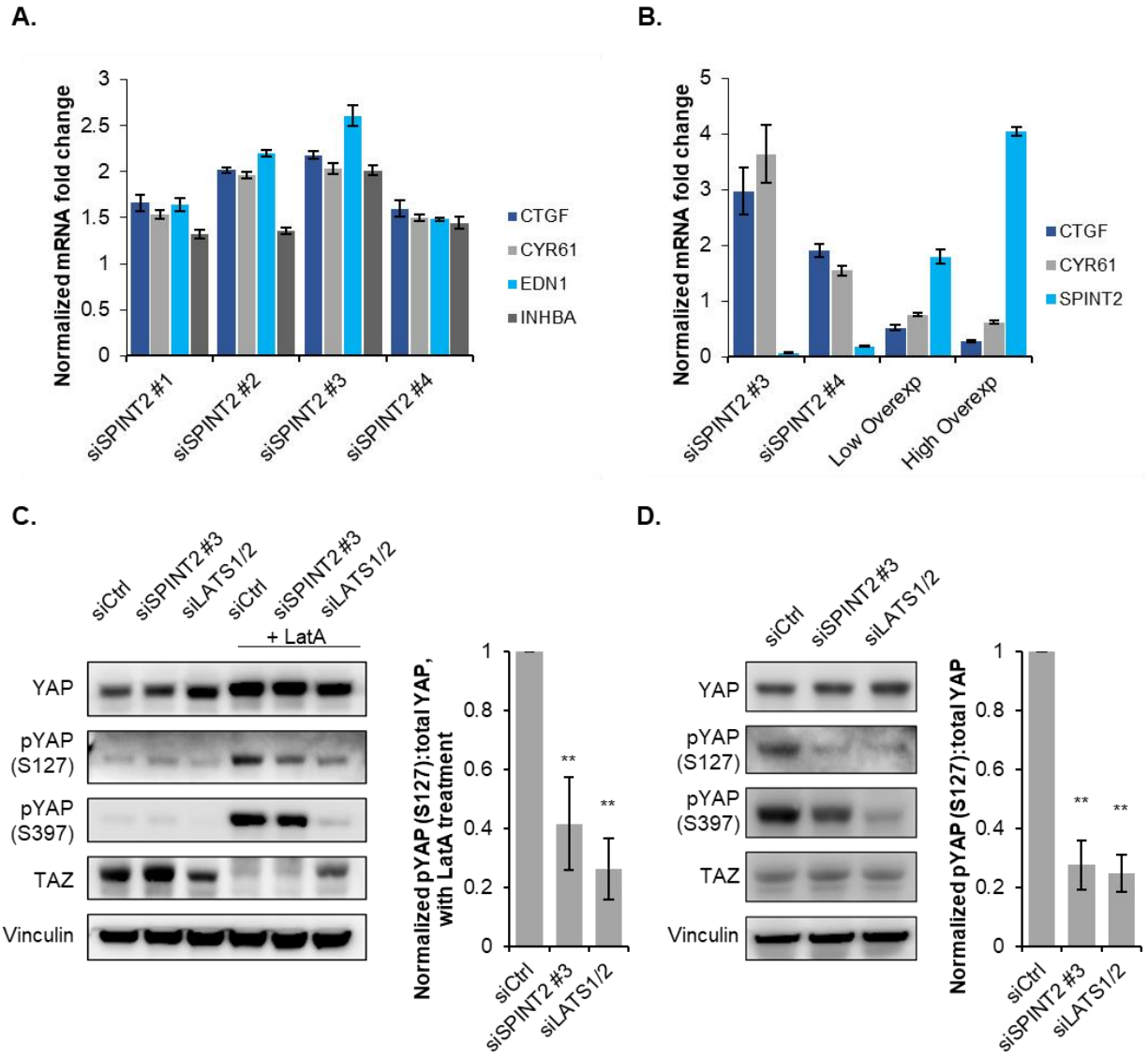

Figure 2-4. YAP target gene expression and dephosphorylation following SPINT2 depletion.

A. SPINT2 depletion induces YAP target gene expression in RPE-1. **B**. *SPINT2* mRNA inversely correlates with YAP target transcripts in HCT-116. Low overexpression, 0.1 µg cDNA/10^6 cells transfected; high, 0.4 µg. **C**. YAP S127 and S397 phosphorylation and TAZ abundance following SPINT2 knock-down in RPE-1 cells. Bar graph, average fold change of pYAP S127:total YAP ratio, with LatA. **D**. YAP phosphorylation in HCT-116 cells with SPINT2 depletion. Bar graph, average fold change of pYAP S127:total YAP ratio. Error bars, SD (n=3). **, $p<0.01$, *t*-test.

Phosphorylation of YAP on serine 127 (S127) promotes YAP 14-3-3 binding and cytoplasmic sequestration, whereas phosphorylation on serine 397 (S397)—sometimes termed S381 in alternative isoforms—mediates YAP ubiquitination and degradation. TAZ, on the other hand, frequently undergoes rapid degradation following phosphorylation as a result of Hippo pathway activation.[103,117,181] I therefore tested the phosphorylation status of YAP on S127 and S397, and the abundance of TAZ following SPINT2 depletion.

As shown in Figure 2-4C–D, SPINT2 knock-down altered YAP phosphorylation but not TAZ abundance in RPE-1 and HCT-116 cells. As evidenced by the relatively high frequency of cells with predominantly nuclear (unphosphorylated) YAP/TAZ in control conditions (Figure 2-2), the low basal levels of phospho-YAP in RPE-1 cells posed a technical difficulty. To overcome this challenge and to provide a sensitized background, RPE-1 cells were treated for 1 h with 500 nM latrunculin A (LatA), a drug that inhibits actin polymerization and promotes YAP/TAZ phosphorylation[179] prior to protein extraction.

Strikingly, in both RPE-1 (with LatA) and HCT-116, SPINT2 knock-down resulted in apparent YAP S127 dephosphorylation akin to that induced by LATS1/2 double knock-down. In contrast, dephosphorylation of YAP S397 was reduced by a moderate extent. Interestingly, in RPE-1 cells treated with LatA, TAZ appeared to be degraded in control cells. This effect was rescued by siLATS1/2 (Figure 2-4C), suggesting that the LatA-induced TAZ degradation is dependent on LATS1 and LATS2—consistent with findings reported by Liu and colleagues (2010)[181] using HEK-293T (transformed human embryonic kidney) and MCF-10A (non-transformed breast epithelial) cells. Notably but perhaps unsurprisingly, SPINT2 depletion did not recapitulate the effect of LATS1/2 knock-down on TAZ abundance in LatA-treated RPE-1 cells.

To test whether SPINT2 may regulate YAP via upstream Hippo pathway kinases,[103,117] my colleague Kristyna Kotynkova (Boston University School of Medicine, Boston, MA) examined the phosphorylation status of LATS1/2 following SPINT2 suppression. Specifically, following knock-down of SPINT2 or LATS1/2, HCT-116 cells were treated for 1 h with 250 nM latrunculin B (LatB; similar to LatA)[179] in order to sensitize the background. Phospho-LATS1/2 (detected by a single antibody),[182] LATS1, and LATS2 were probed. As shown in Figure 2-5, SPINT2 depletion markedly reduced phospho-LATS1/2.

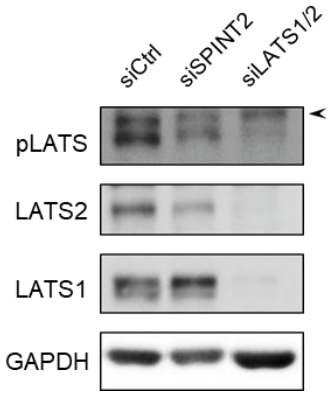

Figure 2-5. SPINT2 knock-down leads to dephosphorylation of LATS1/2.

Immunoblot measuring phospho-LATS1/2 (pLATS), LATS1 and LATS2 abundance. Arrow head, non-specific signal.

It is worth noting that depletion of SPINT2 does not alter cell cycle distribution (discussed in Section 3.2.2; see Figure 3-8), suggesting that the consequent alteration of YAP and LATS are not cell cycle-dependent. Taken together, these results demonstrate that SPINT2 limits YAP activity. Suppression of *SPINT2* by RNAi results in YAP activation as shown by YAP/TAZ nuclear localization, YAP dephosphorylation, and YAP/TAZ target gene expression. Consistent with the observed activation of YAP, SPINT2 depletion also may lead to a reduction in the phosphorylation of LATS kinases.

2.2.2 SPINT2 regulates YAP via PAR1, PAR2, and $G_{i/o}$

To systematically dissect SPINT2's regulation of YAP, I performed transcriptome analysis of SPINT2-depleted RPE-1 and HCT-116 cells. Two independent siRNAs (#2 and #3) against *SPINT2* were used to control for potential off-target effects.[183] The resultant gene expression data were analyzed using clustering-heatmap and gene set enrichment analyses to identify consistently upregulated genes as well as potential biological pathways induced by SPINT2 knock-down.

Clustering-heatmap analysis aims to visualized high-throughput multivariate data by clustering values based on similarities.[184] Using the algorithm Morpheus (Broad Institute),[184,185] I performed clustering of SPINT2-depleted transcriptome data by row (genes) and column (samples), and identified genes consistently induced by SPINT2 depletion (Figure 2-6A). Strikingly, several well-characterized YAP target genes such as *CTGF*, *CYR61*, *COL8A1* (collagen 8α), and *MCL1* (an anti-apoptotic protein) were among the most highly induced.[117,186,187]

Gene Set Enrichment Analysis (GSEA) is an algorithm that detects the enrichment of "biologically defined" sets of genes within gene expression data.[188] Biologically defined gene sets refer to those delineated based on prior biological knowledge such as published information on specific biological pathways. GSEA assesses whether these gene sets enrich in the top or bottom portions of rank-ordered expression data. Two metrics indicate the magnitude and significance of enrichment. First, normalized enrichment scores (NES) measure the degree of enrichment normalized against input size (e.g., number of samples). Second, false discovery rates (FDR, or *q* values) provide information on the statistical significance of detected enrichments. For experiments with <7 samples in each condition, the recommended FDR cutoff is 0.05.[188]

GSEA was performed using SPINT2-depleted transcriptome data from RPE-1 and HCT-116 against the H: Hallmark and C6: Oncogenic Signatures collections curated by the Broad

Institute.[189] In addition, the top 300 genes induced in RPE-1 overexpressing phosphorylation-resistant forms of YAP (YAP-5SA) and TAZ (TAZ-4SA) were included in the analysis. Strikingly, in both RPE-1 and HCT-116 cells, the custom YAP-5SA and TAZ-4SA gene sets were significantly enriched (Figure 2-6B and Table 2-1).

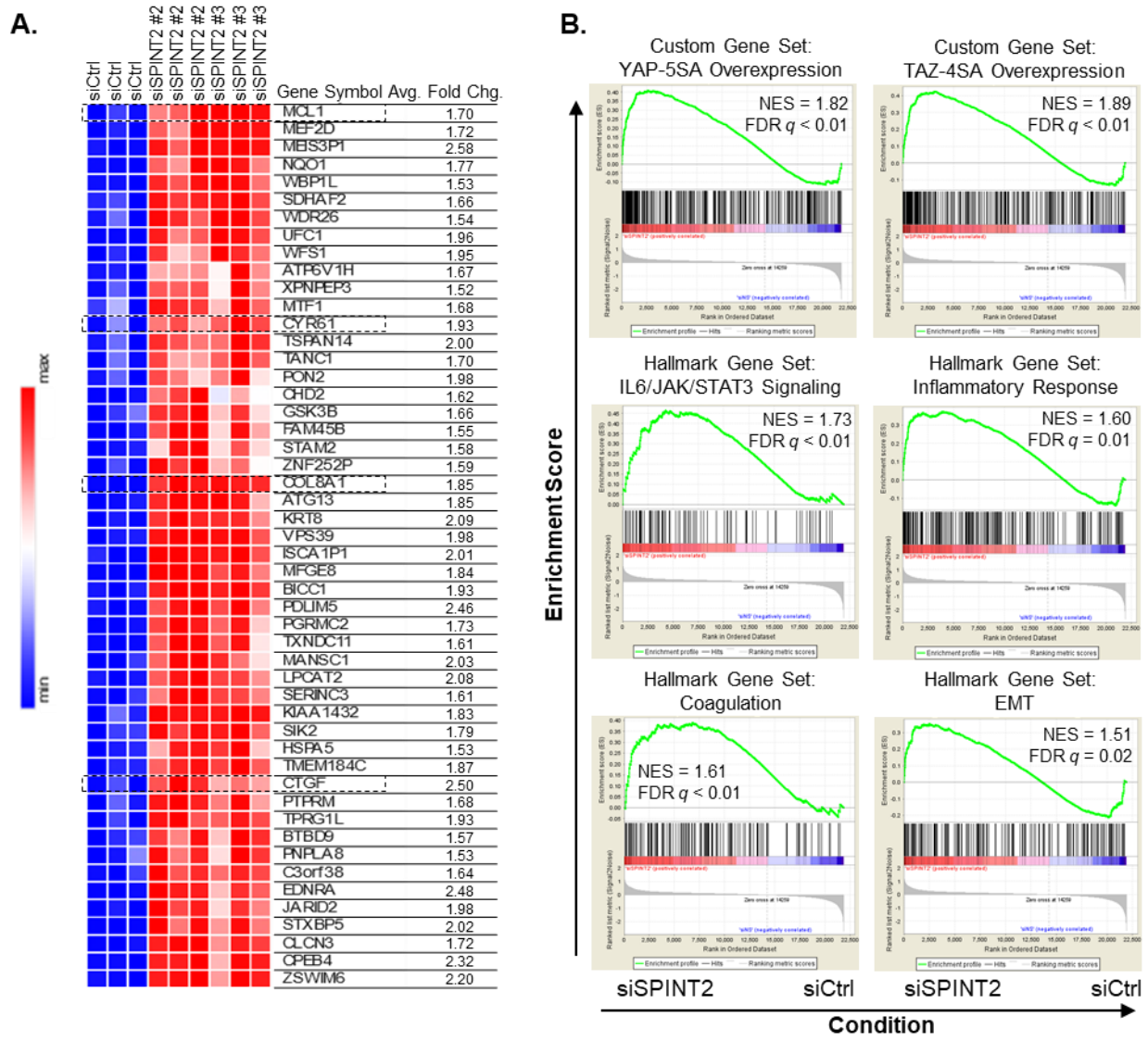

Figure 2-6. Transcriptome analysis of cells depleted of SPINT2.

A. Clustering reveals top 50 genes upregulated following SPINT2 knock-down in RPE-1. Average fold change of each transcript is listed. Dashed rectangles highlight known YAP/TAZ target genes. **B**. Examples of top gene sets enriched in SPINT2-depleted RPE-1 cells. A total of 241 gene sets were included in the GSEA run (189 in C6 collection; 50 in Hallmark collection; 2 custom gene sets). NES, normalized enrichment score; FDR, false discovery rate (*q* value).

Table 2-1. Common top gene sets enriched in SPINT2-depleted RPE-1 and HCT-116 cells.

Gene Set	NES, FDR *q* (RPE-1)	NES, FDR *q* (HCT-116)
HALLMARK_HYPOXIA	2.11, <0.01	1.94, <0.01
HALLMARK_INTERFERON_ALPHA_RESPONSE	2.01, <0.01	2.04, <0.01
HALLMARK_TNFA_SIGNALING_VIA_NFKB	1.96, <0.01	1.94, <0.01
TAZ-4SA (custom gene set)	1.89, <0.01	1.72, <0.01
YAP-5SA (custom gene set)	1.82, <0.01	1.51, 0.01
HALLMARK_IL6_JAK_STAT3_SIGNALING	1.73, <0.01	1.35, 0.05
HALLMARK_TGF_BETA_SIGNALING	1.64, 0.06	1.66, <0.01
HALLMARK_CHOLESTEROL_HOMEOSTASIS	1.63, 0.01	2.23, <0.01
HALLMARK_COAGULATION	1.61, <0.01	1.36, 0.04
HALLMARK_INFLAMMATORY_RESPONSE	1.60, 0.01	1.33, 0.05
HALLMARK_INTERFERON_GAMMA_RESPONSE	1.56, 0.02	1.87, <0.01
HALLMARK_EPITHELIAL_MESENCHYMAL_TRANSITION	1.51, 0.02	1.74, <0.01

Interestingly, gene sets that are indicative of heightened growth factor signaling (in line with prior reports on SPINT2 functions)[86,190,191] such as HALLMARK_KRAS_SIGNALING_UP and HALLMARK_PI3K_AKT_MTOR_SIGNALING[189] were not detected by GSEA (Table 2-1). Instead, genes associated with coagulation, inflammatory response (e.g., IL6/JAK/STAT3 and Inflammatory Response gene sets), and epithelial-mesenchymal transition (EMT) were significantly induced following SPINT2 depletion (Table 2-1). These highly enriched gene sets provided intriguing hypotheses regarding how SPINT2 modulates YAP activity.

Protease-activated receptors (PARs) are well-established modulators of the coagulation cascade and inflammation,[41] and have recently been reported to regulate EMT in solid tumors.[62,192] In addition, Mo et al. (2012)[143] demonstrated that PAR1 and PAR2 activation induced YAP dephosphorylation via their coupled G protein α subunits $G_{12/13}$. Therefore, I hypothesized that SPINT2 may negatively regulate YAP activity through inhibition of PARs.

To test whether PARs mediate SPINT2-YAP signaling, I conducted a candidate-based siRNA screen that examined PARs, common Gα subunits, and known downstream factors of SPINT2 (Figure 2-7 and Figure 2-8).

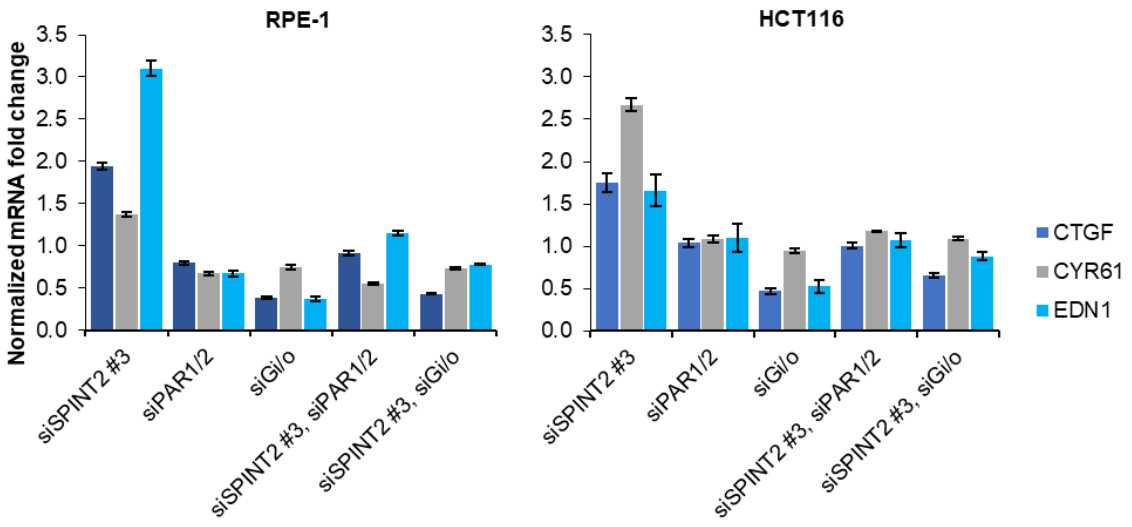

Figure 2-7. Candidate-based screen identifies requirements for YAP activation following SPINT2 knock-down.

Double knock-down of PAR1 and PAR2; and G_i and G_o abrogated YAP target gene expression following SPINT2 depletion. Error bars, SD (n=3).

Interestingly, simultaneous—but not individual—knock-down of PAR1 and PAR2 abrogated YAP target gene expression induced by siSPINT2; suppression of Gα subunits $G_{i/o}$ rescued SPINT2 depletion's effect (Figure 2-7 and Figure 2-8A). These results were acquired using previously validated RNAi reagents (see Table 2-2 in 2.4 Materials and Methods). Of note, transcriptome data (generated for Figure 2-6; not shown) revealed that PAR1 and PAR2 mRNAs were expressed at medium-to-high levels in both RPE-1 and HCT-116 cells; PAR3 mRNA was abundant in RPE-1 but low in HCT-116; PAR4 mRNA had low abundance in both cell lines; and all tested G_α subunits were abundantly expressed.

However, depletion of other factors that are known to be negatively regulated by SPINT2, such as matriptase (ST14)[80] and HGF receptor (MET),[193] as well as knock-down of $G_{12/13}$[143] or $G_{11/q}$ did not interfere with YAP target gene expression following SPINT2 depletion (Figure 2-8A). As a validation of the reagents, the efficiency of siRNAs used in this screen was demonstrated by immunoblotting or qPCR (Figure 2-8B–C). Consistent with these findings, PAR1 and PAR2, but not PAR3 or PAR4, are known to couple with $G_{i/o}$ to effect downstream signaling.[40]

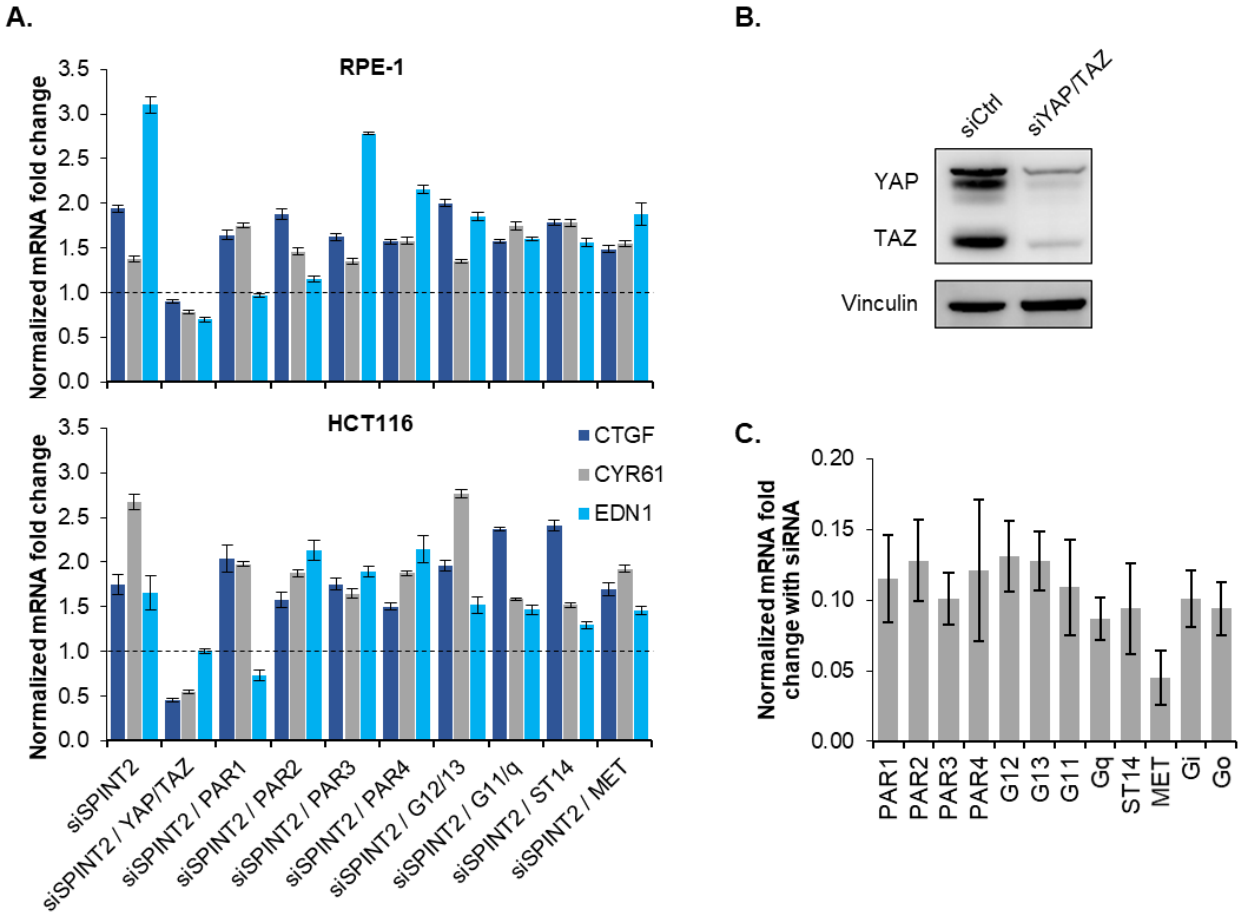

Figure 2-8. Validation of candidate-based screen for dependencies of SPINT2-YAP signaling.

A. Knock-downs that did not abrogate SPINT2 depletion-induced YAP activation. Positive control: YAP/TAZ dual-specific siRNA. **B** and **C**. Validation of siRNAs by immunoblot and qPCR, respectively. Cell line, RPE-1. Error bars, SD (n=3).

My findings confirm the activation of YAP following SPINT2 depletion on the transcriptome level, and suggest that SPINT2 limits YAP activity through both PAR1 and PAR2, as well as their coupled $G_{i/o}$ proteins.

2.2.3 SPINT2 inhibits PAR1 and PAR2 cleavage by endogenous proteases

PARs are activated through proteolytic cleavage of their N-termini by extracellular or membrane proteases, which results in conformational changes of PARs' intracellular domains (C-termini) that trigger downstream G protein-mediated signaling.[41] To test whether SPINT2 directly alters the cleavage of PAR1 and PAR2 by endogenous proteases, I utilized expression constructs of PAR1/2 with N-terminus alkaline phosphatase (AP) fusion. When these fusion proteins are proteolytically cleaved, AP is released into the medium. Therefore, PAR1 and PAR2 cleavage by endogenous proteases was measured through free AP activity in serum-free culture medium of cells transfected with AP-PAR constructs (Figure 2-9).

AP-PAR1 and AP-PAR2 cleavage was measured in both SPINT2 suppression and overexpression using a chemiluminescence-based AP detection assay. Free AP activity in culture medium is expressed as luminescence per million cells (Figure 2-9A). A stable HCT-116 cell line was constructed with a short hairpin RNA (shRNA) targeting *SPINT2*. To control for potential off-target effects, I engineered a cell line expressing a synonymously mutated *SPINT2* open reading frame (ORF) resistant to shSPINT2. Overexpression of SPINT2 was achieved by transfecting HCT-116 with a CMV promoter-driven FLAG-tagged *SPINT2* ORF. SPINT2 overexpression, knock-down, and shRNA rescue were validated by immunoblotting (Figure 2-9B).

As shown in Figure 2-9A, shSPINT2 resulted in moderate, but statistically significant, increases in PAR1 and PAR2 cleavage, whereas the shRNA rescue cell line (shSPINT2+ORF)

exhibited cleavage levels similar to control (shLuc, shRNA targeting firefly luciferase). Consistent with these results, SPINT2 overexpression significantly inhibited PAR1 and PAR2 cleavage compared to control (CMV promoter-driven mCherry).

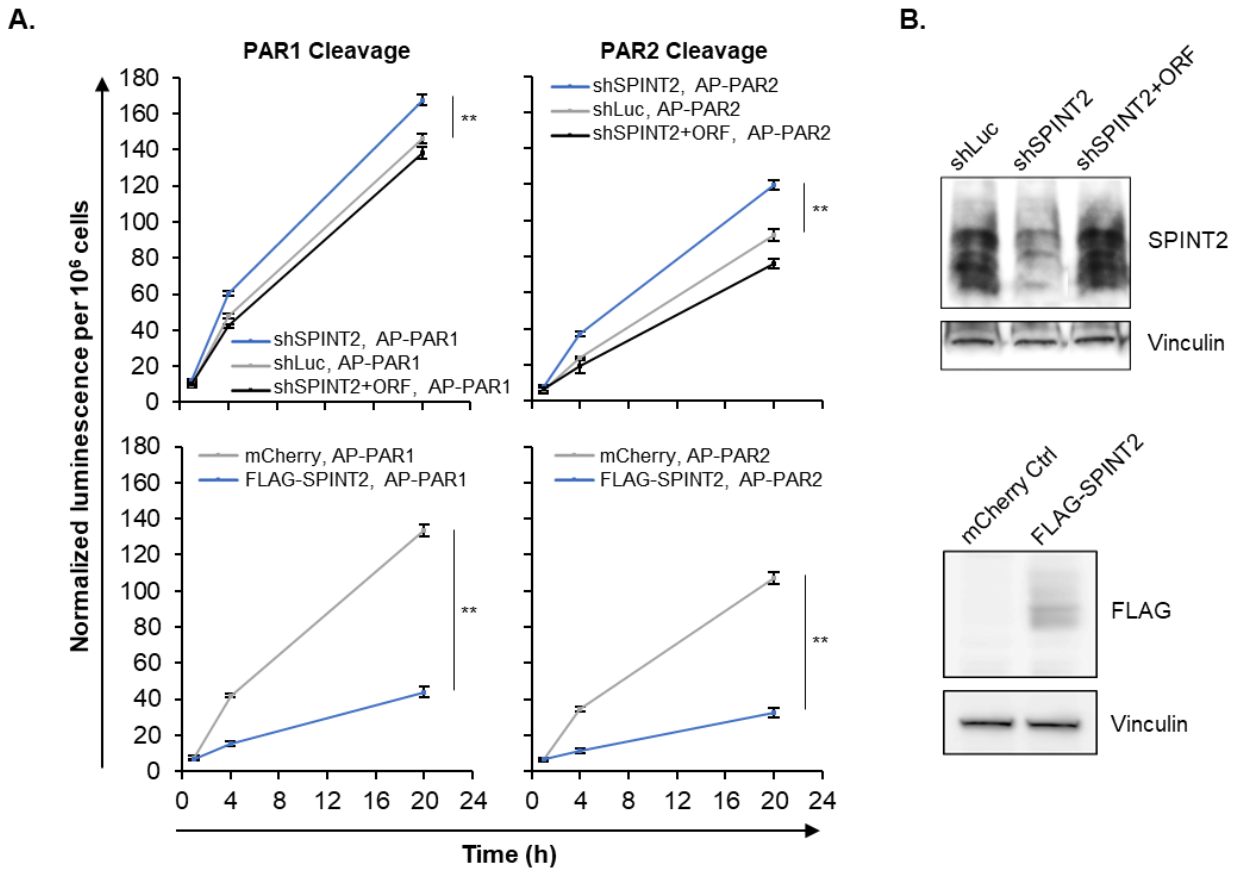

Figure 2-9. SPINT2 regulates PAR1 and PAR2 cleavage by endogenous proteases.

A. AP-PAR1/2 cleavage assay in HCT-116 cells. Free AP activity was normalized to cell numbers at each time point and expressed as normalized luminescence per million cells. **B**. Validation of reagents. Error bars, SD (n=3). **, $p<0.01$, *t*-test.

To allow for maximum sensitivity and accuracy of this assay, AP-PAR1 and AP-PAR2 expression was restricted to modest level (~50% of endogenous levels; Figure 2-10) to minimize secretion or exodomain shedding into the medium.[194,195] In addition, while we have observed cell death following high levels of SPINT2 overexpression, the expression of FLAG-SPINT2 (~10 fold endogenous level; Figure 2-10) appeared to be well-tolerated by cells in this experiment.

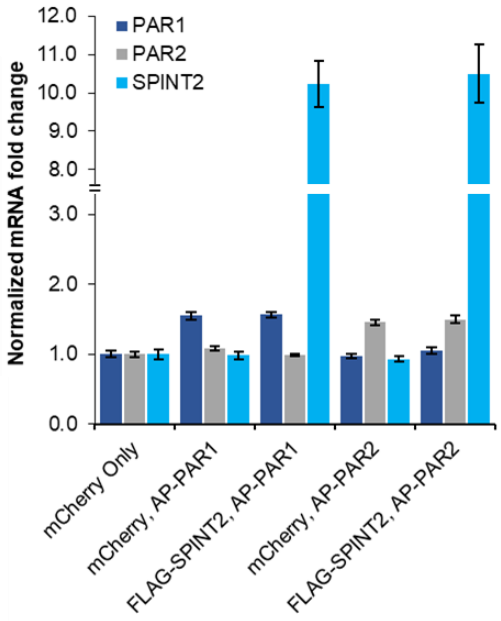

Figure 2-10. qPCR validation of AP-PAR1/2 and SPINT2 overexpression.

AP-PAR1/2 expression was restricted to modest levels; FLAG-SPINT2 was expressed at about 10-fold of endogenous *SPINT2* mRNA. Error bars, SD (n=3).

In summary, both loss- and gain-of-function experiments have shown that SPINT2 directly regulates PAR1 and PAR2 cleavage, and likely activation, by endogenous proteases.

2.2.4 SPINT2 loss is insufficient for anchorage-independent growth

Amplification of a YAP-containing chromosome fragment, 11q22, is observed in human tumors.[136] Considering the frequent silencing of *SPINT2* in cancers,[94-100] I set out to test whether SPINT2 depletion resulted in oncogenic transformation in an MCF-10A human breast epithelial model. Wild-type MCF-10A cells are known to experience anoikis when detached from the extracellular matrix;[196] upon overexpression of oncoproteins such as YAP and $KRAS^{G12V}$, they resist anoikis and exhibit anchorage-independent growth in soft agar suspension.[136,197]

Wild-type (WT) and *TP53* shRNA knock-down[198] MCF-10A cells were transduced with two independent shRNAs against *SPINT2*; shTP53 cells were additionally transduced with an shRNA against *LATS2* or a CRISPR single-guide RNA (sgRNA) construct targeting *SPINT2*. After 42 days, however, I was unable to detect anchorage-independent growth following SPINT2 knock-down, whereas overexpression of $KRAS^{G12V}$ produced robust growth of colonies (Figure 2-11).

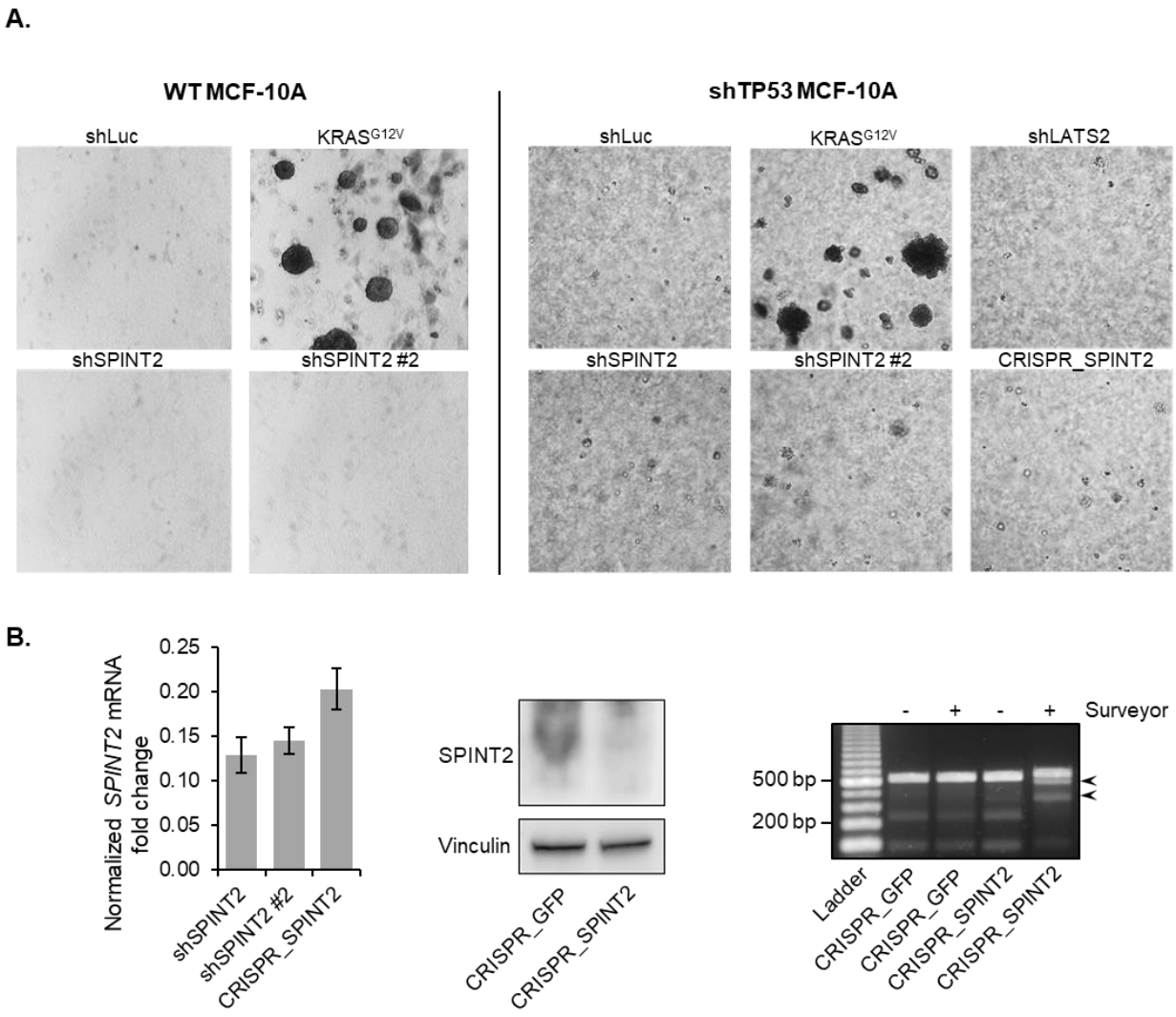

Figure 2-11. Soft agar assay of SPINT2-depleted MCF-10A cells.

A. Crystal violet staining of MCF-10A cell lines grown in soft agar for 42 days (50,000 cell/well seeded in 6-well plates; media replenished twice a week). shLuc and CRISPR_GFP (not shown) produced similar results. Magnification, 20X. **B**. qPCR, immunoblot, and Surveyor validation of shRNA and CRISPR constructs targeting *SPINT2*. Arrow heads, CRISPR-specific Surveyor cleavage products. Error bars, SD (n=3).

It is perhaps unsurprising that SPINT2 depletion alone does not recapitulate the effect of YAP overexpression in promoting anchorage-independent growth. In human cancers, the chromosome 11q22 amplicon harboring *YAP1* usually occurs at high copy numbers and also contains genes encoding other putative oncoproteins including several matrix metalloproteases and the anti-apoptotic cIAP1/2.[199-201]

In the *ex vivo* model, Overholtzer et al. (2006)[136] overexpressed YAP using the highly potent SV40 promoter, and observed dramatic 3-D morphological changes of MCF-10A cells at day 8 and anchorage-independent growth at day 21. By contrast, I did not observe morphological changes in SPINT2-depleted MCF-10A cells in 2-D cultures after a 7-day antibiotic selection for cells expressing shRNA or CRISPR sgRNA constructs. Furthermore, as shown in Figure 2-4, SPINT2 depletion resulted in moderate YAP activation and did not alter YAP abundance.

2.3 Discussion

I have characterized novel functions of SPINT2 in modulating Hippo signaling via YAP suppression, specifically through PAR1 and PAR2, and $G_{i/o}$. This mechanism is conserved in two independent cell lines with distinct tissues of origin and transformation statuses.

2.3.1 SPINT2 as a dual-function tumor suppressor limiting growth factors and YAP

Prior investigations on SPINT2 have focused on its role as a negative regulator of HGF signaling due to its inhibition of hepsin and HGFA, serine protease activators of pro-HGF.[86,190,191] Recently, it was shown that SPINT2 knock-down phenocopied insulin-like growth factor (IGF) treatment in tetraploid RPE-1 cells and induced sustained AKT and ERK phosphorylation, suggesting general activation of growth factor signaling pathways following SPINT2 depletion.[178]

Potential crosstalk between growth factor signaling and the Hippo pathway remains elusive.[102] In 2003, Basu et al.[202] reported that in MCF-7 breast carcinoma cells, expression of active AKT resulted in YAP phosphorylation and its sequestration by 14-3-3, suggesting negative regulation of YAP by AKT signaling.

On the contrary, later studies reported mutual reinforcement between IGF and YAP. Specifically, expression of constitutively active phosphoinositide-3-kinase (PI3K; kinase upstream of AKT) in the *Drosophila* wing disc resulted in tissue overgrowth as well as Yorkie (YAP homolog) transcriptional activity as measured by a transgene reporter; expectedly, expression of a dominant-negative form of PI3K led to the opposite effect.[203] Furthermore, in murine cardiomyocytes, expression of phosphorylation-resistant Yap induced an IGF gene expression signature. This result was corroborated by the observation that Akt phosphorylation was sustained at a higher level in murine cells expressing phosphorylation-resistant Yap.[204]

Additionally, Reddy and Irvine (2013)[205] reported that in *Drosophila*, expression of activated epidermal growth factor receptor (EGFR) induced Yorkie-dependent glial tissue overgrowth. The authors further showed that Yorkie was activated by overexpressed EGFR via a pathway dependent on Ras-Raf signaling. In human cell lines, expression of active EGFR and an activating HRAS mutant ($HRAS^{V12}$) resulted in reduced YAP S127 phosphorylation, although potential downstream mechanisms remained unclear.[205] However, the overexpression and gain-of-function conditions used in these studies represent a caveat: although YAP may be activated by constitutively active mutant growth factor receptors and Ras GTPases, the contribution of growth factor signaling on YAP activity in physiological conditions remains poorly understood.

It is likely that growth factors are not the predominant activator of YAP in unperturbed human cell culture conditions. Yu et al. (2012)[142] showed that in HEK-293A cells, YAP was

activated by serum stimulation after starvation. Remarkably, this activation was preserved when serum was pre-treated with pronase E (a protease cocktail) or heat, conditions that degraded or denatured virtually all proteinaceous factors. The authors further identified two modulators of GPCR signaling, lysophosphatidic acid (LPA) and sphingosine 1-phosphophate (S1P), as the main serum-borne macromolecules responsible for the observed YAP activation.[142] Consistent with these findings, neither RPE-1 nor HCT-116 cells showed growth factor-related gene expression signatures following SPINT2 depletion (Figure 2-6 and Table 2-1), and suppression of HGF receptor (MET) did not inhibit SPINT2 depletion-induced YAP gene expression (Figure 2-8).

Nevertheless, SPINT2 may assume a more potent role in regulating growth factor signaling *in vivo*. It has been shown that HGFA, a serine protease and a regulatory target of SPINT2,[80,89] is required for the conversion of pro-HGF to HGF during murine metanephric kidney morphogenesis.[206] *SPINT2* is highly expressed in murine and human kidney tissues[89,207] and is epigenetically silenced in human renal cell carcinomas.[96,208] Therefore, ablation of SPINT2 *in vivo*, as seen in various cancers,[94-100] may afford significant tumorigenic potential due to SPINT2's dual function in suppressing both growth factor signaling and YAP activity.

Further accentuating SPINT2's relevance as a tumor suppressor are recent observations that oncogenic KRAS may converge with YAP to exert potent tumorigenic signaling. *KRAS* encodes a membrane monomeric G protein that is activated by growth factors, and is among the most frequently mutated genes in human cancers.[209] It has been shown that a combination treatment of PI3K and MEK inhibitors leads to marked tumor regression in $Kras^{G12D}$-driven murine lung cancer, suggesting growth factor dependency of KRAS-driven tumors.[210] In 2014, Kapoor et al.[211] and Shao et al.[212] reported that YAP could functionally substitute for activated KRAS in KRAS-dependent colorectal, lung, and pancreatic cancer cells. In KRAS-dependent

human colorectal cancer cell lines, YAP is required for cell survival, and YAP overexpression rescues KRAS suppression. Activated KRAS and YAP converge on the transcription factor FOS to induce an EMT gene expression program.[212] In murine lung adenocarcinoma and pancreatic ductal adenocarcinoma, Yap drove tumor relapse following Kras suppression.[211,212] In mouse pancreatic ductal adenocarcinoma, Yap mediates the expression of cell cycle genes in conjunction with transcription factors Tead2 and E2f1.[211]

Given these findings, it is conceivable that SPINT2 may represent an *in vivo* tumor-suppressing mechanism that attenuates both growth factors and YAP, as well as their convergent downstream oncogenic transcription program. While Spint2's functions during development have been tested in murine models,[80] the physiological consequences of Spint2 loss in tumorigenesis require further interrogation *in vivo*.

2.3.2 Potential mechanisms linking PAR1/2 and YAP

PARs are a class of GPCRs that are predominantly expressed in epithelial, vascular, immune, and neuronal cells, and are irreversibly activated through proteolytic cleavage to induce cellular responses to extracellular proteases.[40] PARs are known to couple with most major G_α subunits of heterotrimeric G proteins ($G_{i/o}$, $G_{q/11}$, and $G_{12/13}$) with differential and sometimes redundant specificity. For example, all PARs have been shown to couple with $G_{q/11}$ in various cell lines. However, only PAR1, PAR2, and PAR4 are known to couple with $G_{12/13}$; and $G_{i/o}$ predominantly couples to PAR1 and PAR2.[40] The preferential coupling of PARs to G_α subunits is presumed to be tissue- and context-dependent.[40,213]

Mo et al. (2012)[143] initially uncovered PAR1 and PAR2's roles in activating YAP. Specifically, in HEK-293A, HeLa, MCF-10A, and MDA-MB-231 (metastatic breast cancer) cells,

TRAP6 (PAR1-activating peptide) and thrombin induced dramatic but transient reduction of YAP phosphorylation following serum starvation. This phenotype was further shown to be $G_{12/13}$-dependent. A PAR2-activating peptide (SLIGRL) induced a similar effect in all but HeLa cells, although the downstream G protein was not elucidated.[143]

In light of the prior report by Mo and colleagues,[143] several attributes of my data provide novel insights regarding PAR1/2's regulation in tumorigenesis and expand our view of YAP. First, SPINT2 depletion resulted in sustained (48–72 h) dephosphorylation of YAP (Figure 2-4) in proliferating cell populations, whereas YAP dephosphorylation induced by thrombin (1–10 nM), TRAP6 (1–5 μM), and SLIGRL (5–50 μM) started to be attenuated at two (2) hours after treatment of serum-starved cells.[143] Treating RPE-1 and HCT-116 cells with thrombin or TRAP6 at similar concentrations for the duration of 48–72 hours did not result in YAP target gene expression (personal observations; data not shown).

This is an especially interesting distinction given that PARs are known to be rapidly desensitized and internalized following activation.[40] For example, in human pulmonary artery endothelial cells, cell-surface PAR1 is desensitized to thrombin stimulation if pre-treated with 10–25 nM thrombin for 60–120 min.[214] Hence, a transient burst (~2 h) in PAR-mediated YAP dephosphorylation may only correlate with one round of rapid PAR activation, and may not fully recapitulate physiologically meaningful conditions, especially in the context of oncogenesis. SPINT2 depletion's effect may more closely model tumor environments where it induces sustained activation of PARs and subsequently long-term elevation of YAP activity.

Second, $G_{i/o}$ regulates distinct downstream pathways compared to $G_{12/13}$.[215] $G_{12/13}$ activates Rho GTPases (known to regulate the actin cytoskeleton), whereas $G_{i/o}$ inhibits adenylyl cyclase (AC; produces cellular cAMP).[40,215,216] Indeed, PAR1-$G_{12/13}$ dephosphorylation of YAP was

abrogated when cells were treated with *Botulinum* toxin C3 (Rho GTPase inhibitor) and latrunculin B (LatB; actin poison).[143] However, SPINT2 knock-down's suppression of YAP and LATS phosphorylation persisted in the face of actin disruption by LatA or LatB (Figure 2-4C, Figure 2-5), suggesting a mostly actin-independent mechanism. Consistently, RNAi of $G_{i/o}$, but not $G_{12/13}$, cancelled SPINT2 depletion-induced YAP activation (Figure 2-7 and Figure 2-8). Hence, YAP activation induced by SPINT2 depletion via $G_{i/o}$ represents a non-redundant pathway to YAP regulation by other G proteins.[217]

Protein kinase A (PKA) is the main downstream effector of cellular cAMP production, which is inhibited by $G_{i/o}$.[215,218] Recently, Kim et al. (2013)[144] reported that PKA inhibition led to YAP dephosphorylation and activation. Furthermore, they showed that PKA phosphorylated LATS1 and LATS2 *in vitro* and enhanced their activities. These findings were consistent with prior publications that described YAP phosphorylation and inhibition following activation of G_s-coupled receptors, which promote PKA activity.[142,144]

Therefore, our results suggest a SPINT2-PAR1/2-$G_{i/o}$ pathway that feeds into a potential PKA-LATS-YAP axis. We hypothesize that SPINT2 depletion results in $G_{i/o}$ activation and reduction of cellular cAMP, leading to PKA suppression, LATS dephosphorylation, and YAP activation. Approaches to address this hypothesis are discussed in Section 5.2.1.

2.3.3 Which proteases may be involved?

SPINT2 is a broad-spectrum serine protease inhibitor that suppresses the activation of PAR1 and PAR2 by endogenous proteases (Figure 2-9); there are approximately 230 known extracellular or transmembrane human serine proteases.[20,21] Therefore, it is unsurprising that knock-down of matriptase, one of the numerous well-characterized SPINT2 targets,[80,177] did not

rescue the effects of SPINT2 depletion on YAP target gene expression (Figure 2-8). Adding to this complexity is the myriad of thrombin-family and trypsin-family serine proteases that are capable of activating PAR1 and PAR2.[40]

In rare RPE-1 cells that overcome the G_1 cell cycle arrest induced by cytokinesis failure—which activates the Hippo pathway—*SPINT2* is downregulated,[178] consistent with SPINT2's crucial role in regulating YAP activity. Interestingly, transcriptome analysis reveals that *PLAT*, encoding tissue plasminogen activator (tPA), is among the genes most upregulated (personal communications with Prof. N. Ganem, Boston University, Boston, MA). Plasminogen activators are trypsin-like serine proteases that convert plasminogens into active plasmins, which are serine proteases known to regulate extracellular matrix degradation and turnover.[219] Notably, plasmin has been reported to induce the expression of *CYR61*, a YAP target gene.[220] In addition, urokinase plasminogen activator (uPA), another member of the plasminogen family, has been shown to be inhibited by SPINT2.[89] These results yield the hypothesis that the plasminogen activator/plasmin system may be involved in SPINT2-mediated suppression of YAP activity.

2.3.4 SPINT2 in the tumor microenvironment

SPINT2's well-known targets, such as extracellular proteases matriptase and uPA, are frequently deregulated in cancers.[48,221,222] Matriptase activates pro-HGF and contributes to tumor proliferation,[223] and has also been shown to activate PAR2.[224,225] uPA is often overexpressed in breast cancers,[226] and its downstream product plasmin induces migratory phenotypes via PAR1.[227]

Extracellular proteolysis plays key roles in the tumor microenvironment and modulates multiple malignant processes such as angiogenesis, tumor cell EMT, invasion, and metastasis.[46-48] Pericellular proteolysis at the tumor-stromal interface, for instance, is considered an important

initiating event in tumor cell migration and invasion, following tumor-stromal adhesion and tumor cytoskeletal reorganization.[46] Matrix metalloproteases (MMPs) are some of the most extensively investigated proteases in tumorigenesis.[48] MMPs are frequently found to be overexpressed in cancers, and may promote tumorigenesis by contact-dependent proteolytic remodeling of the extracellular matrix, enzymatic cleavage of cell-surface receptors or adhesion molecules, or activate pericellular growth factors.[46] Notably, certain MMPs are regulated by uPA.[228]

On the other hand, intracellular regulators that promote or maintain mesenchymal phenotypes are also crucial for microenvironment remodeling and tumor metastasis.[229] Notably, SPINT2 depletion induced epithelial-mesenchymal transition (EMT) gene expression signatures, including a transforming growth factor β (TGFβ) signature, in RPE-1 and HCT-116 cells (Figure 2-6 and Table 2-1). It is likely that this was a readout reflecting YAP and/or TAZ activation considering well-characterized roles of YAP/TAZ in EMT. TAZ, for instance, has been shown to interact with SMAD2/3-SMAD4 complexes (key effectors of TGFβ signaling) and to be required for TGFβ-induced SMAD nuclear localization and gene expression.[230] Recently, Diepenbruck et al. (2014)[231] and Hiemer et al. (2014)[232] further shed light on the critical roles of YAP/TAZ in modulating cellular EMT. In murine mammary gland and breast cancer cells, EMT induced by TGFβ correlated with nuclear redistribution of Yap/Taz. Knock-down of Tead transcription factors, well-characterized binding partners of Yap/Taz, blocked EMT and reduced Yap/Taz nuclear localization.[231] In human metastatic breast cancer cell line MDA-MB-231-LM2-4, YAP and TAZ are required for cell migration and invasion mediated by TGFβ.[232]

Taken together, these observations suggest that SPINT2, a membrane-resident protease inhibitor, may be part of a tumor suppressor network that regulates multiple facets of the tumor microenvironment including extracellular signal composition and cell-autonomous behaviors.

This is a plausible scenario especially considering SPINT2's documented role in enabling neural tube closure,[80] a developmental process that requires dynamic and delicate remodeling of the extracellular matrix as well as precise signaling control of cell migration and differentiation.[233]

In conclusion, this chapter has complemented prior reports on PAR-based regulation of the Hippo pathway and has added to our understanding of SPINT2's functions as a putative tumor suppressor. Results presented herein have informed refined hypotheses regarding potential regulation of the Hippo pathway by $G_{i/o}$ and PKA, as well as SPINT2's potential functions in modulating the extracellular environment.

2.4 Materials and Methods

Cell lines and culture conditions

RPE-1, HCT-116, MCF-10A, and HEK-293T cells were obtained from the American Type Culture Collection (ATCC), and expanded and stored per vendor instructions. RPE-1, HCT-116, and HEK-293T cells were cultured in phenol red-free DMEM/F12 media (Life Technologies) supplemented with 10% (v/v) fetal bovine serum (FBS; Life Technologies) and 1X Pen/Strep (Life Technologies 15140122). MCF-10A cells were cultured in phenol red-free DMEM/F12 with 5% (v/v) horse serum (Life Technologies), 1X Pen/Strep, 0.02 μg/ml mouse EGF (Sigma-Aldrich E4127), 0.5 μg/ml hydrocortisone (Sigma-Aldrich H0888), 10 μg/ml recombinant human insulin (Life Technologies 12585014), and 0.1 μg/ml cholera toxin (Sigma-Aldrich C8052). All cells were maintained in sterile incubators at 37°C and 5% CO_2.

Latrunculin A (LatA; Life Technologies L12370) or latrunculin B (LatB; Life Technologies L22290) treatment was carried out at the specified concentrations for 1 h with vehicle control (DMSO), using existing media in the plates to avoid adding fresh media to cells.

All experiments were performed at comparable cell densities.

RNAi reagents, immunoblotting, and antibodies

Small interfering RNAs (siRNAs) were obtained pre-made by GE Dharmacon or synthesized as duplex RNAs by Integrated DNA Technologies (Table 2-2). For siRNA transfection, cells were plated at 15–25% density in 6-well plates (2 ml Pen/Strep-free medium each well), and transfected with siRNAs using Lipofectamine RNAiMAX (Life Technologies 13778075) following manufacturer's protocol. Each well was transfected with 3–9 μl of stock siRNA (10 μM), incubated for 4–5 h, and switched to regular growth medium.

Table 2-2. siRNAs: sources, sequences, and references.

siRNA	Catalog #	Target sequence	Reference
Control	D-001810-10	ON-TARGETplus pool	-
SPINT2 (#1)	J-010216-06	GAAGACCACUCCAGCGAUA	-
SPINT2 (#2)	J-010216-07	GCUCAAAGGUGGUGGUUCU	-
SPINT2 (#3)	J-010216-08	GCAAUAAUUACCUGACCAA	-
SPINT2 (#4)	J-010216-09	CCUGCCAGCUGUUUGUGUA	-
LATS1	L-004632-00	ON-TARGETplus pool	-
LATS2	L-003865-00	ON-TARGETplus pool	-
YAP/TAZ (dual)	Synthesized	UGUGGAUGAGAUGGAUACA	[232]
PAR1	Synthesized	AGAUUAGUCUCCAUCAAUA	[61]
PAR2	Synthesized	GGAAGAAGCCUUAUUGGUA	[61]
PAR3	L-005491-00	ON-TARGETplus pool	-
PAR4	L-005492-03	ON-TARGETplus pool	-
G_{i1}/G_{i3} (dual)	Synthesized	CCGAAUGCAUGAAAGCAUG	[234]
G_o	Synthesized	CCUCCGAACCAGGGUCAAA	[234]
G_q	L-008562-00	ON-TARGETplus pool	-
G_{11}	L-010860-00	ON-TARGETplus pool	-
G_{12}	L-008435-00	ON-TARGETplus pool	-
G_{13}	L-009948-00	ON-TARGETplus pool	-
ST14 (Matriptase)	L-003712-00	ON-TARGETplus pool	-
MET	L-003156-00	ON-TARGETplus pool	-

Short hairpin RNAs (shRNAs), shSPINT2-resistant ORF, and CRISPR single-guide RNAs (sgRNAs) are listed in Table 2-3. shRNAs (pLKO.1 backbone)[235] were obtained from the RNAi Consortium via Sigma-Aldrich. The shSPINT2-resistant ORF was synthesized by Integrated DNA Technologies. sgRNAs (lentiCRISPRv2 backbone)[236] were obtained from the Genome Engineering Production Group at Harvard Medical School.

Table 2-3. shRNAs, rescue construct, and sgRNAs.

shRNA	Catalog #	Target sequence	Notes
shLuc (luciferase)	TRCN0000072253	ACACTCGGATATTTGATATGT	-
shSPINT2	TRCN0000073578	CTCCTGCAATAACTTCATCTA	-
shSPINT2-resistant ORF	Synthesized	Mutated sequence: tagtTGtAAcAAtTTCATaTA	Partial ORF shown; compare to shRNA
shSPINT2#2	TRCN0000073582	CCAGCAGGAATGCAGCGGATT	-
shLATS2	TRCN0000000880	CCGTCGATTACTTCACTTGAA	-
CRISPR_GFP	Pre-made	GGGCGAGGAGCTGTTCACCG	-
CRISPR_SPINT2	Pre-made	GGCCCCTCTCTCGTCCTCAG	-

Plasmid vectors, cloning, and viruses

SPINT2 overexpression was achieved by transfecting cells with the pCMV6-FLAG-SPINT2 vector (OriGene RC202044) using Lipofectamine 2000 (Life Technologies 11668019).

The HCT-116 shSPINT2 rescue cell line was made using cumate-inducible expression of shSPINT2-resistant ORF in the shSPINT2 background. Cells expressing the cumate repressor at low titer (~1 MOI) were made by viral transduction of the pCDH-EF1-CymR-T2A-Puro vector (System Biosciences QM200PA-2). shSPINT2-resistant ORF was cloned into the cumate promoter/T2A-RFP co-expression vector pCDH-CuO-MCS-T2A-RFP (System Biosciences QM522A) using XbaI (5') and NotI (3') restriction enzymes followed by T4 ligation (New England Biolabs). The stop codon of the SPINT2 ORF (TGA) was mutated to Glycine (GGA) to allow for the continued translation of the T2A-RFP self-cleaving marker. Experiments and validations were performed based on manufacturers' protocols. shRNA-resistant SPINT2 expression (as evidenced by co-expression of RFP) was able to restore total SPINT2 to wild-type level without cumate induction due to low titer of the CymR repressor.

For lentivirus production, 80–90% confluent HEK-293T cells were co-transfected with 6 μg construct, 4.5 μg psPAX2 (Addgene), and 1.5 μg pMD2.G (Addgene) using Lipofectamine 2000 in 8 ml Pen/Strep-free DMEM/F12 medium (with 10% FBS) per 10-cm plate. Viral media were harvested 24 h to 72 h post-transfection, and were filtered with Steriflip 0.22 μm PVDF (EMD Millipore SE1M179M6). To generate stable cell lines, viral infection was carried out by incubating 200,000 cells per well (6-well plate) in 2 ml viral medium with 8 μg/ml polybrene (Thermo Fisher Scientific NC9515805) for 24 h. Transduced/infected cells were given 24 h to recover, and were then maintained in puromycin (Sigma-Aldrich P7255; 1.5 μg/ml used for HCT-116 and MCF-10A; 5 μg/ml used for RPE-1) for at least 5 days to achieve effective antibiotic

selection. Cells with fluorescent markers were enriched by fluorescence-activated cell sorting (FACS) at least twice for positive cells.

The shTP53 MCF-10A cell line (Figure 2-11A) was constructed and validated by Susana Godinho in our lab.[198]

Confocal and light microscopy

Immunofluorescence staining was performed as follows: cells were plated and treated with specified conditions in 12-well plates with sterile #1.5 round glass coverslips (Warner Instruments 64-0714). For HCT-116 cells, coverslips were pre-coated with poly-D-lysine (Sigma-Aldrich P7280) to enhance cell attachment; briefly, coverslips were incubated with 15 μg/ml poly-D-lysine in PBS for 20 min at room temperature, and washed 3 times with PBS. When ready for imaging, cells were washed with PBS and were then fixed for 20 min in 2 ml 4% paraformaldehyde (Electron Microscopy Sciences NM15700) at room temperature. After, samples were washed 3 times with PBS, and were permeabilized using 0.5% (v/v) Triton X-100 (Thermo Fisher Scientific NC9160286) in PBS for 5 min. Samples were subsequently blocked in 3% (w/v) BSA in PBS for 30 min, followed by incubation with primary antibodies in 3% BSA/PBS for 1 h at room temperature. Primary antibodies were washed away using 0.05% Triton X-100 in PBS for 3 times (each 5 min). Secondary antibody incubation was performed in 3% BSA/PBS protected from light for 45 min at room temperature and washed using 0.05% Triton X-100 in PBS for 3 times (each 5 min). For nuclear counter-staining, cells were incubated with Hoechst 33342 (Cell Signaling Technology 4082S) at 1:2,500 dilution in PBS for 10 min. Samples were mounted using ProLong Gold antifade reagent (Life Technologies P36930).

Primary antibody with dual-specificity against YAP/TAZ (Santa Cruz Biotechnology sc-101199) was used at 1:200 dilution; secondary antibody (goat anti-mouse IgG cross-adsorbed-Alexa Fluor 488, Molecular Probes A-11001) was used at 1:1,000 dilution.

Fluorescence confocal and light microscopy was conducted using an Eclipse Ti-E inverted microscope (Nikon). For fluorescence imaging, laser excitation of the fluorophores was performed sequentially using the 405 nm and 488 nm lasers. Signals acquired from the 405 nm laser were pseudo-colored blue for presentation; 488 nm, pseudo-colored red. Images were collected using a 60X Plan Apo NA 1.4 oil objective (Nikon) with a CoolSnapHQ2 CCD camera (Photometrics). Image quantification was performed using ImageJ (National Institutes of Health). Bright-field (phase-contrast) images of crystal violet staining was acquired using a 20X Plan Fluor NA 0.5 objective (Nikon).

Microarray and Gene Set Enrichment Analysis (GSEA)

Microarray data of SPINT2-depleted cells were generated at the Dana-Farber Cancer Institute Molecular Biology Core. RNA from RPE-1 and HCT-116 cells treated with siRNAs (48 h) was extracted using RNeasy Plus (Qiagen 74134) and each sample was quantified using a NanoDrop 3300 spectrophotometer (Thermo Fisher Scientific) to ensure proper 260/280 and 260/230 absorbance ratios. Transcriptomes were profiled using the Human Genome U133+ 2.0 microarray (Affymetrix) and analyzed using Affymetrix Expression Console. Normalized linear data were clustered by Morpheus (Broad Institute) by row and column with default parameters.

GSEA (Broad Institute) was performed by defining two phenotypic classes: siSPINT2 and siCtrl. Triplicates of siSPINT2#2 and siSPINT2#3 were pooled as the “siSPINT2” class and compared to triplicates of siCtrl. Gene sets tested included the two custom gene sets (YAP-5SA

and TAZ-4SA; see below), the Hallmark collection (H; 50 gene sets) and the Oncogenic Signatures collection (C6; 189 gene sets), resulting a total of 241 gene sets. Due to the limited sample size (<7 per phenotypic class), gene set permutation was used (1000 permutations).

The custom YAP-5SA and TAZ-4SA gene sets were generated by virally transducing RPE-1 cells using pBABE-Puro_YAP-5SA and pLVX-Puro_TAZ-4SA vectors, with cells transduced with the empty pBABE-Puro vector as control. After selection, cells were grown to 70% confluency, and RNA was extracted as described above. Microarray analysis was performed using the Human Gene 2.0 ST microarray (Affymetrix) at Boston University. The top 300 upregulated genes from each cell line were selected as YAP-5SA and TAZ-4SA gene sets.

Quantitative PCR (qPCR) and immunoblotting

Equal amounts of RNA were reverse-transcribed into cDNA using the SuperScript III Reverse Transcriptase kit (Life Technologies 18080093) each experiment. qPCR was performed using Power SYBR Green Master Mix (Thermo Fisher Scientific 4367659) and measured with a ViiA 7 Real-Time PCR system (Thermo Fisher Scientific) in triplicates (96-well format) following manufacturers' protocols. All measurements were normalized against *ACTB* (β-actin) transcripts. qPCR primers are listed in Table 2-4.

Immunoblotting was performed following standard RIPA buffer-based (EDTA-free, with protease and phosphatase inhibitors) protocols except for SPINT2, LATS1/2, and phospho-LATS. Unless otherwise stated, cells were lysed at 4°C using RIPA buffer (Boston BioProducts BP-115); protein samples were denatured and reduced at 100°C for 5 min using Laemmli SDS Sample Buffer (Boston BioProducts BP-110R), and separated using NuPAGE 4–12% Bis-Tris Protein Gels (Life Technologies NP0321) with the NuPAGE MOPS-SDS Running Buffer (Life

Technologies NP0001). Transfer was performed using Trans-Blot (Bio-Rad) or iBlot 2 (Life Technologies) devices, and membranes were blocked for at least 1 h using 5% (w/v) bovine serum albumin (BSA) in 1X TBST (1X TBS buffer with 0.05% v/v Tween-20). Membranes were subsequently incubated with primary antibodies in 2% BSA in TBST at 4°C overnight. Blots were then washed extensively using TBST (at least 3 times; 20 min each) and incubated with secondary antibodies with 2% BSA/TBST for 1 h at room temperature. Signals were developed using ECL Prime reagents (GE Healthcare RPN2232), and images were acquired by ImageQuant LAS4000 (GE Healthcare). Image quantification was performed using ImageJ (National Institutes of Health).

Table 2-4. qPCR primers: SPINT2, YAP targets, and candidate-based screen validation.

Target	Forward sequence (5'-3')	Reverse sequence (5'-3')
ACTB	GCGAGAAGATGACCCAGAT	CCAGTGGTACGGCCAGA
SPINT2	TCTGAGGAGGCCTGCAT	TCAACACCATCACGAACAGC
CTGF	GCTCGGTATGTCTTCATGCTG	GAAGCTGACCTGGAAGAGAAC
CYR61	GGGATTTCTTGGTCTTGCTG	CCAATGACAACCCTGAGTGC
EDN1	AAGTAAATTCTCCAAGGCTCTCT	GTGTCTACTTCTGCCACCTG
YAP1 (YAP)	CACCTGTATCCATCTCATCCAC	ACGACCAATAGCTCAGATCCT
TAZ	TCCTTGGTGAAGCAGATGTC	CCAATCACCAGTCCTGCAT
LATS1	ATGATAGGCCACACTTTCTCC	CTGCCAGACCTATTAATGCCA
LATS2	GTCCGTTTCTGTAGTCCGTATG	GTGGGCAGTCTGTCAGTAAA
F2R (PAR1)	GGCCAGACAAGTGAAGGAA	CGCCTCTATCTTGCTCATGAC
F2RL1 (PAR2)	CGTTCTTTGCATGATCCCTGA	GCCATGTCTATGCCCTGTA
F2RL2 (PAR3)	AGGTCTTAATGGGTAAGGTTGG	GACTCAGGTCATCAAAATGAAAGC
F2RL3 (PAR4)	TGTCATTGGCACAGACTTGG	GGGTTCAGCCTGTCTGG
GNAI1 (G_{i1})	GCTGCTGAAGAAGGCTTTATG	GTACTCTCGGGATCTGTTGAAA
GNAO1 (G_o)	CACCATTGTGAAGCAGATGAAG	GGACTGGATAGTGTTGCTGTAG
GNAQ (G_q)	GCCACAGACACCGAGAATATC	GGTGTCTAGGAGGCACAATTAG
GNA11 (G_{11})	CTGACGTACTGATGCTCGAAG	GACGCTCAAGATCCTCTACAAG
GNA12 (G_{12})	GAAGTCATGCTCCACAATTCC	GTACTTCCTGGACAACTTGGA
GNA13 (G_{13})	GTTGTTGGTTTGAGTTGTCTCC	CACCATCTACAGCAACGTGA
ST14	CAGCAGGTAGAAGAATTTGAAGC	ACTACCCACCCAACATTGAC
MET	AAATGTGTCGCTCCGTATCC	GCACTATGATGTCTCCCAGAAG

For detection of endogenous SPINT2, RIPA-extracted cell lysates were concentrated 5–10X using the Amicon Ultra 3 kDa filter units (EMD Millipore UFC500324) following manufacturer's instructions at 4°C using a bench-top microcentrifuge. Electrophoresis (NuPAGE 4–12% gels) was run at ≤70V, and gels were loaded with samples of similar concentrations to minimize lane/band distortion.

Detection of LATS1/2 and phospho-LATS1/2 was achieved under the following conditions. Lysis buffer: 50 mM Tris-HCl pH8.0; 2% (w/v) SDS; 10% (v/v) glycerol; in ddH_2O. Cells were mixed with 100 µl lysis buffer, detached by cell scrapers, and sonicated at 20% power for 20 seconds on ice. Lysates were denatured using the Laemmli SDS Sample Buffer (100°C, 5 min) and run on 7.5% SDS-PAGE protein gels. Transfer buffer: 50 mM Tris; 40 mM glycine; 10% (v/v) methanol; in ddH_2O. Blocking was carried out at 5% (w/v) milk in 1X TBS with 0.1% v/v Tween-20. Antibody incubation was performed using 1% milk in 0.1% Tween-20/1X TBS (primary, 4°C overnight; secondary, room temperature 1.5 h).

Primary antibodies and dilution for blots: Vinculin (1:400, Sigma-Aldrich V9131); GAPDH (1:5,000, Cell Signaling Technology 2118); SPINT2 (1:800, R&D Systems AF1106); YAP/TAZ (1:200, Santa Cruz Biotechnology sc-101199); phospho-YAP S127 (1:2,000, Cell Signaling Technology 4911); phospho-YAP S397 (Cell Signaling Technology 13619); LATS1 (1:1,000, Cell Signaling Technology 3477); LATS2 (1:1,000, Cell Signaling Technology 13646); phospho-LATS (1:500, Cell Signaling Technology 8654 [detects both pLATS1 and pLATS2]); FLAG/DDK (1:1,000, OriGene TA50011).

Secondary antibodies and dilution for blots: ECL anti-mouse IgG-HRP (1:8,000, GE Healthcare NXA931); ECL anti-rabbit IgG-HRP (1:8,000, GE Healthcare NA9340); anti-goat IgG-HRP (1:5,000, Santa Cruz Biotechnology sc-2354).

PAR cleavage assay and alkaline phosphatase (AP) measurement

HCT-116 cells with described genetic backgrounds were plated at 1.5×10^6/well density in 6-well plates. Duplicate plates were made to allow for cell counting at each time point. pcDNA3-AP-PAR1 and pcDNA3-AP-PAR2 (kind gift from Sylvain Le Gall in Prof. E. Camerer's lab at INSERM, Paris, France)[237] were transfected at 0.5 μg/well using Lipofectamine 2000. pCMV6-FLAG-SPINT2 (OriGene RC202044) and control (pCMV-mCherry; Addgene) were transfected at 1.5 μg/well. Transfection was carried out overnight, and cells were given another 24 h to recover and express transfected ORFs. Subsequently, cells were washed twice with PBS and once with serum-free growth media (10 min each wash). Cells were then incubated in 2.5 ml fresh serum-free media and these media were sampled at 3 time points: 1 h, 4h, and 20 h. In parallel, cell numbers were acquired using a Vi-Cell counter (Beckman Coulter). AP concentration in each sample's medium was measured using the SensoLyte Luminescent AP Assay Kit (AnaSpec AS-72122) per manufacturer's protocol. Luminescence was measured by a FLUOstar Omega plate reader (BMG LABTECH). Values from buffer-only wells were subtracted, and luminescence per million cells was normalized against control samples.

Surveyor assay

Genomic DNA from CRISPR_GFP, CRISPR_SPINT2, and wild-type cells was isolated using the DNeasy Blood and Tissue Kit (Qiagen 69504). CRISPR_SPINT2 sgRNA target locus (and flanking areas) was amplified by Phusion high-fidelity PCR polymerase (New England Biolabs M0530) using the forward primer 5'-GCTCTCAGCCCTCCCAGC-3' and the reverse primer 5'-CCCCAGTCCTCTTGGCGAC-3'. Amplified DNA fragments were analyzed using the Surveyor Mutation Detection Kit (Integrated DNA Technologies 706025) following manufacturer's

instructions. Briefly, an equal amount of DNA from CRISPR_GFP or CRISPR_SPINT2 was hybridized with the wild-type reference fragment, and digested with the Surveyor nuclease (cleaves mismatched DNA duplexes). The digestion products were separated using standard DNA agarose gel electrophoresis, stained with ethidium bromide, and imaged using a ChemiDoc XRS transilluminator (Bio-Rad).

Soft agar assay

Agar underlays in 6-well plates were created using 0.5% low-gelling temperature agarose (Sigma-Aldrich A4018) melted in PBS (2 ml each well), solidified at 4°C, and warmed to 37°C. Overlays, each with 50,000 MCF-10A cells of the specified genetic background, were created by resuspending cells in 4% melted agarose in 37°C growth media. Liquid overlays were gently pipetted atop underlays and incubated at 4°C for 15–20 min for solidification. The resultant soft agars were incubated at 37°C for up to 42 days, with addition of growth media twice/week.

Each sample was fixed and stained using crystal violet at the endpoint, and imaged using phase-contrast light microscopy. Briefly, colonies were simultaneously fixed and stained using PBS containing 0.05% (w/v) crystal violet (Sigma-Aldrich C3886), 1% (v/v) formaldehyde (Sigma-Aldrich F8775), and 1% (v/v) methanol, for 20 min at room temperature. Samples were washed with PBS twice (5 min each), and air-dried prior to imaging.

Statistical analysis

Student's *t*-tests (two-sample assuming unequal variances, two-tail) were performed using Microsoft Excel unless stated otherwise. Statistical significance was defined as $p<0.05$.

2.5 Chapter Contributions

I have enjoyed the greatly enriching collaboration with Prof. Neil Ganem's group (Boston University School of Medicine, Boston, MA): Kristyna Kotynkova contributed Figure 2-5 and respective methods; Ryan Quinton provided the custom YAP-5SA and TAZ-4SA gene sets analyzed in Figure 2-6 and Table 2-1, and respective methods; and Sanghee Lim offered important insights on the experimental methods used in Figure 2-4C.

I thank my colleague Selwin Wu for constructive comments on this chapter.

Chapter 3 : Elevation of Cellular Tolerance for Aneuploidy Following SPINT2 Depletion

Summary

I demonstrate that SPINT2 loss is linked to the survival of aneuploid cells; specifically, aneuploid RPE-1 cells epigenetically silence *SPINT2* gene expression via promoter methylation, and SPINT2 depletion in HCT-116 cells leads to persistent aneuploidy after chromosome missegregation. I then discuss potential mechanisms contributing to these phenotypes.

3.1 Introduction

Genome instability, defined as continued alterations of sequence or dosage information within the genome, is a hallmark of cancer and is widely considered an "enabling characteristic" that promote tumorigenesis.[9,238]

Chromosome instability (CIN) refers to an increased rate of chromosome missegregation, and is a form of genome instability that leads to the loss of structural or numerical integrity of the chromosome complement.[239-242] The altered numerical composition of chromosomes, or aneuploidy, is prevalent in cancer: nearly all solid tumors and half of hematopoietic cancers exhibit varying degrees of aneuploidy.[148-151] Moreover, 37% of cancers show signs of whole-genome duplication, which correlate with increased rates of somatic copy number alterations.[243] These observations highlight the role of CIN and the consequent ploidy alterations in driving tumor karyotype evolution.

It is important to note that, while related to CIN, aneuploidy is a distinct term representing the cellular state of lacking a euploid chromosome complement (multiples of a haploid set of chromosomes).[147,244] For instance, an aneuploid cell may result from a rare missegregation event, but may continue to proliferate without CIN.

Interestingly, aneuploid primary cells generally have poor proliferative capacity, unlike aneuploid tumor cells.[168] Mechanisms that limit aneuploidy in normal somatic tissues and tumorigenic roles of aneuploidy in cancer cells remain partially understood .[159,161] Recently, aneuploidy has been shown to induce defects in autophagy and proteasomal functions,[171,245,246] as well as features of senescence in non-transformed human cells.[247] On the other hand, aneuploidy is correlated with evasion from immune surveillance[248] and contributes to karyotype heterogeneity in human tumors.[173] Considering the stark contrast between the physiological consequences of

aneuploidy in normal somatic tissues and tumors, it is crucial to investigate cellular mechanisms that allow cells to tolerate aneuploidy, especially in the context of tumor development.

In this chapter, I demonstrate that *SPINT2*, encoding a putative tumor suppressor, is epigenetically silenced in cells with a variety of aneuploidies. I further show that SPINT2 depletion allows aneuploid cells to persist in the population, potentially contributing to karyotype heterogeneity. Combined with Chapter 2, these results illustrate SPINT2's roles in regulating multiple tumorigenic characteristics of the cell. My findings raise the interesting possibility that cellular tolerance for aneuploidy may be a built-in component of oncogenic signaling, and inform future lines of work to test this hypothesis.

3.2 Results

3.2.1 SPINT2 is epigenetically silenced in aneuploid cells

Tetraploid cells, resulting from cytokinesis failure or cell fusion, are thought to promote aneuploidy in cell populations.[178,242] In 2014, Ganem and colleagues[178] reported that SPINT2 is required in RPE-1 cells for the G_1 cell cycle arrest following cytokinesis failure and is downregulated in rare tetraploid cells that continue to proliferate after aborted cytokinesis. Similar observations were made in HCT-116 cells (personal communications with Prof. Z. Storchova, University of Kaiserslautern, Kaiserslautern, Germany). Interestingly, while many proliferating tetraploid RPE-1 cells possess completely tetraploid chromosome complements,[178] I found that some have accrued extra copies of chromosome 12 as measured by chromosome fluorescent *in situ* hybridization (FISH) (Figure 3-1). These findings are consistent with prior observations that trisomy-12 cells tend to arise in diploid RPE-1 populations during routine passaging (possibly due to a heterozygous *KRAS* activating mutation on chromosome 12).[249-251]

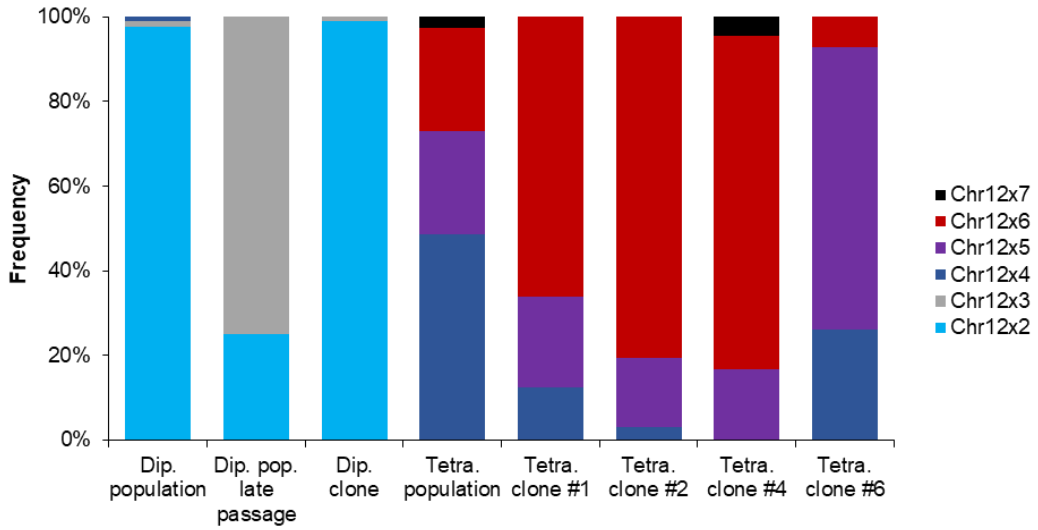

Figure 3-1. Proliferating tetraploid RPE-1 cells accrue chromosome 12 aneuploidy.

FISH scoring of chromosome 12 copy numbers in various RPE-1 cell lines. Dip., diploid; Tetra., proliferating tetraploid. Dip. clone underwent the identical cloning procedure as Tetra. clones. 200 cells were scored in each sample.

In light of these observations, I hypothesized that SPINT2 downregulation is a common feature associated with aneuploidy. To test this hypothesis, my colleagues David Gordon and Hubo Li and I took advantage of the spontaneous chromosome 12 gain in RPE-1 cells and microcell-mediated chromosome transfer (MMCT; a technique for generating defined aneuploidies),[252,253] and created a collection of 10 proliferating RPE-1 cell lines with aneuploidies of chromosomes 8, 12, and 21 (Table 3-1).

Table 3-1. Summary of aneuploid RPE-1 cell lines.

Cell line	Specific aneuploidy	Ploidy of parent cell line (control)	Generated by
#74	Chromosome 8, 4 copies	Diploid	MMCT
#304	Chromosome 8, 3 copies	Diploid	MMCT
#312	Chromosome 8, 3 copies	Diploid	MMCT
#B1	Chromosome 12, 3 copies	Diploid	Single-cell sorting
#E3	Chromosome 12, 3 copies	Diploid	Single-cell sorting
Tetra#4	Chromosome 12, 6 copies	Tetraploid	Single-cell sorting
Tetra#6	Chromosome 12, 5 copies	Tetraploid	Single-cell sorting
#2	Chromosome 21, 3 copies	Diploid	MMCT
#3	Chromosome 21, 3 copies	Diploid	MMCT
#7	Chromosome 21, 4 copies	Diploid	MMCT

Parental cell lines underwent identical experimental procedures and were used as isogenic controls. Each aneuploid cell line was validated using karyotyping, single-nucleotide polymorphism (SNP) array, or chromosome FISH (Figure 3-2).

Consistent with my hypothesis, I found that *SPINT2* mRNA was significant downregulated in all aneuploid cell lines compared to diploid controls that underwent mock MMCT (not shown) or single-cell sorting (Figure 3-3A), suggesting that *SPINT2* suppression is generally linked to continued proliferation of aneuploid cells regardless of the specific aneuploid chromosome.

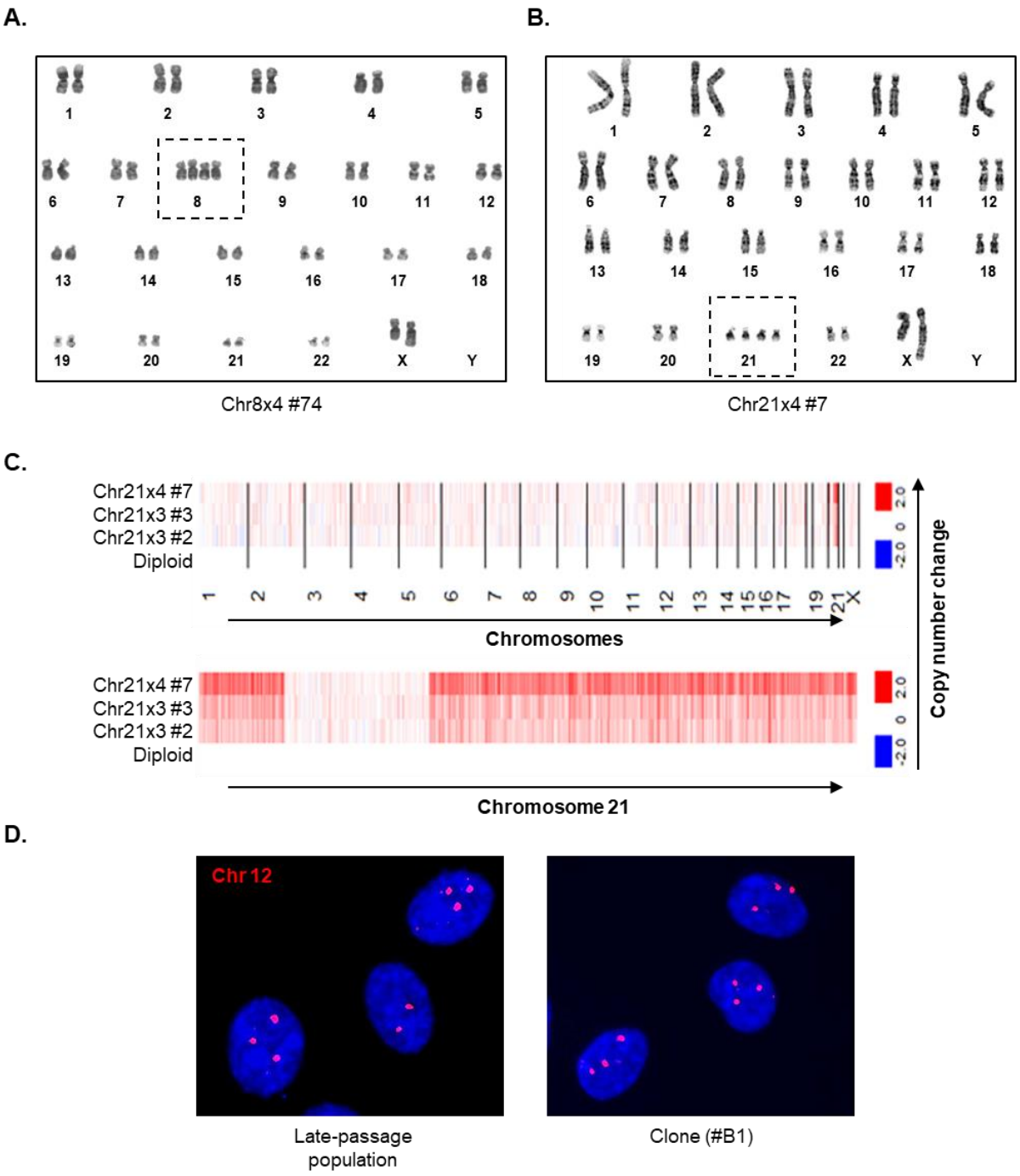

Figure 3-2. Validation of aneuploid RPE-1 cells by karyotyping, SNP array, or chromosome FISH.

Examples of karyotype validation of tetrasomy-8 (**A**) and tetrasomy-21 (**B**) cell lines. **C**. SNP array comparing trisomy- and tetrasomy-21 cell lines with diploid control, with whole-genome and chromosome 21-specific views. **D**. Chromosome FISH validation of trisomy-12 cells, with Hoechst nuclear counter-stain shown in blue.

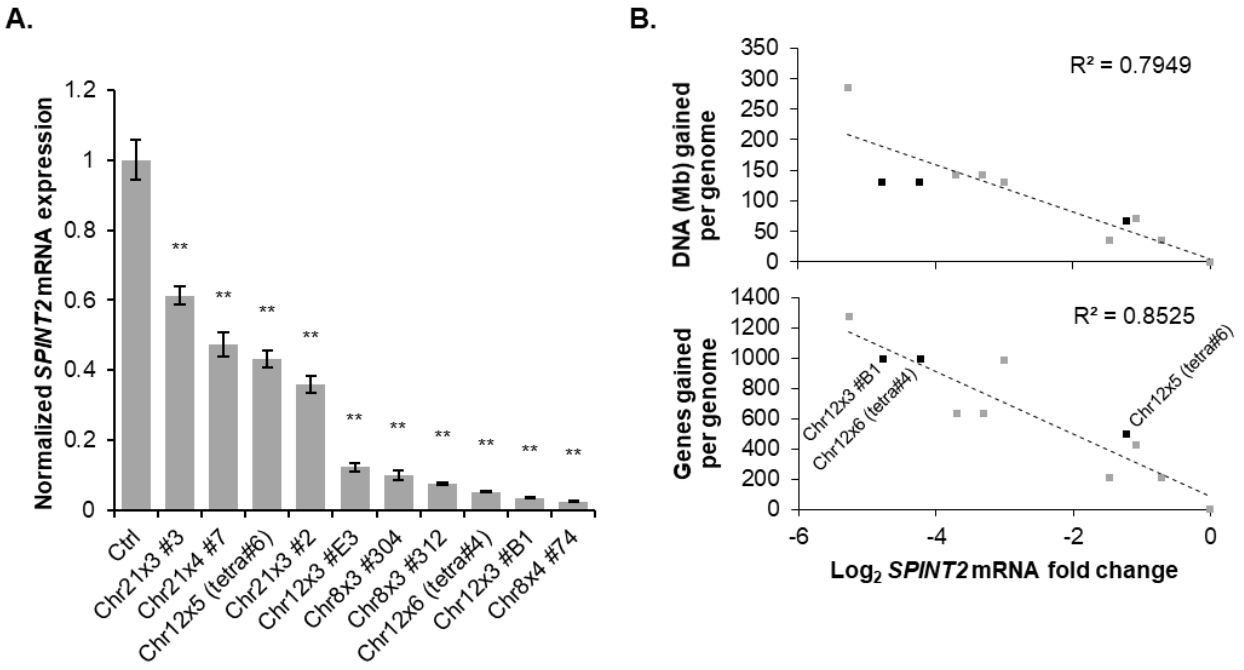

Figure 3-3. *SPINT2* is downregulated in proliferating aneuploid RPE-1 cells.

A. qPCR measurement of *SPINT2* mRNA in aneuploid RPE-1 cells. **B**. Correlation between per-genome gain of genetic material and *SPINT2* downregulation in aneuploid cells. Example cell lines are marked, and annotated in the lower panel. Error bars, SD (n=3). **, $p<0.01$, *t*-test.

It has been proposed that aneuploidy causes a decrease in cellular fitness due to the dosage gain or loss of gene products associated with aneuploid chromosomes.[168,254] In other words, perturbations to stoichiometric ratios within the proteome are responsible for the common cellular stress response to aneuploidy.[168] It is expected that the magnitude of cellular stress response to aneuploidy correlates with the level of per-genome dosage imbalance of protein-coding genes caused by each specific aneuploidy. For example, Torres et al. (2007)[162] reported that the G_1 cell cycle delay caused by chromosome gains in haploid yeast cells was longer in strains with gains of larger chromosomes or multiple copies of the same chromosome. In addition, diploid-derived yeast cells carrying one extra chromosome appear to be more stress-tolerant compared to haploid-derived cells that are disomic for the same chromosome.[239]

Consistent with this model, tetraploidy represents an aneuploidy-tolerating condition due to a larger pre-existing "genomic buffer."[168] Strikingly, when parental cell ploidy is taken into account, the degree of *SPINT2* downregulation showed a strong correlation with the per-genome gain of genetic material in each aneuploid cell line (Figure 3-3B). These correlations suggest that *SPINT2* downregulation scales with the stress induced by each aneuploidy and implicate a direct role of *SPINT2* in regulating the fitness of aneuploid cells.

Considering the wide-spread silencing of *SPINT2* by promoter hypermethylation in cancers,[94-100] I asked whether aneuploid RPE-1 cells recapitulated this tumor phenotype. Using the DNA-demethylating agent 5-aza-2-deoxycytidine (5-AdC), I detected dramatic upregulation of *SPINT2* mRNA in aneuploid cells (Figure 3-4A), indicating epigenetic silencing of *SPINT2* via promoter hypermethylation.

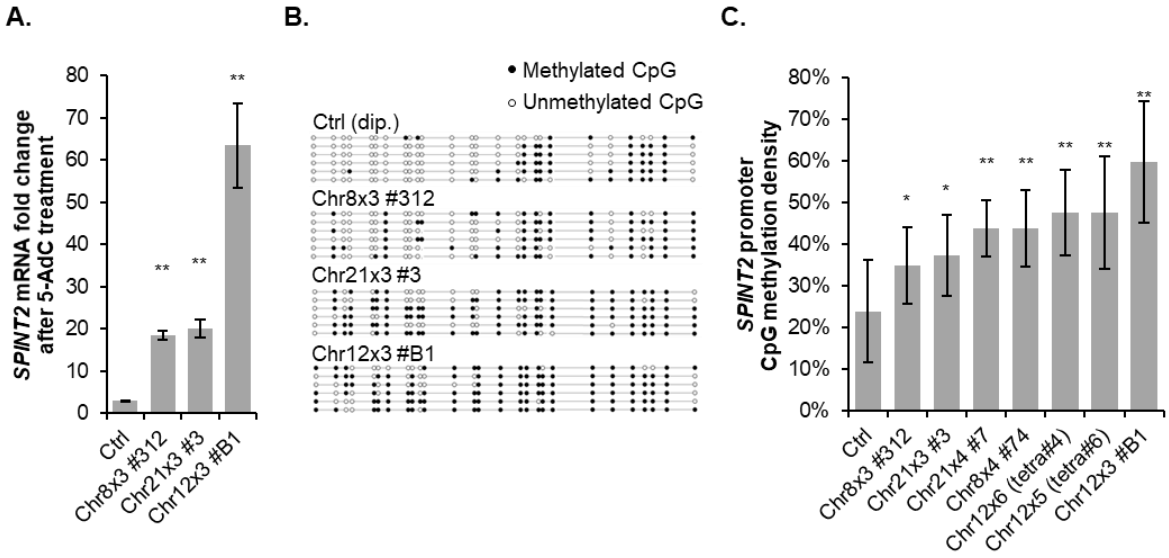

Figure 3-4. *SPINT2* is downregulated in aneuploid RPE-1 via promoter hypermethylation.

A. *SPINT2* mRNA expression following 5-AdC treatment (10 μM, 48 h). **B**. Examples of *SPINT2* promoter CpG methylation (6 fragments of a promoter sub-region shown). **C**. *SPINT2* promoter methylation density in aneuploid RPE-1 cells. 72 out of 88 predicted CpGs were tested. Error bars, SD (n=3 for A; n=10 for C). *, $p<0.05$; **, $p<0.01$, *t*-test.

Next, I performed bisulfite sequencing to detect specific CpG methylation within the *SPINT2* promoter. Bisulfite treatment converts unmethylated cytosine residues into uracils but leaves methylated cytosines (5-methylcytosines) intact.[255] On average, aneuploid cells harbored at least 11–26% more methylated CpGs within the *SPINT2* promoter compared to controls, which averaged at 24% (Figure 3-4C). Consistent with these findings, knock-down of DNA methyltransferase 1 (DNMT1), known to maintain DNA methylation,[256] resulted in upregulation of *SPINT2* mRNA in trisomy-12 RPE-1 cells (Figure 3-5A).

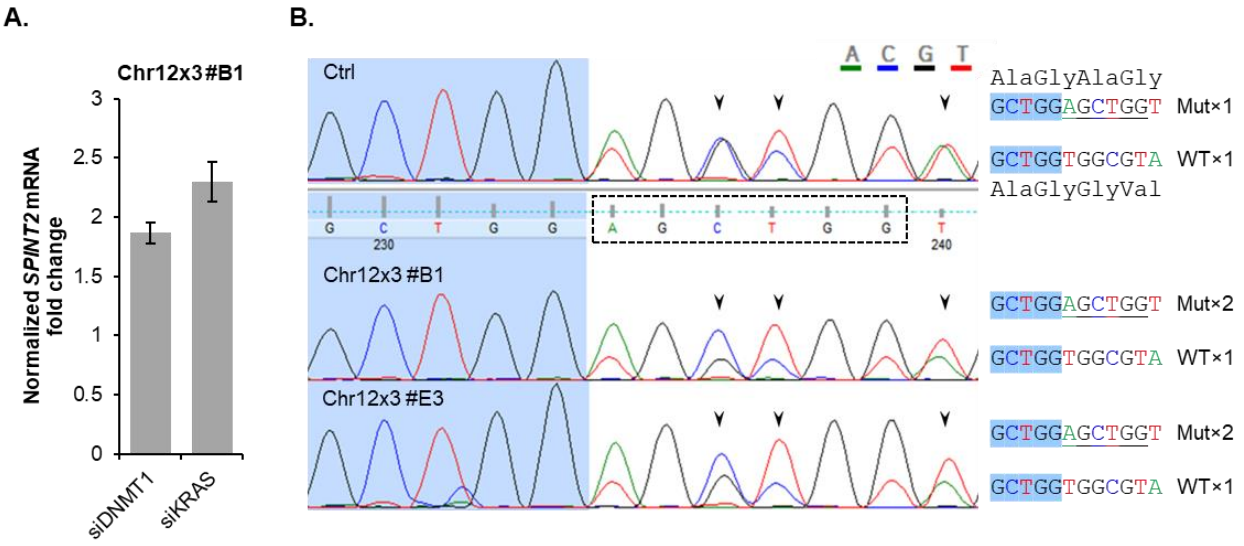

Figure 3-5. Epigenetic silencing of *SPINT2* in aneuploid RPE-1 cells may involve both DNMT1 and KRAS.

A. qPCR measurement of *SPINT2* mRNA following DNMT1 or KRAS knock-down. **B**. Sanger sequencing chromatograms indicating copies of mutant (Mut) *KRAS* in trisomy-12 vs. diploid RPE-1 cells. Mutated sequence is circled by dashed line in the chromatogram or underlined in the text on the right. Arrow heads, sequencing peaks indicating copy gain. Error bars, SD (n=3).

Recently, Serra and colleagues (2014)[257] reported that KRAS, a Ras family proto-oncogene, mediates a methylation-based transcriptional silencing mechanisms through DNMT1 and ZNF304 (a zinc-finger protein) in certain human colorectal cancer cells. Considering RPE-1 cells' putative tendency to accrue extra copies of chromosome 12 harboring the activating *KRAS*$^{G12\_G13insAG}$

mutation[249-251] and the associated silencing of *SPINT2* (Figure 3-3A, Figure 3-4), it is intriguing to consider whether KRAS may play a role in mediating *SPINT2* silencing. Indeed, KRAS depletion by siRNA resulted in *SPINT2* upregulation in trisomy-12 cells (Figure 3-5A). Additionally, I performed Sanger sequencing of genomic DNA from two independent trisomy-12 RPE-1 clones (#B1 and #E3) and obtained data confirming their postulated preferential gain of the chromosome 12 copy with the $KRAS^{G12\_G13insAG}$ allele (Figure 3-5B).

In summary, these results have revealed that aneuploid RPE-1 cells recapitulates the epigenetic silencing of *SPINT2* in human tumors, and have implicated the role of *SPINT2* silencing in facilitating the proliferation of aneuploid cells.

3.2.2 SPINT2 depletion confers heightened tolerance for aneuploidy

To test whether SPINT2 depletion would directly allow cells to tolerate aneuploidy, I experimentally induced chromosome missegregation in HCT-116 cells using monastrol, an inhibitor of KIF11 (also known as Eg5, a mitotic kinesin), and AZ3146, an inhibitor of TTK (also known as Mps1, a critical kinase regulating the spindle assembly checkpoint).[171,258]

HCT-116 cell lines with shSPINT2 plus or minus the shRNA-resistant ORF (described in Section 2.2.3; controls for RNAi specificity), as well as with biallelic *TP53* knock-out (kind gift from Prof. B. Vogelstein at Johns Hopkins University, Baltimore, MD), were subjected to drug treatments. Specifically, after an eight-hour incubation in monastrol (100 μM), mitotic cells were isolated by shake-off, thoroughly washed, and re-plated. For AZ3146 treatment, cells were incubated with AZ3146 (2 μM) for 24 hours and washed thoroughly. Cells were fixed at day 2 and day 6 following removal of each drug, and levels of aneuploidy were measured by chromosome FISH of two arbitrary chromosomes (chromosomes 7 and 12).

As shown in Figure 3-6, SPINT2-depleted cells had higher levels of persistent aneuploidy (Figure 3-6A), as measured by deviation from modal chromosome numbers (Figure 3-6B–C).

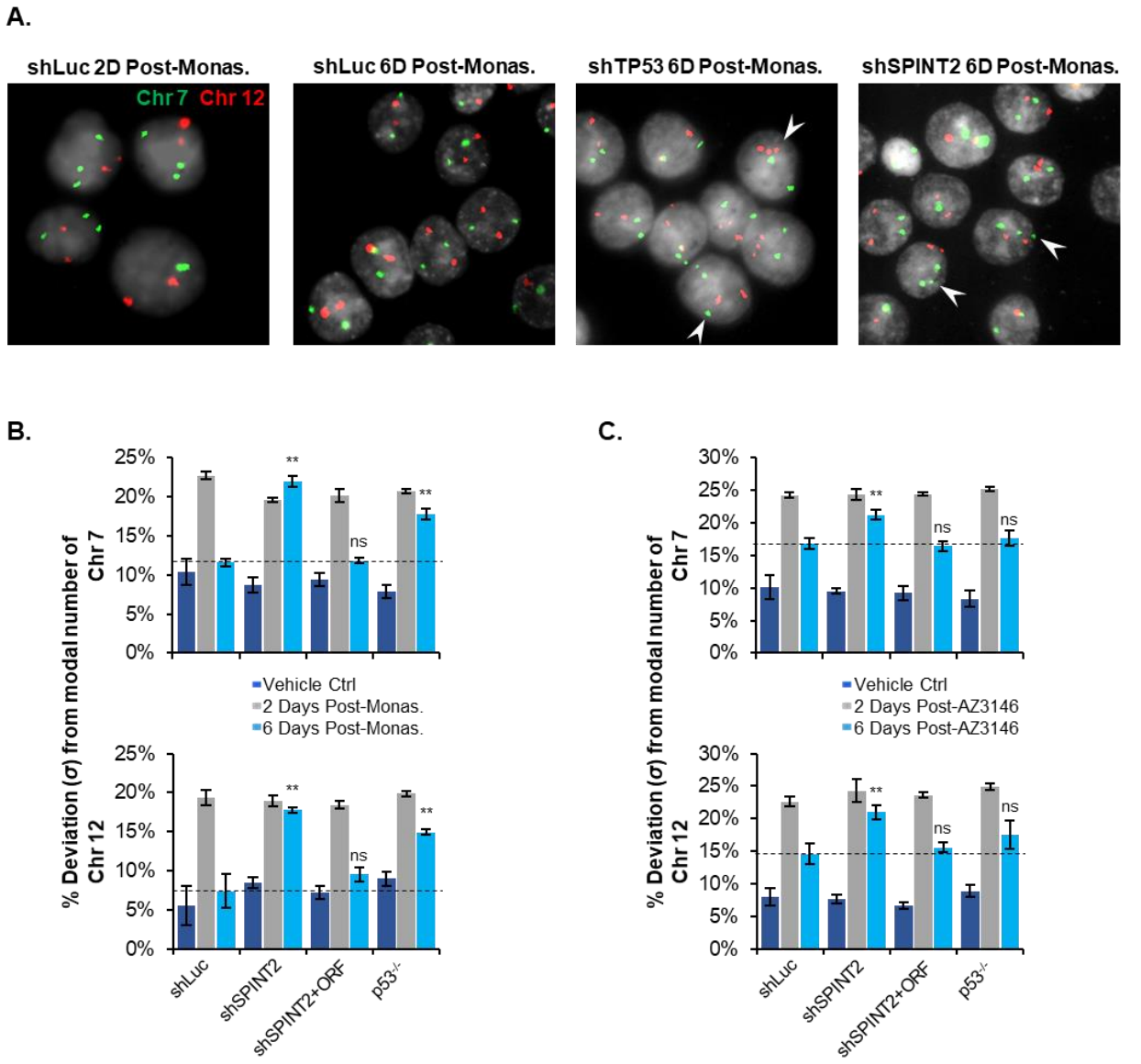

Figure 3-6. SPINT2 depletion confers increased tolerance for aneuploidy following chromosome missegregation.

A. Example images of chromosome FISH following monastrol shake-off/wash-out. Nuclear counter-stain is shown in gray. **B**. Deviation from modal chromosome numbers of chromosomes 7 and 12 (both cases, mode=2) at different time points after monastrol treatment. An additional *SPINT2* shRNA (shSPINT2#2; described in Table 2-3) yielded similar results as shSPINT2. **C**. AZ3146 treatment. Error bars, SD (n=3; ≥250 cells were scored in each triplicate). **, $p<0.01$; ns, non-significant, *t*-test; Day 6 samples were compared with control (dashed line).

Percent deviation (σ) from modal chromosome numbers (Figure 3-6B–C) was calculated using the following formula:

$$\sigma = \sqrt{\frac{\sum(x-m)^2}{n}} \Big/ m \times 100\%$$

where x is each cell's count of the probed chromosome, m is the modal number of that chromosome (m=2 for chromosomes 7 and 12 in HCT-116 cells), and n is the total number of cells scored.[258] Note that this formula is akin to the calculation of a population's percent standard deviation (replacing mean with mode). While σ is a useful indicator of aneuploidy due to its weighted incorporation of all non-disomy scenarios, it may be skewed by a small percentage of high-copy chromosome gains. Therefore, I also quantified the frequency of chromosome-specific aneuploidy (defined as any non-disomy) and observed nearly identical trends, as exemplified in Figure 3-7.

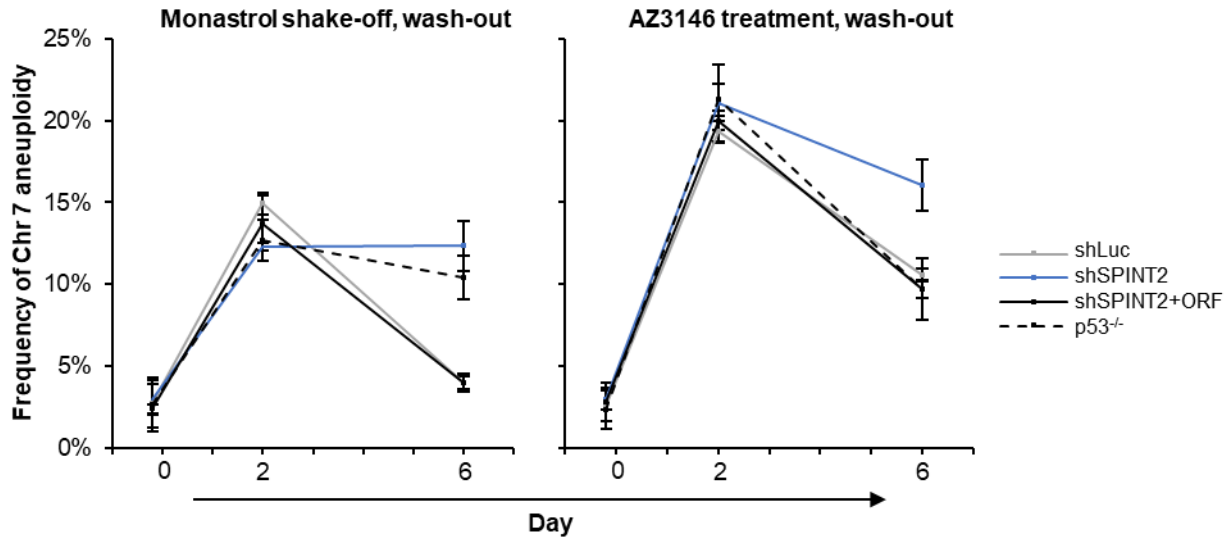

Figure 3-7. Alternative quantification of aneuploidy following chromosome missegregation.

Frequency of aneuploid cells in monastrol and AZ3146 experiments. Each non-diploid cell was counted as an "aneuploid" cell; shown are examples of chromosome 7 measurements. Drug treatments were administered at Day 0; first timepoint represents pre-treatment. Error bars, SD (n=3; ≥250 cells were scored in each triplicate).

It is important to note that in contrast to monastrol treatment, $p53^{-/-}$ cells did not exhibit persistent aneuploidy following AZ3146 treatment. These findings are consistent with prior reports on cellular responses to mitotic delays.

Uetake and Sluder (2010)[259] reported that when cells experienced prolonged (more than ~100 min) mitotic arrest before completing mitosis, their daughter cells would enter a p53-dependent G_1 arrest. Treatment with spindle poisons such as monastrol activates the spindle assembly checkpoint (SAC),[260] arrests cells in mitosis, and attains an increased rate of chromosome missegregation following drug wash-out due to the occurrence of lagging, merotelically attached (kinetochores attached to multiple spindle poles) chromosomes.[259] Hence, the monastrol shake-off I performed resulted in up to eight hours of mitotic delay, whereas HCT-116 cells complete mitosis within 30–40 minutes in unperturbed conditions.[261] While $p53^{-/-}$ and shSPINT2 cells both showed increased frequencies of aneuploidy in the following days (Figure 3-6B), it is difficult to distinguish whether this was due to bypass of mitotic delay-related cell cycle arrest or was a direct result of tolerance for aneuploidy alone.

SAC inhibitors such as AZ3146, by contrast, do not delay but rather accelerate mitosis due to impaired checkpoint mechanisms. The majority of cells following SAC inhibitor treatment are expected to continue dividing without mounting a long-term p53 response.[247] Therefore, AZ3146 treatment was an orthogonal assay that isolated SPINT2's effect on cellular aneuploidy tolerance.

Taken together, these findings have demonstrated that SPINT2 limits tolerance for aneuploidy in HCT-116 cells; depletion of SPINT2 increases persistent aneuploids in a cell population following disruptions to the mitotic machinery and contributes to karyotype variation.

Two main hypotheses exist regarding how SPINT2 suppresses aneuploidy tolerance. First, depletion of SPINT2 may provide general proliferative advantage via shortening of the cell cycle

or alteration of cell cycle distribution.[262] Second, SPINT2 knock-down may confer resistance to aneuploidy-induced stresses such as autophagy defects[171] or apoptosis.[245]

It is unlikely that SPINT2 depletion shortens the cell cycle as SPINT2 knock-down cells exhibit identical growth rates as controls during routine passaging. To test whether SPINT2 depletion alters cell cycle distribution, I performed flow cytometry analyses. As shown in Figure 3-8A, cell cycle distribution in RPE-1 cells measured by nuclear DNA content did not change following SPINT2 knock-down.

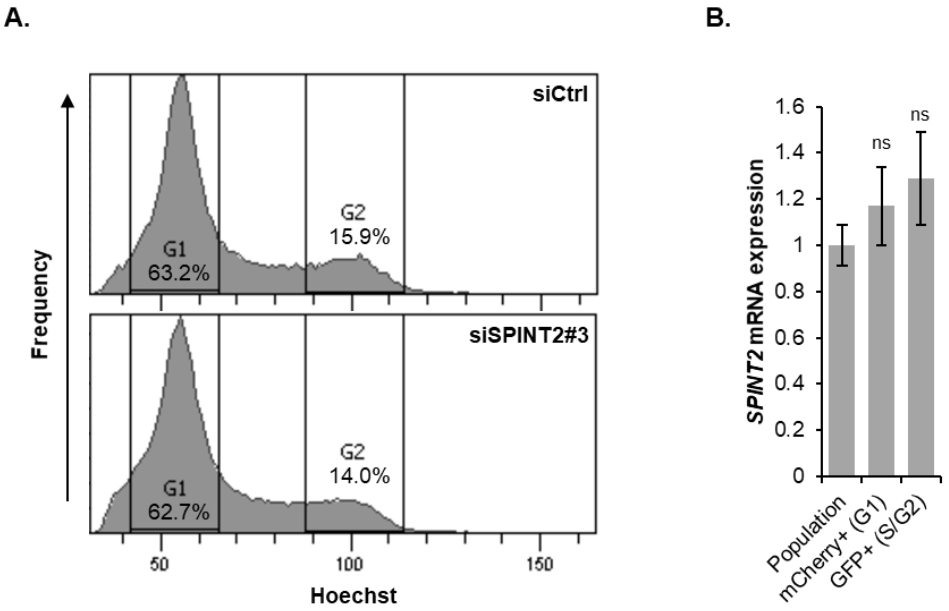

Figure 3-8. SPINT2 depletion does not alter cell cycle distribution, and its expression is not cell cycle-dependent.

A. Cell cycle distribution measured with Hoechst by flow cytometry. **B**. qPCR measurement of *SPINT2* mRNA at different cell cycle phases. Error bars, SD (n=3). ns, non-significant.

Furthermore, using RPE-1 cells expressing fluorescence ubiquitination cell cycle indicators (FUCCI; G_1 is marked by mCherry-CDT1, and S/G_2, GFP-Geminin),[263] I did not detect significant differences in *SPINT2* mRNA expression among cells at G_1 or S/G_2 (Figure 3-8B). These data suggest that SPINT2 does not regulate, and is not regulated by, the cell cycle.

In addition, it was recently reported that chromosome missegregation and the resultant aneuploidy induced the accumulation of LC3-labeled structures in cells. Specifically, LC3-II (a modified form of LC3-I, indicative of autophagy) was progressively upregulated in aneuploid RPE-1 cells 24–72 h following chromosome missegregation.[171] However, as shown in Figure 3-9A, SPINT2 knock-down did not significantly alter AZ3146-induced LC3-II upregulation. Cells starved of glucose and serum were used as positive controls for LC3 immunoblot.

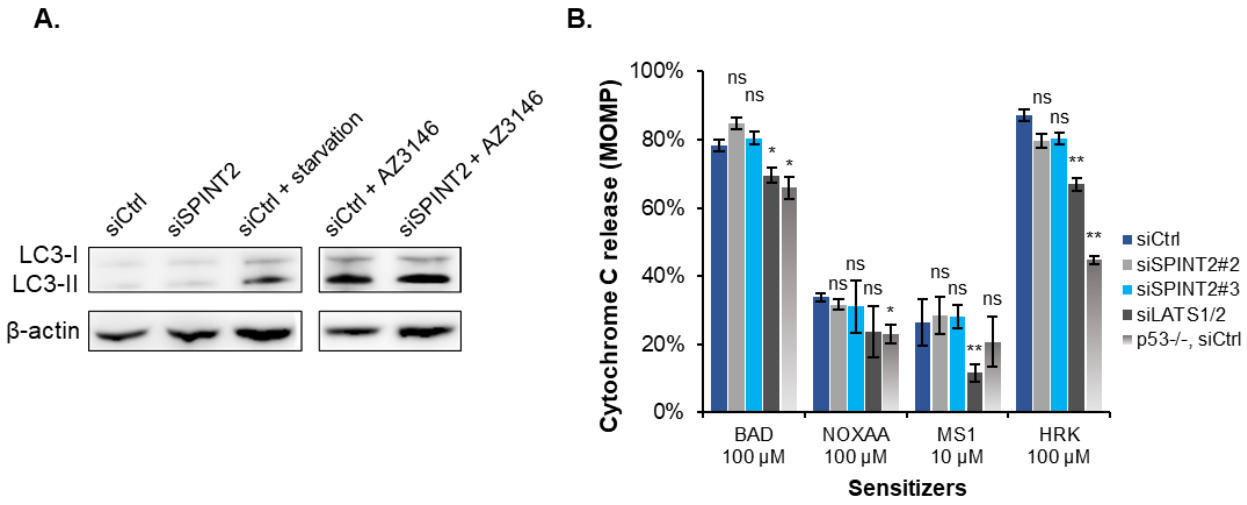

Figure 3-9. SPINT2 does not directly regulate autophagy or apoptosis.

A. Immunoblots of LC3 with glucose- and serum-starvation as positive control in RPE-1. For AZ3146 treatment, cells were treated for 48 h (2 µM), washed, and allowed to recover for 24 h. Glucose and serum starvation was carried out for 24 h. **B**. BH3 profiling of HCT-116 with pro-apoptotic peptides. Error bars, SD (n=3); *, $p<0.05$; **, $p<0.01$; ns, non-significant, *t*-test.

To test whether SPINT2 depletion affords anti-apoptotic effects, my colleague Jeremy Ryan and I performed BH3 profiling to measure tendencies for apoptosis in HCT-116 cells. Briefly, cells were permeabilized and treated with BH3-domain containing pro-apoptotic peptides. The propensity of each cell line to undergo apoptosis was measured by mitochondria outer membrane permeabilization (MOMP) following treatment.[264]

Among the panel of pro-apoptotic peptides, four exhibited differential behaviors among the cell lines profiled (Figure 3-9B): BAD peptide, based on BAD, a promoter of apoptosis related to BCL-2;[265] NOXAA, derived from NOXA, a mediator of p53-dependent apoptosis;[266] MS1, a synthetic peptide that binds to MCL1;[264] and HRK, derived from Harakiri, a BCL-2 and BCL-$_{XL}$ binding protein.[267] Specifically, double knock-down of LATS1 and LATS2 reduced sensitivity to MS1 and HRK. p53 knock-out (treated with control siRNA) decreased NOXAA and HRK sensitivity. However, depletion of SPINT2 did not result in detectable reductions of apoptotic propensity following sensitizer treatment.

The behavior of p53-null cells confirmed the efficiency of sensitizing peptide treatment. p53 is known to induce apoptosis both through transactivation of target genes such as PUMA, and transcription-independent binding to pro-apoptotic partners such as BAK.[268,269] LATS1 and LATS2, on the other hand, have also been reported to induce apoptosis.[270,271]

Collectively, my findings demonstrate SPINT2's role in limiting cellular tolerance for aneuploidy. However, mechanisms contributing to this phenotype remain to be defined.

3.2.3 Relevance and potential mechanisms of SPINT2 loss-induced aneuploidy tolerance

Considering SPINT2's suppression of YAP (Chapter 2), we asked whether elevated YAP activity may be responsible for the increased aneuploidy tolerance that I observed following SPINT2 depletion. To address this question, my collaborator Prof. Amity Manning (Worcester Polytechnic Institute, Worcester, MA) performed FISH-based measurement of aneuploidy in RPE-1 cells expressing YAP-5SA, a phosphorylation-resistant YAP mutant (described in Section 2.4). As shown in Figure 3-10, YAP-5SA overexpression resulted in a dramatic increase of aneuploidy within the population.

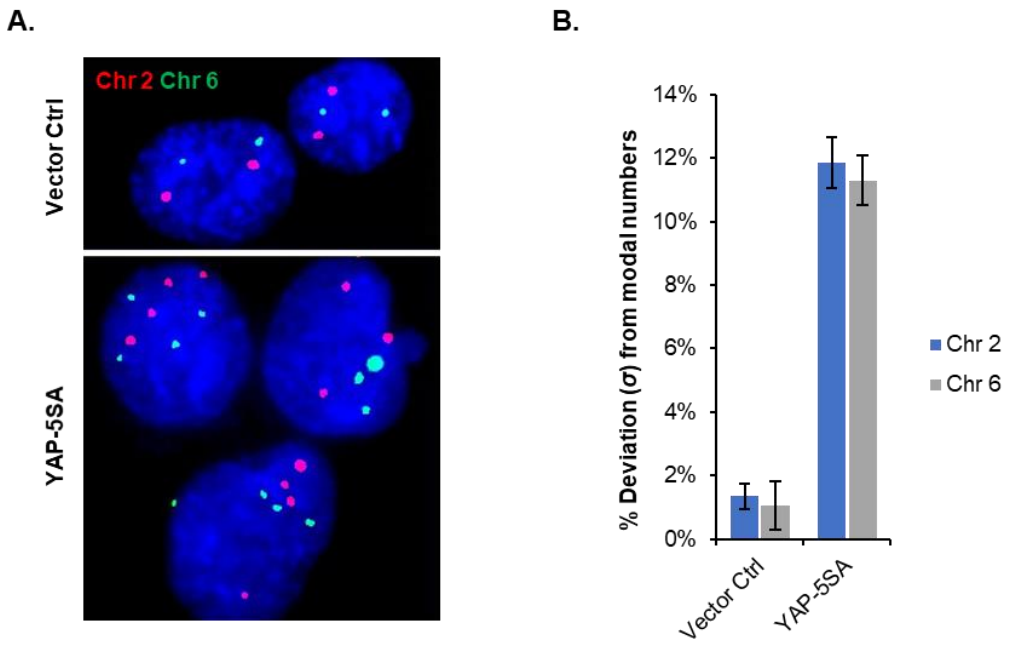

Figure 3-10. Overexpression of active YAP results in aneuploidy in RPE-1 cells.

A. Example images of chromosome FISH following YAP-5SA expression. Nuclear counter-stain is shown in blue. **B**. Aneuploidy quantified by deviation from modal chromosome numbers of chromosomes 2 and 6. Error bars, SD (n=3; ≥500 cells were scored in each triplicate).

It is important to highlight that the persistent aneuploid cells generated by monastrol shake-off or AZ3146 treatment following SPINT2 knock-down primarily exhibited trisomies (Figure 3-6A), whereas YAP-5SA overexpression resulted in predominantly polyploid derivatives (Figure 3-10A). These observations are consistent with prior reports showing that ablation of Lats1 and/or Lats2, or overexpression of Yap-5SA, led to polyploidy in mouse cells.[272,273] Considering polyploidy's role in promoting subsequent chromosome missegregation[242] and the Hippo pathway's known role in suppressing tetraploidy,[178] the induction of cellular polyploidy following YAP-5SA overexpression (Figure 3-10A) confounds the distinction between: 1) an aneuploidy phenotype stemming from increased tolerance for aneuploidy-specific stress, and 2) aneuploidy as a consequence of polyploidy—which may result from defects such as cytokinesis failure—and the

subsequent chromosome missegregation. Current work aiming to resolve this ambiguity, as well as the associated experimental challenges, are discussed in Section 3.3.2.

How is the silencing of *SPINT2* in aneuploid cells relevant to physiological or pathological contexts? It is unclear whether epigenetic silencing of *SPINT2* in human cancers[94-99] is related to the aneuploidy tolerance phenotype that I observed. Prompted by this question, I conducted a literature review of cancers that have cytogenetic and *SPINT2* expression data.

Interestingly, in thyroid cancers, *SPINT2* mRNA is almost completely silenced in anaplastic thyroid carcinomas (ATCs) compared to papillary thyroid carcinomas (PTCs).[274,275] ATCs represent a highly malignant form of thyroid tumors that are frequently derived from PTCs.[274-276] Notably, based on published data,[277-279] ATCs are associated with higher levels of cytogenetic and ploidy aberrations (Figure 3-11). I assessed aneuploidy levels based on the available cytogenetic or karyotypic characterization of tumor samples within the PTC and ATC subtypes (Table 2-1).

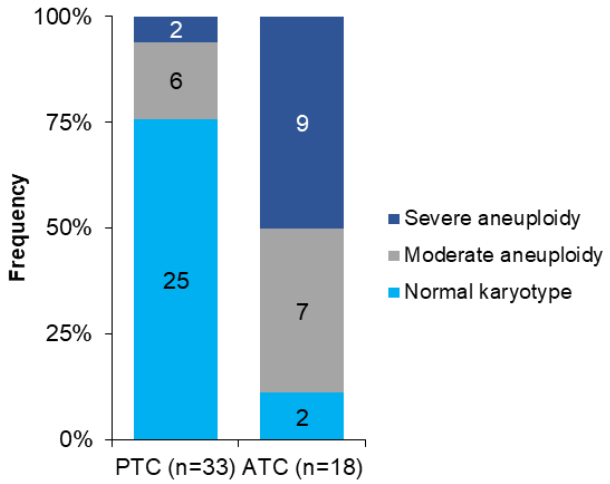

Figure 3-11. Thyroid cancers downregulating *SPINT2* have high levels of aneuploidy. Cytogenetic data (Table 3-2) reveal that ATCs are highly aneuploid compared to PTCs.

Table 3-2. Aneuploidy scoring of papillary and anaplastic thyroid cancers.

Type	Cytogenetics/karyotype	Note; reference	Scoring*
PTC	+5q23.3-qter, +7, +17, +21q22.1-qter	Age 81;[277]	Severe
PTC	+5 or +20 or +X +5 +7	[278]	Severe
PTC	+1q23-qter	Age 73;[277]	Moderate
PTC	+5q14-23.3	Age 78;[277]	Moderate
PTC	Normal or -Y	[278]	Moderate
PTC	Normal or -Y	[278]	Moderate
PTC	Normal, or +5	[278]	Moderate
PTC	Normal, with some clones showing aneuploidy	[278]	Moderate
PTC	24 samples; normal	Ages 6-80;[277]	Normal
PTC	Normal, or with inv(10)(q11.2q21.2)	[278]	Normal
ATC	+2q11.1-q24, +5q34-qter, +8q21.3-qter, +19q13.1-q13.2, +7p22-pter	Age 60;[277]	Severe
ATC	+3q13.3-qter, +5p, +Xq12-qter, +7p13-p5\ter, +8q22-qter, +9, +10q25-qter, +11p11.2-Q23.3, +12q21-qter, +15q22-qter, +20q, -4Q34-qter, -13	Age 64;[277]	Severe
ATC	+X, +7p21-pter	Age 69;[277]	Severe
ATC	Modal chromosome number 93±2	Age 72;[279]	Severe
ATC	Modal chromosome number 107±4	Age 74;[279]	Severe
ATC	Modal chromosome number 82±3	Age 76;[279]	Severe
ATC	Modal chromosome number 83±2	Age 76;[279]	Severe
ATC	Modal chromosome number 136±4	Age 77;[279]	Severe
ATC	-18p, -22	Age 78;[277]	Severe
ATC	+8q21-qter	Age 48;[277]	Moderate
ATC	+3q, -18q	Age 72;[277]	Moderate
ATC	+3p12-p21	Age 74;[277]	Moderate
ATC	+9q22.3-pter	Age 74;[277]	Moderate
ATC	+9q34-qter, +21q22-qter	Age 74;[277]	Moderate
ATC	+6p12-pter, +5p13-pter	Age 83;[277]	Moderate
ATC	+Xq11.2-pter, +7p21-pter	Age 87;[277]	Moderate
ATC	Normal	Age 77;[277]	Normal
ATC	Normal	Age 86;[277]	Normal

**: Scoring criteria are as follows:*
***Normal**, defined as normal karyotype and chromosome complement;*
***Moderate** aneuploidy: structural or numerical alteration of ≤ 2 chromosome arms;*
***Severe** aneuploidy: structural or numerical alteration of >2 chromosome arms.*

To assess the relationship between *SPINT2* expression and aneuploidy in thyroid cancers in an unbiased manner, my colleague William Gibson and I analyzed PTC copy number and expression data in the Cancer Genome Atlas (TCGA).[280] DNA copy number, a proxy of ploidy,

was quantified using ABSOLUTE, a computational method that infers ploidy based on transcriptome data.[281] As shown in Figure 3-12, no statistically significant differences in *SPINT2* expression were detected between ABSOLUTE-inferred diploid and aneuploid PTCs.

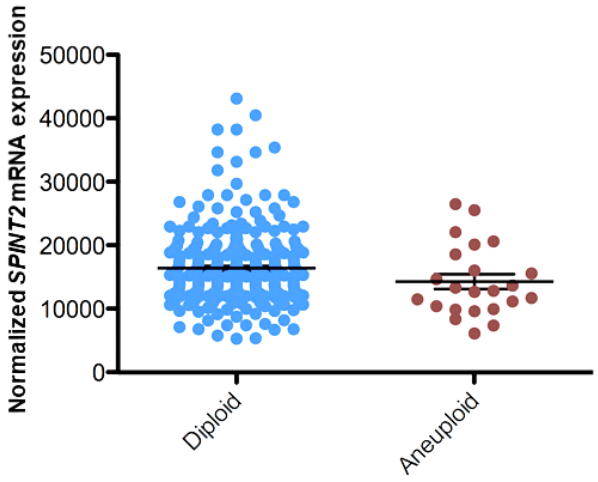

Figure 3-12. Expression of *SPINT2* in papillary thyroid carcinomas by ploidy status.

Normalized *SPINT2* mRNA expression (measured by RNA-Seq) in PTCs as part of TCGA. Ploidy statuses are defined by ABSOLUTE. "Diploid" is defined as 2±0.1 ("aneuploid", remaining samples) based on ABSOLUTE quantification. There was no statistically significant difference between the groups (*t*-test).

While providing a large sample size, TCGA data and ABSOLUTE analyses do not afford the same resolution as cytogenetic and karyotypic data. ABSOLUTE, for example, computes a single "ploidy value" for each sample that is representative of total DNA content. This inferred ploidy masks complex aneuploidy scenarios such as the simultaneous gain and loss of similarly-sized chromosome fragments, a significant imbalance of the genome that would result in an ABSOLUTE value of ~2.0. In addition, considering that *SPINT2* may be downregulated in mild aneuploidy (e.g., single copy gain of chromosome 21, as shown in Figure 3-3A) and that the vast majority of solid tumors experience various levels aneuploidy,[146,168] TCGA may not provide the optimal data source for stratification based on *SPINT2* gene expression.

In summary, we have obtained preliminary results suggesting that YAP activation may mimic SPINT2 depletion in conferring aneuploidy tolerance, and that *SPINT2* silencing in thyroid cancers is potentially associated with high levels of aneuploidy in ATCs.

3.3 Discussion

I have demonstrated that SPINT2 limits cellular tolerance for aneuploidy. Specifically, *SPINT2* is epigenetically silenced in proliferating aneuploid RPE-1 cells, and the degree of its silencing correlates with the level of genomic imbalance associated with each aneuploidy. In HCT-116 cells, SPINT2 depletion leads to persistent aneuploids in the cell population following chromosome missegregation, irrespective of whether cells mount a sustained p53 response. My data further suggest that SPINT2's regulation of aneuploidy does not rely on alterations to the cell cycle, the autophagy machinery, or tendencies for apoptosis.

3.3.1 SPINT2, a pleiotropic suppressor of aneuploidy?

While the mechanisms that mediate SPINT2's inhibition of aneuploidy are presently unclear, it is conceivable that SPINT2 may modulate multiple machineries that limit the survival and proliferation of aneuploid cells.

Mechanisms that confer cellular or organismal tolerance for aneuploidy are under active investigation. Recently, López-García and colleagues (2017)[282] showed that depletion of BCL9L resulted in persistent aneuploidy in HCT-116 cells following chromosome missegregation induced by reversine, a SAC inhibitor with similar efficacy as AZ3146.[171] BCL9L has been shown to regulate Wnt signaling by mediating β-catenin's translocation from the nucleus to the cell membrane.[283] Specifically, 15 days after a 15-day treatment with 125 nM reversine, HCT-116 cells

stably expressing *BCL9L* shRNA showed heightened levels of aneuploidy as measured by deviation from modal numbers of four arbitrary chromosomes as well as by karyotyping.[282] Notably, this observation was largely unchanged in $p53^{-/-}$ cells,[282] consistent with prior observations that SAC inhibition does not lead to long-term p53 activation.[247] The researchers further observed that a shorter reversine treatment (250 nM, 72 h) led to cleavage of caspase-2 in both wild-type and p53-null cells, and that BCL9L suppression resulted in lowered *CASP2* (caspase-2) mRNA expression.[282] These observations illustrate an apoptosis-dependent pathway for aneuploidy tolerance.

Additionally, Dodgson et al. (2016)[246] reported that in budding yeast, deletion of *UBP3*, a gene encoding a deubiquitinase that promote proteasomal degradation of cellular proteins, significantly reduced the fitness of aneuploid cells. Knock-down of the mammalian homolog of Ubp3, USP10, impaired the proliferation of aneuploid RPE-1 cells induced by reversine treatment.[246] Interestingly, spautin-1, a USP10 inhibitor, appeared to suppress autophagosome accumulation following lysosome inhibition, suggesting defects in early steps of autophagy following USP10 inhibition.[246] These observations are consistent with prior reports that aneuploidy causes accumulation and delayed clearing of autophagosomes,[171,245] and hence delineate a pathway for aneuploidy tolerance that is proteasome/autophagy-dependent.

SPINT2 depletion did not lead to alterations to the cell cycle or propensity for apoptosis in otherwise unperturbed conditions (Figure 3-8, Figure 3-9B), and did not detectably reduce LC3-II following reversine treatment (Figure 3-9A). Considering SPINT2's potential roles in regulating both growth factor and YAP signaling (discussed in Section 2.3.1), it is possible that SPINT2 depletion confers individually moderate but additively significant effects as a consequence of upregulated growth factor signaling and YAP activity. For instance, based on transcriptome data

generated for Figure 2-6, SPINT2 depletion by siRNAs correlated with reductions of *CASP2* (caspase-2) mRNA by 33% in RPE-1 cells ($p<0.01$) and by 23% in HCT-116 cells ($p<0.05$), a similar but more subtle effect compared to the approximately 60–75% *CASP2* mRNA reduction that followed BCL9L knock-down as observed by López-García et al.[282]

On the other hand, growth factors are known to suppress autophagy through the PI3K-AKT-mTOR pathway.[284-286] Upon growth factor stimulation, AKT, along with other kinases such as ERK and p90RSK1, phosphorylates and inactivates inhibitors of mTOR such as TSC2,[285,287-290] resulting in mTOR-mediated inhibition of the core autophagy initiation machinery.[291,292]

Additionally, AKT signaling has well-documented anti-apoptotic functions. For instance, it has been established that AKT phosphorylates pro-apoptotic factor BAD and thus prevents BAD-induced cell death.[286,293-295] Interestingly, Tumaneng et al. (2012)[296] reported that YAP may promote PI3K-AKT-mTOR signaling by upregulating the transcription of miR-29 microRNAs. miR-29 microRNAs suppress PTEN, the main negative regulator of PI3K.[296]

Therefore, it is possible that SPINT2 loss promotes aneuploidy tolerance through a combination of pro-proliferation and pro-survival mechanisms (e.g., elevation of YAP activity, promotion of autophagy, and inhibition of apoptosis). Considering the moderate magnitude of YAP activation (Figure 2-2, Figure 2-4) and AKT/ERK phosphorylation[178] following SPINT2 depletion, future work may be best-served with optimized experimental sensitivity and dynamic range. For example, instead of depleting SPINT2 and assay for autophagy or apoptotic propensities (Figure 3-9), overexpressing SPINT2 may help us isolate SPINT2-regulated cellular machineries.

3.3.2 Connecting YAP activation and aneuploidy tolerance

Is aneuploidy tolerance driven by YAP activation following SPINT2 depletion? We have obtained preliminary data that YAP-5SA overexpression recapitulates some aspects of an aneuploidy phenotype (Figure 3-10). Nevertheless, as discussed in Sections 2.2.4 and 3.2.3, YAP-5SA overexpression may render results difficult to interpret due to prevalent polyploidy.

In order to overcome this challenge, we aimed to achieve moderate activation of YAP using LATS1/2 double knock-down. We prioritized partial loss-of-function mediated by LATS1/2 shRNAs over CRISPR-based complete knock-out due to prior findings that LATS1/2 double knock-out induced widespread polyploidy.[272,273] Neomycin-selectable *LATS1* shRNA and puromycin-selectable *LATS2* shRNA were transduced into HCT-116 cells by lentiviral infection. Strikingly, following antibiotic selection, I observed a high level of compensatory expression of *LATS1* in cells stably expressing both shRNAs (shown and discussed in Section 5.2.2). Similar observations were made in RPE-1 cells (personal communications with Prof. N. Ganem).

Furthermore, several recent lines of evidence have suggested that YAP/TAZ activity is tightly constrained by robust feedback mechanisms within the core Hippo circuit. For instance, active YAP has been shown to provoke potent transcription of *LATS2* in addition to moderate expression of *LATS1*, and also reduce cellular abundance of TAZ.[182,297] In addition, overexpression of wild-type YAP induces disproportionately dramatic YAP phosphorylation and significantly milder colony-forming phenotypes compared to phosphorylation-resistant YAP mutants overexpressed at similar levels.[132,298] Therefore, the Hippo regulatory network exerts a long-term self-stabilizing control that limits YAP/TAZ activity through phosphorylation.

These observations inform both technical and scientific thinking regarding our ongoing work that aims to address whether a moderate increased in YAP activity contributes to SPINT2

loss-mediated aneuploidy tolerance. Regarding the technical aspects, it is increasingly evident that moderate YAP activation should be attained via titratable and inducible systems that exogenously express wild-type or phosphorylation-resistant YAP, hence circumventing the need to manipulate LATS1/2, which appear to be part of a robust feedback mechanism (discussed in Section 5.2.2).

In terms of how we scientifically frame our inquiries, the time scales of molecular signaling and cellular responses following SPINT2 suppression become an interesting issue to consider. In other words, is it possible that short-term and long-term phenotypes associated with SPINT2 loss are mediated by distinct mechanisms?

I have observed that shSPINT2 HCT-116 cells that have been passaged for several weeks exhibit attenuated induction of YAP target genes compared to freshly transduced cells (data not shown). This observation is consistent with the self-attenuating properties YAP/TAZ signaling.[132,182,297,298] Of note, compared to YAP/YAP-5SA overexpression, SPINT2 knock-down does not introduce exogenous YAP activity and thus is presumably more susceptible to physiological feedback mechanisms within the Hippo pathway. In this chapter, *SPINT2* expression was silenced through epigenetic mechanisms or by virally transduced shRNAs for durations of multiple weeks; the shortest time frame during which I detected a significant phenotype (Figure 3-6) was approximately one week. In contrast, most results regarding YAP activation in Chapter 2 were acquired after 2–3 days of SPINT2 depletion using siRNAs. Therefore, it is possible that YAP activation may represent a near-term response to SPINT2 knock-down, whereas additional mechanisms contribute to the longer-term phenotypes (such as aneuploidy tolerance) under persistent SPINT2 suppression.

Nevertheless, it is distinctly possible that increased YAP activity drives long-term phenotypes associated with *SPINT2* silencing. Indeed, transient early signals may alter long-term

cell fate as short-term effects can be transmitted, amplified, and subsequently prolonged in downstream signaling.[299] For example, mathematical modeling of experimental data has shown that in HT-29 human colorectal cancer cells, transient early activation (≤90 min) of tumor necrosis factor-α (TNFα) signal transmitters such as JNK1 and MK2 predicts cellular apoptotic behaviors that occur 24–48 hours later.[300]

Therefore, to deepen our understanding of short-term and long-term effects of SPINT2 depletion, it is important to document SPINT2-mediated growth factor signaling and YAP/TAZ activity with temporal sensitivity. Additionally, transcriptomic characterization of cells with permanent SPINT2 loss (via *SPINT2* shRNA or CRISPR knock-out) may provide insights on the long-term biological consequences of SPINT2 depletion.

In conclusion, this chapter demonstrates that SPINT2 plays a crucial role in limiting cellular aneuploidy tolerance. Evaluation of cellular mechanisms by which SPINT2 exerts this effect requires a well-rounded understanding of SPINT2's potential short-term and long-term roles within multiple signaling pathways.

3.4 Materials and Methods

Generation of aneuploid cells

Microcell-mediated chromosome transfer (MMCT) was performed as previously described[252] with modifications. Five 15-cm dishes of human/mouse hybrid A9 cells were cultured to ~70% confluency and treated with 75 ng/ml colcemid (Sigma-Aldrich 360406) for 48 h. Cells were collected and resuspended in 1:1 DMEM:Percoll (GE Healthcare 17-0891-01) and 10 μg/ml cytochalasin B (Sigma-Aldrich C6762), and then spun at 17,000 rpm for 75 minutes using a Beckman JA-17 rotor. Supernatant was collected and filtered. Approximately 2 million RPE-1 cells growing at exponential phase were collected by trypsin, and were mixed with filtered microcells. The mixture was treated with 100 μg/ml PHA-P (Sigma-Aldrich L1668) for 30 minutes and fused by PEG 1500 (Roche 10783641001) in solution, per manufacturer's instructions. Hybrid cells were washed 3 times and then plated in 4 10-cm dishes. 48 hours later, 500 μg/ml Geneticin (Life Technologies 10131035) were added and cells were selected for 12-14 days. Colonies were picked with cloning cylinders, and expanded in 96-, 24-, and 6-well plates. Clones were verified for specific aneuploidies.

Single-cell cloning of RPE-1 cells with aneuploidy-12 was performed at the Dana-Farber Cancer Institute Flow Cytometry Core. Briefly, RPE-1 cells were trypsinized, filtered with a cell strainer, and resuspended in regular growth media. Single cells were then sorted into 96-well plates using the "single-cell" parameters on a FACSAria II UV cell sorter (BD Biosciences) and were expanded into clonal populations. Clones were screened for chromosome 12 gain. Diploids from the same sort were collected as controls.

Proliferating tetraploid RPE-1 cells were isolated by treating at least 4 15-cm plates of ~50% confluent cells with 4 μM dihydrocytochalasin B (Sigma-Aldrich D1641) for 16 h to disrupt

cytokinesis. Cells were given 24 h to recover, and were subsequently incubated in 4 µg/ml Hoechst 33342 (Cell Signaling Technology 4082S) for 30 min. Cells were then trypsinized, filtered, and resuspended in growth media containing 4 µg/ml of Hoechst. Sorting for cells containing 8C DNA content (signifying G_2 tetraploid cells) measured by UV excitation of Hoechst was performed using a FACAria II UV cell sorter (BD Biosciences) and the resultant cells were washed and expanded. Usually, 4–6 such sorts were necessary to obtain a pure population of proliferating tetraploids. Cycling populations of diploid cells were used during each sort to control for Hoechst staining and DNA content. Diploid cells were sorted based on 2C DNA content and used as controls.

Karyotyping validation was performed by KaryoLogic, Inc. (Durham, NC). Genomic DNA was extracted with the DNeasy Blood and Tissue Kit (Qiagen 69504), and SNP array was performed at the Dana-Farber Cancer Institute Molecular Biology Core Facilities using the Human Mapping 250K Nsp platform (Affymetrix).

DNA methylation studies

Treatment with 5-aza-2-deoxycytidine (5-AdC; Sigma-Aldrich A3656) was carried out at 10 µM for 48 h with vehicle (DMSO) control. RNA extraction and gene expression methods have been described in Section 2.4.

For bisulfite sequencing analysis, *SPINT2* promoter sequence was obtained from genecards.org and was consistent with prior publications.[94-100] The 729-bp promoter was divided into 3 regions of 240-250 bp due to the size limit of bisulfite sequencing. Bisulfite-specific primers were designed using the Zymo Research Bisulfite Primer tool and are listed in Table 3-3. Matching

genomic sequences (had the primers not been designed to account for bisulfite conversion) are also provided. Note that R refers purines and Y, pyrimidines.

Table 3-3. Bisulfite sequencing primers and target genomic sequences.

Promoter region	Forward primer (5'-3')	Reverse primer (5'-3')
#1 bisulfite-specific primers	GTGTTTGTYGTTTTTTTTTTT ATTTTGAGGTTAG	CAAACRCAAAAAACAAACACCT AC
#1 target genomic sequence	*CGTGTCTGCCGCCCCCTCCTCC CACCCTGAGGCCAG*	*GCAGGTGCCTGCCCTTTGCGCC TG (sense)*
#2 bisulfite-specific primers	GTTTTTTYGGATTTTTAGTGTG GGG	CCCAACTCRCCCTACCTAACCA AATAC
#2 target genomic sequence	*CCCCACACTGAAGGTCCGGAAA GGC (sense)*	*CCCAGCTCGCCCTGCCTAGCCA GGTGC*
#3 bisulfite-specific primers	GATTTTYGGGGGTTTTGGTATT TGG	ACCRCCAAAACCCCAAAAAAAA ACAAC
#3 target genomic sequence	*GACTTCCGGGGGCTTTGGCACC TGG*	*GCTGCTCCTCTCTGGGGTCCTG GCGGC (sense)*

Genomic DNA was extracted using the DNeasy Blood and Tissue Kit (Qiagen 69504) and was subjected to bisulfite conversion using the EZ-DNA Methylation Gold kit (Zymo Research D5005), following manufacturer's instructions. Bisulfite-converted DNA was amplified using the ZymoTaq DNA polymerase (Zymo Research E2001) to prepare for TA-cloning. Due to multiple mutations in the primer sequences to accommodate for potentially unmethylated cytosines (converted to uracils by bisulfite), PCR amplification temperature was determined empirically using a Bio-Rad gradient PCR machine. PCR products were then TA-cloned using the TOPO TA Cloning kit (Life Technologies K4575J10), and the resultant plasmid DNA from single transformed *E. coli* colonies was Sanger-sequenced. Ten (10) fragments for each promoter region were sequenced per sample. CpGs in primers were excluded from the analyses. Overall, methylation status of 72 out of 88 CpGs in *SPINT2* promoter was determined.

Sanger DNA sequencing

Sequencing was performed by Genewiz, Inc. (Cambridge, MA). The *KRAS* locus was PCR-amplified using the following primers: forward 5'- GCGTCGATGGAGGAGTTTGT-3'; reverse 5'- GGTCCTGCACCAGTAATATGC-3'.

Chromosome fluorescent* in situ *hybridization (FISH)

Chromosomes counted for measurement of aneuploidy were probed by specific satellite enumeration probes targeting centromeric or pericentromeric regions of each chromosome (Cytocell; chromosome 2: LPE 002R-A; chromosome 6: LPE 006G-A; chromosome 7: LPE 007G-A; chromosome 12: LPE 012R-A) to eliminate the need to control for cell cycle (i.e., each probed chromosome emits one positive signal irrespective of DNA replication status).

Cells were plated in 12-well plates with sterile #1.5 round glass coverslips. HCT-116 cells were plated on coverslips pre-coated with poly-D-lysine (described in Section 2.4). Before fixation, cells were washed with PBS and incubated with 2 ml of 75 mM KCl at 37°C for 20–30 min. Subsequently, 1.5 ml of cold (-20°C) 3:1 methanol:acetic acid solution was added drop-wise to the KCl incubation to fix each sample. The solution was removed by aspiration and 1.5 ml of cold (-20°C) 3:1 methanol:acetic acid solution was added for the second fixation; this step was repeated for the third (and final) fixation, followed by aspiration.

Coverslips were air-dried overnight to reduce DNA over-denaturation, and were incubated at 37°C for 15–30 min in 2X SSC buffer with 0.5% v/v NP-40. Subsequently, samples were dehydrated sequentially with cold (-20°C) 70%, 85%, and 100% ethanol (2 min each incubation). Coverslips were air-dried.

Satellite enumeration probes were warmed to room temperature and mixed 1:5 to 1:8 with the Hybridization Buffer (Cytocell HB1000L). Ten (10) µl probe/Hybridization Buffer was added onto a sterile glass slide for each coverslip, and coverslips were gently placed atop the solution. Subsequently, coverslips were sealed onto the glass slides by rubber cement (Electron Microscopy Sciences MS72170) and heated to 75°C for 5 min to denature DNA. Samples were then incubated at 37°C overnight for hybridization. Following hybridization, rubber cement was removed, and samples were washed with PBD Buffer (100 mM NaH_2PO_4, 100 mM Na_2HPO_4, 0.1% v/v NP-40) for 10–15 min, and washed with pre-heated Wash Buffer (0.5X SSC with 0.1% w/v SDS) at 70–72°C for 5 min (temperature was determined empirically to optimize signal). Subsequently, samples were incubated with PBD Buffer containing 4 µg/ml Hoechst 33342 (Cell Signaling Technology 4082S) at room temperature for 10 min for nuclear counter-staining. Coverslips were mounted on glass slides for fluorescent imaging (described in Section 2.4).

FUCCI and flow cytometry

Fluorescence ubiquitination cell cycle indicator (FUCCI)[263] vectors expressing fluorophore-tagged, truncated CDT1 and GMNN—mCherry-hCdt1(30/120) and mAG-hGem(1/110)—were kind gifts from Prof. Atsushi Miyawaki (Riken, Tokyo, Japan). Lentiviruses carrying the respective vectors were produced and transduction/infection was carried out as described in Section 2.4. For cell cycle-dependent gene expression analysis, 100,000 G_1 or S/G_2 RPE-1 cells were sorted based on $mCherry^+/GFP^-$ or GFP^+ using a FACSAria II UV cell sorter (BD Biosciences) and were immediately lysed for qPCR.

For DNA content-based cell cycle analysis, cells were treated with siRNAs for 72 h (Section 2.4), and were incubated in 4 µg/ml Hoechst 33342 (Cell Signaling Technology 4082S)

for 30 min. Cells were then trypsinized, filtered, and resuspended in growth media containing 4 μg/ml of Hoechst, and were analyzed using FACSAria II UV (BD Biosciences).

Immunoblotting

Standard RIPA buffer-based immunoblotting was performed to detect LC3-I and LC3-II. Primary antibody against LC3 (Sigma-Aldrich L7543) was used at 1:500.

BH3 profiling

BH3 profiling was performed as described[264] with modifications. Staining Solution contains 20 μg/ml oligomycin, 50 μg/ml digitonin, 2 μM JC-1 (Thermo Fisher Scientific T3168), 10 mM 2-mercaptoethanol, in Mitochondrial Buffer (MEB). MEB consists of 150 mM mannitol, 10 mM HEPES-KOH pH 7.5, 50 mM KCl, 0.02 mM EGTA, 0.02 mM EDTA, 0.1% w/v bovine serum albumin, and 5 mM succinate.

BH3 peptides (sensitizers) were prepared at 100X concentration, and 15 ul 2X peptide solutions were added in triplicates in 384-well plates. Cells were trypsinized, washed, and resuspended in MEB at about 10^6 cells/ml. 15 ul of cells was added to the peptide solution in each well. A Tecan Safire 2 fluorescent plate reader was used to measure JC-1 emission (excitation, 545-560 nm; emission 580-600 nm). Fluorescent emission was measured every 5 min for 90 min at 28°C.

TCGA data analysis

TCGA data on thyroid cancers[280] was obtained from the Genomic Data Commons (National Cancer Institute). RNA-Seq expression data were quantile-normalized, and ABSOLUTE

analysis was performed using the GenePattern platform (genepattern.broadinstitute.org) and as previously described.[281]

Gene expression, imaging, and statistics

Gene expression, imaging, and statistical methods are described in Section 2.4.

Plasmids, constructs, and cloning

shLATS1 (TRCN0000001776) and shLATS2 (TRCN0000000880) were obtained from the RNAi Consortium through Sigma-Aldrich. shLATS2 was used without modification and with puromycin selection. shLATS1 was cloned into the pSIH-H1-Neo vector (System Biosciences) with neomycin/Geneticin selection following manufacturer's protocols. FLAG-YAP-WT and FLAG-YAP-5SA constructs (Addgene 18881 and 146858) were kind gifts from Profs. Y. Shaul (Weizmann Institute of Science, Rehovot, Israel) and K. Guan (University of California San Diego, San Diego, CA) and were cloned into cumate-inducible vectors as described in Section 2.4.

3.5 Chapter Contributions

Hubo Li and David Gordon in our group created and validated chromosome-8 and -21 aneuploid RPE-1 cells, and contributed Figure 3-2A–C and respective methods. Jeremy Ryan in Prof. Anthony Letai's lab (Dana-Farber Cancer Institute, Boston, MA) contributed Figure 3-9B and corresponding methods. Prof. Amity Manning (Worcester Polytechnic Institute, Worcester, MA) contributed Figure 3-10. William Gibson in Prof. Rameen Beroukhim's group (Dana-Farber Cancer Institute) contributed Figure 3-12 and corresponding methods.

I thank my colleague I-Ju Lee for offering helpful feedback on this chapter.

Chapter 4 : Modulation of Acute Myeloid Leukemia (AML) Differentiation by ZEB2

Summary

I show that depletion of ZEB2, a transcription factor known for its role in epithelial-mesenchymal transition (EMT), results in aberrant differentiation and impaired proliferation of human acute myeloid leukemia (AML) cells. I discuss these findings' biological and potential therapeutic relevance, discuss their links to Chapters 2 and 3, and outline future directions.

Part of this chapter was adapted from the following publication:

Li H,[*] Mar BG,[*] **Zhang H**, Puram RV, Vazquez F, Weir BA, Hahn WC, Ebert B, and Pellman D. (2017). The EMT regulator ZEB2 is a novel dependency of human and murine acute myeloid leukemia. *Blood*: 129(4), 497-508.[301] [*]: equal contribution.

adhering to the journal's Rights and Permissions guidelines.[302]

4.1 Introduction

4.1.1 Hematopoiesis, leukemia, and AML

Leukemias are cancers of the hematopoietic system—the physiological process that forms and replenishes blood cells.[303,304] The hematopoietic system is composed of stem cells, progenitor cells, and terminally differentiated cells, which represent sequential stages of differentiation. Most upstream are the hematopoietic stem cells (HSCs), which are rare cells predominantly residing in the bone marrow. HSCs self-renew and possess the potential to differentiate into more than 10 types of mature blood cells. During hematopoiesis, HSCs first diverge into either the myeloid or the lymphoid lineage by differentiating into common myeloid progenitors (CMPs) or common lymphoid progenitors (CLPs). In the myeloid lineage, CMPs give rise to megakaryocyte-erythroid progenitors (MEPs) and granulocyte-monocyte progenitors (GMPs).[304] MEPs, in turn, differentiate into megakaryocytes and erythroid cells, whereas GMPs differentiate into granulocytes and monocytes. In the lymphoid lineage, CLPs are responsible for deriving B-cells, T-cells, and nature killer (NK) cells. Together, B-cells and T-cells constitute the basis of the adaptive immune system, whereas NK cells, granulocytes, monocytes, and such cell types as dendritic cells make up the innate immune system.[304]

Leukemias are broadly divided into acute and chronic forms.[305] Acute leukemias progress rapidly, and the malignant cells tend to be undifferentiated. Chronic leukemias, on the other hand, accumulate abnormal but relatively mature cells over longer periods. The myeloid and lymphoid lineages are also used as broad categories. Four major types of leukemia are hence delineated: acute myeloid leukemia (AML), acute lymphoblastic leukemia (ALL), chronic myeloid leukemia (CML), and chronic lymphocytic leukemia (CLL).[305] AML is the most common type of leukemia:

in the United States, AML is currently estimated to affect more than 21,000 individuals every year and result in more than 10,000 deaths in 2017.[306]

AML is characterized by heterogenous pathogenesis, complex pathobiology, and poor prognosis.[307] Genetic lesions that contribute to AML development often occur in lineages such as HSCs or myeloid progenitor cells.[308] When defined based on differentiation phenotypes, AML is historically categorized into eight subtypes (the FAB classification): the M0 subtype, where cells have no significant signs of differentiation; the M1, M2, and M3 subtypes, where cells show varying degree of granulocytic differentiation; the M4 subtype with both granulocytic and monocytic differentiation; and the M5, M6, and M7 subtypes, where the disease is characterized by respective accumulation of immature monocytes, erythroid cells, and megakaryocytes.[309] The World Health Organization (WHO) system, currently implemented in clinical practice, classifies AMLs based on recurrent genetic abnormalities and differentiation status.[310]

AML also possesses heterogeneous cytogenetic and karyotypic characteristics. In addition to the FAB subtypes, cytogenetic abnormalities are used to classify patients into three prognostic groups: favorable, intermediate, and adverse (unfavorable).[311] Major favorable cytogenetic factors include t(8;21) (translocation of chromosome 8 and 21), inv(16) and t(16;16) (inversion or internal translocation of chromosome 16), and t(15;17). Adverse risks include complex karyotype, monosomy 5 or 5q deletion, monosomy 7, and several other rare translocations. t(9;11) and trisomy-8 are intermediate-risk. Cytogenetically normal AML is usually characterized by mutations in *FLT3*, *NPM1*, *CEBPA*, *DNMT3A*, *IDH1*/2 and *TET2*, and can range from favorable to adverse prognoses.[311]

4.1.2 Physiological functions of ZEB2

ZEB2, or *Zinc Finger E-Box Binding Homeobox 2*, encodes a transcription factor that regulates epithelial-mesenchymal transition (EMT). EMT is a process by which epithelial cells acquire properties of motile mesenchymal cells: during EMT, epithelial cells lose their junctions and apical-basal polarity, undergo reorganization of the cytoskeleton and alteration of molecular signaling, and develop invasive phenotypes. This transformation is crucial for physiological processes such as embryonic development, wound healing, and stem cell behavior, and contributes to pathological processes such as fibrosis and tumorigenesis.[312]

Along with transcription factors SNAIL and bHLH, the ZEB family factors repress epithelial marker genes such as E-cadherin and Crumbs3, and activate mesenchymal genes such as N-cadherin and matrix metalloproteases (MMPs).[312] The ZEB family consists of ZEB1 and ZEB2, homologs that share highly similar zinc-finger domains at the N- and C-termini. ZEB1 and ZEB2 play overlapping but non-redundant roles in EMT and cell physiology, primarily due to tissue dependency and differential regulation of their specificity and activity.[313,314]

Consistent with its role in cellular EMT, ZEB2 has long been known as a key player in organ development.[314,315] For example, it was reported in 2003 by Van de Putte and colleagues[316] that in mice, *Zeb2* knock-out results in embryonic lethality (E9.5), as well as severe defects in neural crest and neural plate detectable as early as E8.5.[314,316] These defects are related to Zeb2's core function as a transcriptional repressor and EMT regulator, since Zeb2's repression of BMP (bone morphogenic proteins) is essential for early neural development. BMP belongs to the TGFβ superfamily, a predominant signaling component in EMT.[312,314-317]

Recently, increasing evidence has pointed towards ZEB2's roles in blood development and disease. In 2011, Goossens and colleagues[318] characterized Zeb2's expression in mouse embryonic

and adult HSCs. Using endothelial and HSC lineage-specific conditional knock-out of *Zeb2*, the authors showed that Zeb2 was essential for fetal hematopoietic cell localization and downstream differentiation. Zeb2 depletion appeared to suppress HSC differentiation and result in an enrichment of under-differentiated HSCs.[318] Further studies by Scott et al. (2016)[319] and Wu et al. (2016)[320] showed Zeb2's role in the development of murine dendritic cells and monocytes, sub-lineages of CMPs. Specifically, Zeb2's transcriptional repression of Id2, a regulator of myeloid differentiation, was crucial for the lineage commitment of conventional dendritic cells[319] and the development of plasmacytoid dendritic cells and monocytes.[319,320]

Regarding hematopoietic malignancies, recent studies reported that human T-cell ALLs showed heightened *ZEB2* expression,[321] and that overexpression of *Zeb2* drove the development of murine T-cell ALL[321] and B-cell ALL.[322] For example, mice with endothelial-specific overexpression of *Zeb2* did not exhibit blood abnormalities at ages of 6–8 weeks, but started to die from precursor T-cell lymphoblastic leukemia at five months.[321] In mice with acute leukemia driven by the *CALM-AF9* fusion oncogene, upregulation of *Zeb2* mRNA due to promoter disruption accelerated B-cell ALL onset.[322]

In summary, ZEB2 plays crucial roles in the development of a broad range of tissues. It is conceivable, therefore, that misregulation of ZEB2 may contribute to a plethora disorders including various subtypes of leukemia.

4.1.3 Measuring differentiation in AML

Considering the prevalence of aberrant differentiation in AML,[323] it is of interest to examine any AML regulator's role in differentiation. To measure subpopulations and their differentiation status in blood cells, researchers commonly utilize cluster of differentiation (CD)

markers. Specific cell lineages express unique combinations of CD markers, which are a variety of cell-surface gene products following a standardized nomenclature.[324] For example, CLPs are distinguished from CMPs based on CLPs' expression of CD10, an endoprotease encoded by the *MME* gene.[325,326] Given that AML FAB subtypes M1–M5 constitute >90% of cases with aberrant differentiation,[327] we focused on GMP sub-lineage CD markers (Table 4-1).[328-330]

Table 4-1. CD markers for the GMP sub-lineage.

Marker	Gene name (description)	Expression in GMP	Expression in granulocytes	Expression in monocytes
CD11b	*ITGAM* (Integrin Subunit α M)	−	+	+
CD13	*ANPEP* (Membrane Alanyl Aminopeptidase)	+	+	+
CD14	*CD14* (Myeloid Cell-Specific Leucine-Rich Glycoprotein)	−	+	+
CD16	*FCGR3A* (Fc γ Receptor IIIa)	−	+	+
CD66	*CEACAM1* (Biliary Glycoprotein)	−	+	−

4.1.4 Project rationale and significance

Treatment strategies against AML have remained largely unchanged for the past three decades.[331] Currently, AML treatments differ by subtypes.[332] The FAB M3 subtype, also known as AML with PML-RARα fusion or acute promyelocytic leukemia (APL), is treated with all-trans retinoic acid (ATRA) and arsenic trioxide (ATO), along with chemotherapy. ATRA and ATO represent differentiation therapies, and are considered more effective and less toxic than conventional chemotherapy.[333] The treatment for APL is effective, with over 90% of patients achieving long-term remission.[332] All other subtypes of AML are treated by two stages of chemotherapy: induction and consolidation. Induction chemotherapy aims to attain complete remission, whereas consolidation chemotherapy is administered to eliminate residual leukemia

cells. Allogeneic HSC transplant is also used after consolidation to replenish bone marrow cells, which has been demonstrated to improve survival in adverse- and intermediate-risk patients.[334] Nevertheless, this treatment regimen is woefully limited in effectiveness, with the majority of patients eventually succumbing to relapse after induction chemotherapy.[307,331]

Development of effective next-generation therapeutics against AML mandates mechanistic understanding of AML biology, especially AML's molecular regulators as well as genetic dependencies of AML pathogenesis. The latest genomic technologies have led to the generation of large-scale cancer data sets, such as the Cancer Cell Line Encyclopedia (CCLE)[335] and the Cancer Genome Atlas (TCGA).[336] CCLE provides copy number, mutation, gene expression, and pharmacological profiling of over 1,000 cancer cell lines, and includes 34 AML cell lines.[335] TCGA profiles copy number, mutation, RNA expression, and methylation status in more than 30 types of cancer and contains 200 AML samples.[336] These studies have identified multiple genes and microRNAs that are altered in AML. However, a major challenge to interpreting these findings is to establish the functional relevance of these genes in AML and other cancers, and to understand their molecular mechanisms.

To address this challenge, my colleagues combined cancer genomic data with *in vitro* and *in vivo* RNAi screens to systematically examine the genetic dependencies of AML.[301] They identified novel genes regulating AML proliferation using both an *in vitro* genome-scale shRNA screens in multiple AML cell lines and an *in vivo* secondary screen in a syngeneic murine AML model driven by the MLL-AF9 oncogenic fusion protein. In collaboration, we established the transcription factor ZEB2 as a previously unknown regulator of AML proliferation and differentiation. While ZEB2 is known for its role in repressing E-cadherin and promoting EMT,[337] our study uncovered its critical roles in AML pathogenesis.

4.2 Results

A genome-scale shRNA drop-out screen was performed in 17 AML cell lines (Table 4-2 in Section 4.4) as part of Project Achilles,[338] a massively parallel shRNA screening endeavor in 216 cancer cell lines aiming to identify genetic requirements for tumor proliferation.[338] Lentivirus-delivered shRNAs that impaired proliferation were expected to "drop out" of the population by subsequent sequencing analysis, indicative of potential hits.[301,338]

To identify genes uniquely required for the survival of AML (but not other cancers), my colleagues utilized the ATARiS (Analytic Technique for Assessment of RNAi by Similarity) score and the shRNA score. ATARiS represents a computational method that takes advantage of RNAi data across multiple samples and isolates effects caused by on-target shRNA knock-down.[339] In short, the ATARiS score measures the consistency of shRNA reagents targeting each gene and accounts for off-target effects. Genes whose suppression by multiple shRNAs produces consistently no effect will have ATARiS scores centering around 0; genes whose shRNAs drop out of the population consistently will have negative ATARiS scores.[301,339] The shRNA score, on the other hand, is an aggregate measurement of fold depletion of all shRNAs targeting each gene in the drop-out screen; it mainly reflects the magnitude of each gene knock-down's effect.[301,338]

Comparing the ATARiS and shRNA scores of gene knock-downs in AML cells with non-hematopoietic cancer cell lines yielded a list of 353 hits unique to AML. Specifically, with a false discovery rate (FDR) cutoff of 0.001, ATARiS provided a list of 214 genes; shRNA score with an FDR cutoff of 0.01 revealed 197 genes. Fifty-eight (58) genes overlapped between the two lists, representing high-priority hits. These lists have been published in Li et al. (2017).[301] Figure 4-1A shows examples of knock-downs that uniquely impaired AML proliferation.

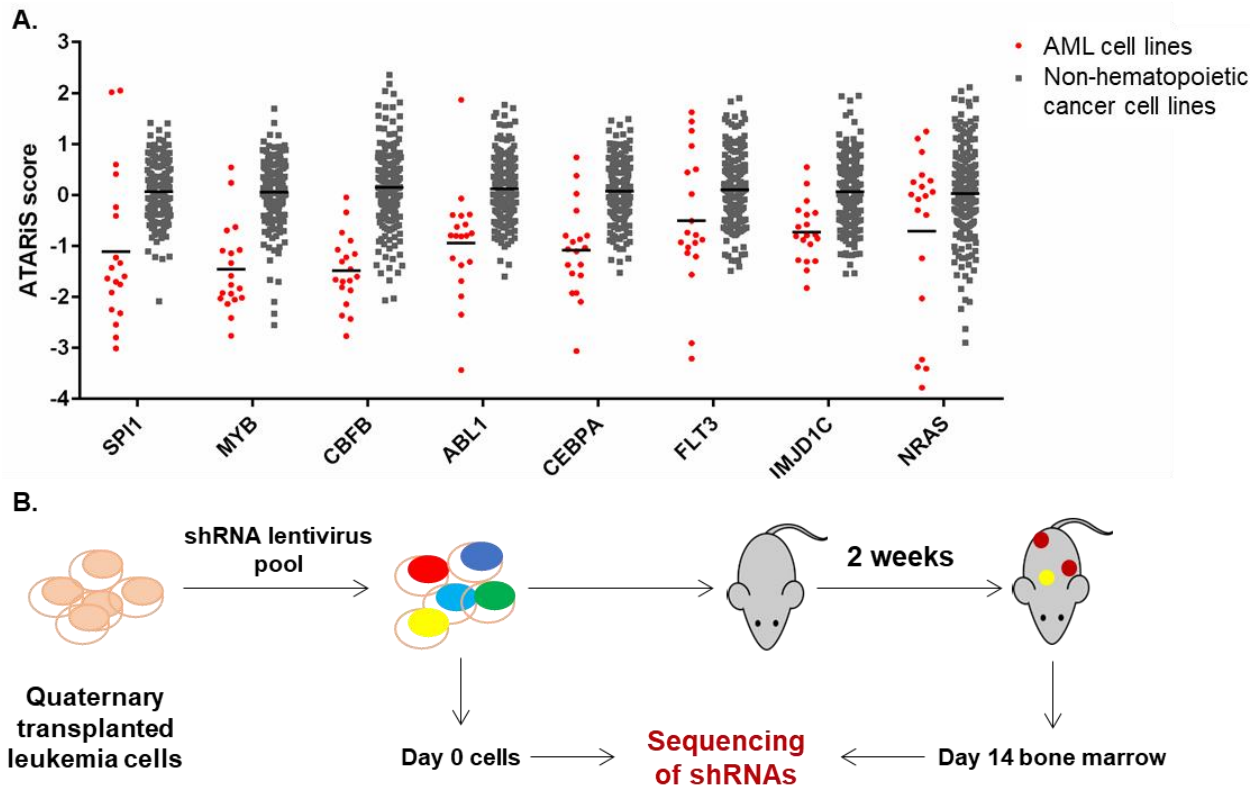

C.

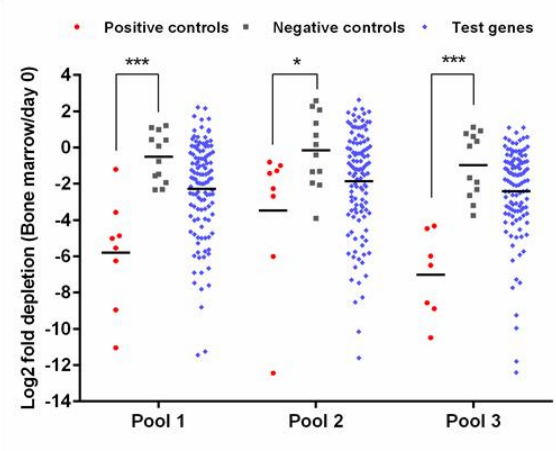

D.

Gene	# shRNAs >= 8-fold depletion	# shRNAs >= 16-fold depletion
Ogfr	4/5	3/5
Tgif2	4/5	3/5
Lclat1	3/5	3/5
Csf2rb	4/5	2/5
Bag4	3/5	2/5
Lrch4	3/5	2/5
Rab15	3/5	2/5
Zeb2	3/5	2/5
Mocs2	2/5	2/5
Pts	2/5	2/5
Taf3	2/5	2/5
Tbxas1	2/5	2/5
Ngb	3/5	1/5

Figure 4-1. AML human cell line and murine *in vivo* shRNA screens.

A. ATARiS score distribution in AML vs. non-hematopoietic cancer cell lines of example hits. **B**. Schematic representation of murine *in vivo* screen. **C**. Validation of murine *in vivo* screen. **D**. Top hits from murine *in vivo* screen.

As a confirmation of the screen's effectiveness, several genes known to be mutated in AML, including *NRAS*, *FLT3*, *CEBPA*, and *ABL1*, were among the hits (Figure 4-1A). To further validate the results of the cell line screen, my colleagues tested the top 37 hits using an *in vivo* secondary drop-out screen in mice with AML driven by the MLL-AF9 fusion oncoprotein.[340] The *MLL-AF9* fusion oncogene has been shown to drive leukemic transformation of lineage-committed GMPs, progenitor cells in the myeloid lineage.[341] The *in vivo* screening strategy is schematically represented in Figure 4-1B. shRNAs targeting the top 37 hits were grouped into three pools with respective positive and negative controls, and each pool was individually validated (Figure 4-1C). Ultimately, 13 *in vivo* hits were identified (Figure 4-1D).

Among those hits, *ZEB2* stood out as a highly expressed gene in AML and MDS (myelodysplastic syndrome; frequently diagnosed preceding AML onset[342]) compared to more-differentiated hematopoietic lineages (Figure 4-2A) based on my analysis of transcriptome data reported by Rapin et al. (2014)[343] and the Cancer Genome Atlas (TCGA).[336] This suggests that *ZEB2* may be important for AML survival and differentiation.

To experimentally test *ZEB2* knock-down's effect on human AML cells, my colleague Hubo Li transduced three independent shRNAs targeting human *ZEB2* into AML cell lines MOLM-13, SKM-1, THP-1, and U-937, and monitored the growth of the derivative cell lines. The knock-down efficiency of each sRNA in these cell lines is shown in Figure 4-2B. Remarkably, *ZEB2* depletion resulted in significant reduction in cell numbers: by the 11th day after the initial transduction of shRNAs, ZEB2-depleted cell lines showed at least 60% decrease in cell numbers relative to controls (Figure 4-2C).

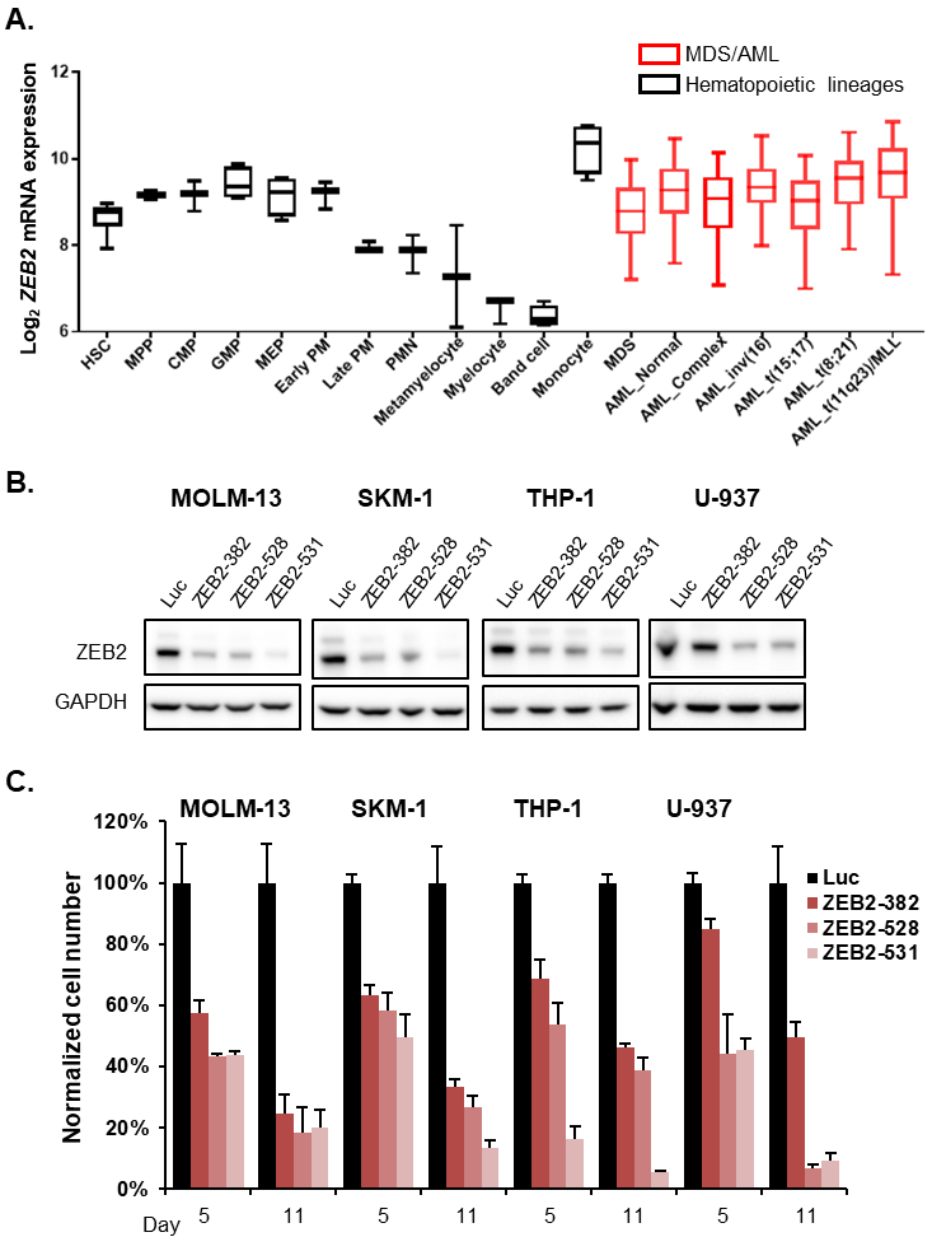

Figure 4-2. Human AML cell lines are sensitive to ZEB2 depletion.

A. *ZEB2* mRNA expression in hematopoiesis and AML. Error bars indicate 5% and 95% percentiles. **B**. Immunoblotting of ZEB2 at day 6 after shRNA lentivirus infection. **C**. Viability of AML cells after *ZEB2* knock-down. Error bars, SD (n=3).

ZEB2-382, -528, -531 refer to different shRNAs targeting *ZEB2*. Luc, control shRNA targeting luciferase. AML_Complex, complex karyotype; AML_Normal, normal karyotype; CMP, common myeloid progenitors; GMP, granulocyte monocyte progenitors; HSC, hematopoietic stem cells; MDS, myelodysplastic syndrome; MEP, megakaryocyte-erythroid progenitors; MPP, multipotential progenitors; PM, promyelocytes; PMN, polymorphonuclear cells.

Considering the differential expression of *ZEB2* in MDS/AML and normal hematopoiesis (Figure 4-2A), I set out to test whether ZEB2 regulates the differentiation of AML cells. To control for shRNAs' off-target effects,[344] I utilized a "seed control" for shZEB2-531.[301] Briefly, seed controls for shRNAs harbor 3-bp substitutions in the mid-region of the RNAi sequence, lose their ability to deplete target transcripts, and are expected to preserve any off-target effects.[345] Expectedly, the seed control for shRNA ZEB2-531, ZEB2-531-sc, no longer depletes ZEB2.[301]

Notably, flow cytometric measurement of cellular side scatter (SSC, indicative of cellular granularity),[346] as well as major GMP sub-lineage CD markers (described in 4.1.3 and Table 4-1), revealed significant shifts in distribution following *ZEB2* knock-down (Figure 4-3). Specifically, ZEB2 depletion caused induction of CD11b, CD13, and CD14 in both HL-60 and THP-1 cells, and induction of CD16 and CD66 in HL-60 cells. The seed control shRNA (ZEB2-531-sc) showed largely unchanged distributions from the control shRNA against luciferase.

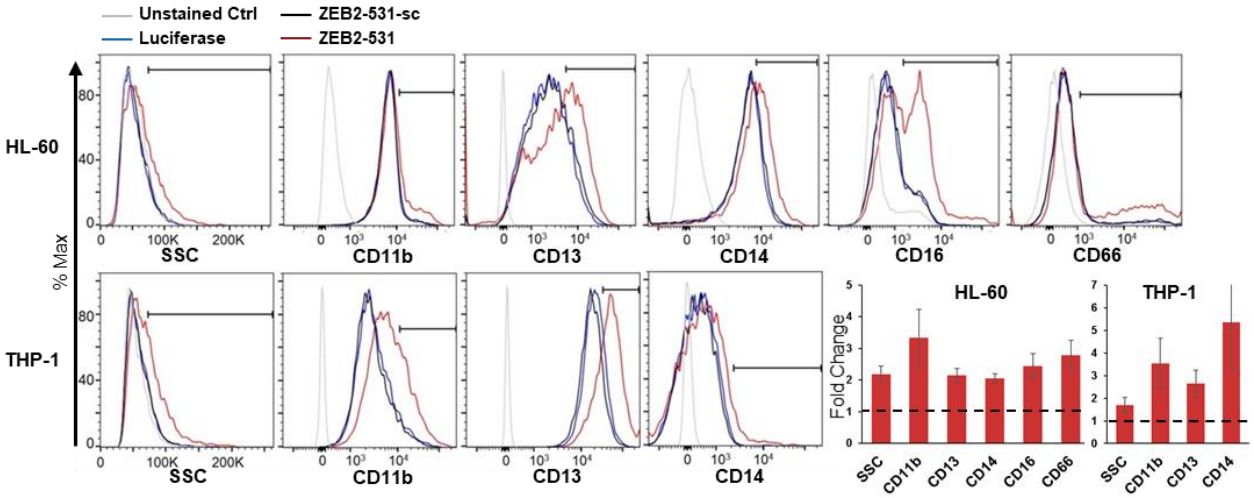

Figure 4-3. ZEB2 depletion causes aberrant differentiation in human AML cells.

HL-60 and THP-1 cells were analyzed day 6 following shRNA transduction. The bar graph quantifies average fold change of the gated populations in each panel. Error bars, SD (n=3).

To document the defects caused by ZEB2 depletion in more detail, I performed May-Grunwald-Giemsa staining in HL-60 and THP-1 cells, as well as flow cytometric measurement of their bromodeoxyuridine (BrdU) incorporation (Figure 4-4). Expectedly, 10 days following shRNA transduction, both cell lines showed increased heterogeneity, with the emergence of large, vacuolated cells (Figure 4-4A). In addition, as early as day 6 post-shRNA transduction, both cell lines exhibited lowered BrdU incorporation, indicative of impaired proliferation.[347]

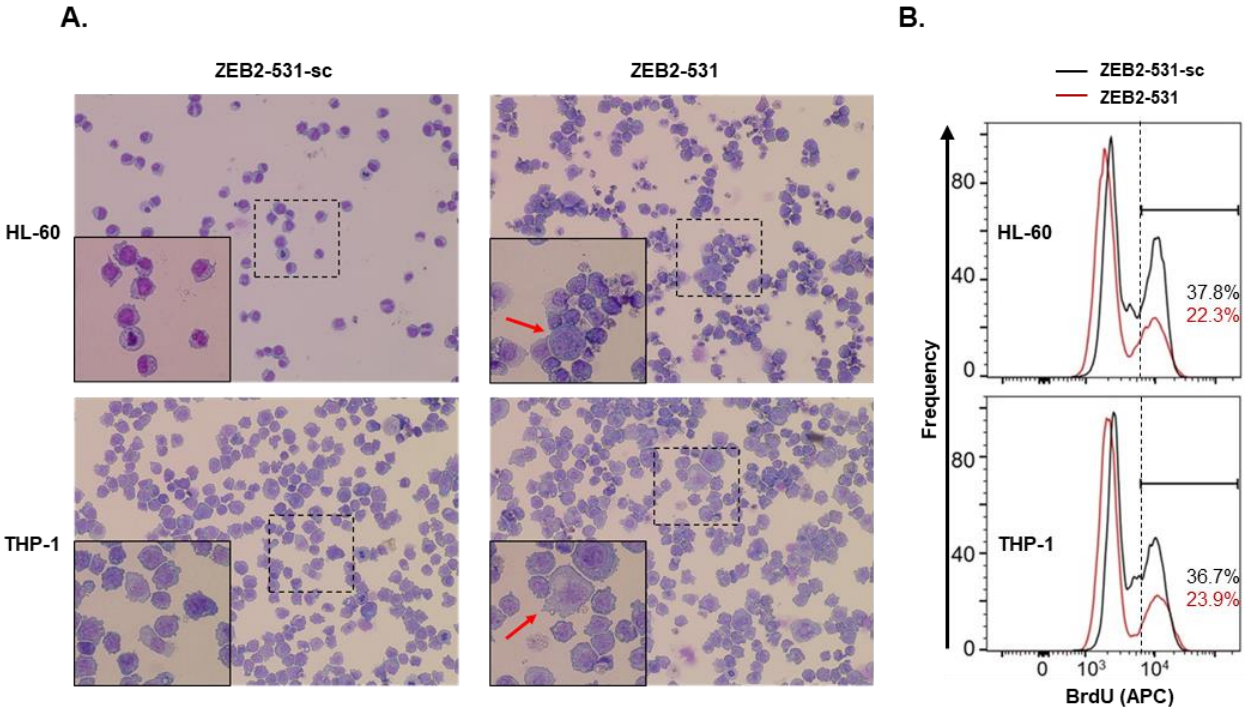

Figure 4-4. ZEB2 depletion alters AML morphology and impairs AML proliferation.

A. Representative May-Grunwald-Giemsa staining of HL-60 and THP-1 cells at day 10 after shRNA transduction. Magnification, 20X; magnification for insets, 40X. **B**. Flow cytometric analysis of BrdU incorporation in HL-60 and THP-1 cells at day 6 after shRNA transduction.

Phorbol myristate acetate (PMA) has been used by researchers to stimulate myeloid-lineage differentiation in AML cells.[348] To understand whether ZEB2 depletion mimics this more "physiologic" scenario, my collaborator Brenton Mar (Brigham and Women's Hospital, Boston, MA) and I compared PMA-induced differentiation and ZEB2 depletion in HL-60, THP-1, and U-

937 cells using flow cytometric measurement of side-scatter profiles and the panel of GMP sub-lineage CD markers (described in 4.1.3 and Table 4-1). As shown in Figure 4-5, ZEB2 depletion recapitulates some, but not all, CD marker induction by PMA.

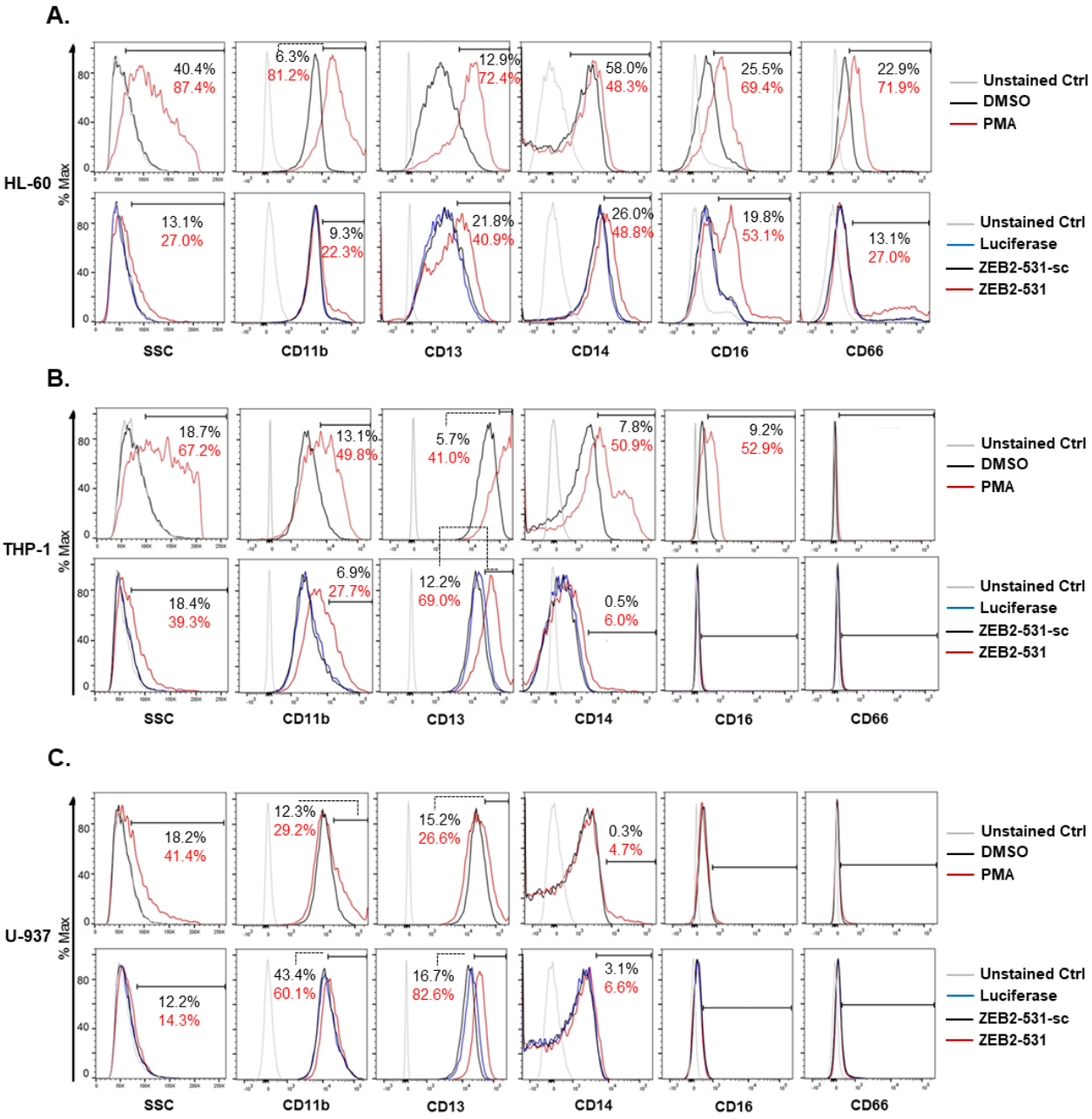

Figure 4-5. Detailed examination of ZEB2's role in regulating human AML differentiation.

Quantification of CD markers and SSC of HL-60 (**A**), THP-1 (**B**), and U-937 (**C**) cells by flow cytometry. PMA treatment was carried out at 100 ng/ml PMA or DMSO control for 4 days before analysis. For shRNA knock-down, cells were analyzed 6 days after transduction.

Given the induction of GMP sub-lineage CD markers in multiple AML cell lines by ZEB2 depletion and ZEB2's role as a transcriptional repressor during EMT, we asked whether ZEB2 may regulate myeloid differentiation through transcriptional repression. To this end, my colleague Hubo Li conducted gene set enrichment analysis (GSEA)[188] of genes upregulated in AML cell lines following ZEB2 depletion against published transcriptome data comparing neutrophils and granulocytes (both derived from GMPs)[304] to less-differentiated cells such as AML and HSCs.[349,350] Rationales for and advantages of GSEA are described in Section 2.2.2.

Specifically, the top 283 genes commonly upregulated in both THP-1 and U-937 following 72 h of ZEB2 knock-down[301] showed preferential enrichment in two independent sets of expression data comparing neutrophils to AML cells, and granulocytes to HSCs, respectively (Figure 4-6). This suggests that ZEB2 represses genes associated with myeloid phenotypes.

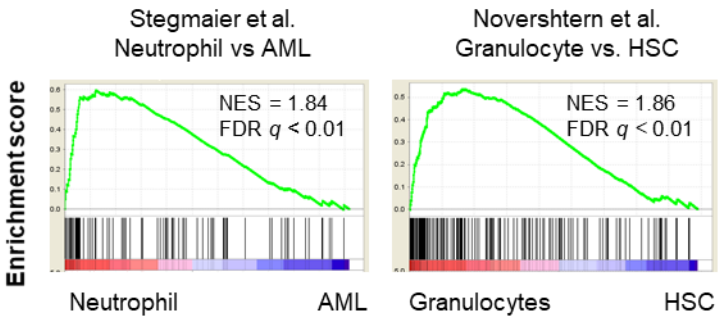

Figure 4-6. ZEB2 represses genes associated with myeloid phenotype.

GSEA analysis shows that genes upregulated after ZEB2 knock-down are enriched in neutrophils or granulocytes. FDR, false discovery rate (*q* value); NES, normalized enrichment score.

In summary, our results demonstrate that ZEB2 promotes AML proliferation and may facilitate the maintenance of AML's undifferentiated state through the repression of genes associated with the myeloid lineage.

4.3 Discussion

We have established *ZEB2* as a genetic dependency of AML through a human cell line screen coupled with an *in vivo* murine validation screen. ZEB2 depletion appears to attenuate AML proliferation by triggering aberrant differentiation via ZEB2's transcriptional repression of myeloid genes, strongly suggesting that ZEB2 is an essential regulator of AML development.

Murine *Zeb2* is required for embryonic hematopoiesis, and depletion of Zeb2 results in embryonic lethality.[318] Nevertheless, it is remarkable that adult mice with hematopoiesis-specific *Zeb2* knock-out survive for multiple months, albeit with differentiation defects that lead to cytopenias—reduction of blood cells.[351] These complementary results not only confirm ZEB2's important role in hematopoiesis, but also raise the possibility that a meaningful therapeutic window may exist: our work in mice shows that *Zeb2* knock-down induces rapid differentiation of AML cells within days to weeks.[301]

While transcription factors represent a class of difficult drug targets, recent endeavors have shown that it is possible to selectively degrade transcription factors by specific recruitment of E3 ubiquitin ligases. For instance, lenalidomide, a small molecule with clinical efficacy in multiple myeloma, causes selective ubiquitination and degradation of lymphoid transcription factors IKZF1 and IKZF3.[352,353] Furthermore, a similar strategy has been used to selectively degrade the leukemia essential protein, BRD4, via the conjugation of the small-molecule BRD4 inhibitor JQ1 to the aryl ring of thalidomide; this results in the targeting of BRD4 for proteasomal degradation by recruiting E3 ubiquitin ligases.[354] Understanding whether there is an opportunity for therapeutic ZEB2 inhibition requires rigorous evaluation.

Are ZEB2's roles in AML differentiation related to its better-known functions in transcriptionally repressing epithelial genes during EMT? Interestingly, EMT transcription factors

such as SNAI1 and SNAI2 have been reported to induce AML in mouse models,[355,356] although it is unclear whether their roles in AML are directly related to EMT pathways. It is worth noting that *Tgif2*, another top *in vivo* hit (Figure 4-1D), encodes a TGFβ-induced transcription factor known to promote EMT.[357] Furthermore, additional data from our group reveal that the transcriptional program repressed by ZEB2 in AML significantly overlaps with the genes downregulated by ZEB2 during EMT.[301] Consistent with these findings, *Zeb2* knock-out induces cell adhesion genes integrin β1 and Cxcr4, resulting in the hematopoietic stem cell retention in murine fetal livers.[318] Hence, ZEB2's core transcriptional output in epithelial cells appears to be preserved in AML.

Remarkably, *SPINT2*, the gene of interest in Chapters 2 and 3, was recently reported to be silenced in bone marrow mesenchymal stromal cells of MDS and AML patients.[97] *SPINT2* downregulation not only is part of an EMT gene expression signature,[358] but also appears to induce EMT gene expression in adherent human cells (Figure 2-6 and Table 2-1). While *SPINT2* is not expressed in whole blood,[91] stromal SPINT2 may regulate hematopoietic stem cell niche by modulating HSC and progenitor cell adhesion.[97] For instance, depletion of SPINT2 in stromal cell lines resulted in increased adhesion with HSCs and U-937 cells.[97,359] Still more intriguing, *SPINT2* and microRNAs targeting *ZEB2* are frequently downregulated in renal cell carcinomas.[208] It is therefore increasingly evident that both SPINT2 suppression and ZEB2 activity promote EMT and tumorigenesis. While it is well-established that EMT promotes stem cell characteristics,[360] these observations raise the possibility that EMT induces mutually reinforcing intrinsic and extrinsic signaling programs in both hematopoietic progenitors and their niches.

In conclusion, this and other studies[318-322,351] have demonstrated that ZEB2 is a critical regulator of hematopoietic development and malignancies. Future directions of this work may follow three main tracks. First and foremost, most of the *in vivo*-validated hits (Figure 4-1D) have

not been well-characterized in the context of AML differentiation and proliferation. *Taf3*, for instance, is a transcription factor that regulates myoblast differentiation.[361] It is therefore interesting, and feasible, to leverage techniques used in this chapter to dissect functions of additional genetic dependencies of AML. Second, ZEB2 target genes and protein binding partners during AML development remain to be elucidated. These questions can be addressed using methods such as chromatin immunoprecipitation-sequencing (ChIP-Seq) and mass spectrometry following co-immunoprecipitation. Lastly, it is unclear whether ZEB2 promotes AML onset. In this study, we utilized human AML cell lines and mice with AML driven by a well-characterized oncogene (*MLL-AF9*).[301] These systems are not suitable for testing ZEB2's roles during the initial stages of AML development. Mouse models of ZEB2 gain- or loss-of-function in myeloid lineages will enable the *in vivo* examination of ZEB2's functions in AML initiation.

4.4 Materials and Methods

Screening and screen data analysis

Seventeen (17) AML cell lines were obtained from CCLE or DSMZ (Table 4-2), and contributed to the RNAi screen platform (Broad Institute). Screening and analytical methods were described previously.[338] To select genes with at least 2 significant shRNAs, an additional filter was created to exclude genes with only 2 significant shRNAs but more than 5 shRNAs included in the library (<40% significant shRNAs). ATARiS score is computed based on the confidence that each RNAi reagent's observed phenotypic effects are the result of on-target gene suppression.[339] *In vivo* screen and analysis protocols are described in Li et al. (2017).[301]

Table 4-2. AML cell lines used in the human shRNA screen.

Cell line	Source	FAB subtype	Known gene fusions	NRAS status
AML-193	CCLE	M5		$NRAS^{G13V}$
F-36P	CCLE	M6		
HL-60	CCLE	M2		$NRAS^{Q61L}$
HNT-34	DSMZ	M4	BCR-ABL1	
KASUMI-1	CCLE	M2	AML1-ETO	
MOLM-13	CCLE	M5a	MLL-AF9	
MONO-MAC-1	CCLE	M5	MLL-AF9	
MONO-MAC-6	CCLE	M5	MLL-AF9	
MV4-11	CCLE	M5	MLL-AF4	
NB-4	CCLE	M3	PML-RARA	
NOMO-1	CCLE	M5a	MLL-AF9	
OCI-AML-2	CCLE	M4		
OCI-AML-3	CCLE	M4		$NRAS^{Q61L}$
OCI-AML-5	CCLE	M4		
PLB-985*	DSMZ	M2		$NRAS^{Q61L}$
SKNO-1	DSMZ	M2	AML1-ETO	
THP-1	CCLE	M5	MLL-AF9	$NRAS^{G12D}$

* *PLB-985 is a sub-clone of HL-60.*

Cell culture, viral transduction of shRNA vectors, and antibodies

HL-60, THP-1, and U-937 cells were cultured in RPMI-1640 (Life Technologies) supplemented with 10% (v/v) FBS and 1X Pen/Strep. Phorbol myristate acetate (PMA; Sigma-

Aldrich P8139) treatment was carried out at 100 ng/ml and a duration of 4 days. Viral production followed the procedure described in Section 2.4. In addition, viral media were concentrated by PEG-it (System Biosciences LV810A-1). To virally transduce shRNA vectors, spin infection of human AML cells was performed at 2,500 rpm for 2 hours at 30°C with 8 μg/ml polybrene (Thermo Fisher Scientific NC9515805).

The following antibodies and dilution were used for standard immunoblots in this chapter: GAPDH (1:10,000, Abcam ab8245); ZEB2 (1:1,000, Bethyl Laboratories A302-474A).

Plasmid vectors and cloning

shRNAs (Table 4-3) targeting ZEB2 and firefly luciferase in puromycin resistant vectors (pLKO.1 or pLKO_TRC005), as well as empty shRNA vector labeled with GFP (pLKO_TRC019) were obtained from the RNAi Consortium. All shRNAs were cloned into pLKO_TRC019 from the original puromycin vector using standard cloning protocol. Seed control shRNA for ZEB2-531 (ZEB2-531-sc) was cloned into TRC019 using the protocol provided by the RNAi Consortium and described in Li et al. (2017)[301].

Table 4-3. shRNA sequences targeting human and murine ZEB2.

Gene (species)	Name	TRC #	Target sequence
ZEB2 (human)	ZEB2-382	TRCN0000420382	CTGTACTTTCCTTTCGCTATT
ZEB2 (human)	ZEB2-528	TRCN0000013528	GCAGTTCCTTAGTTTACATAT
ZEB2 (human)	ZEB2-531	TRCN0000013531	CCCGAAACGATACGAGATGAA
ZEB2 (human)	ZEB2-531-sc	-	CCCGAAAGCTTACGAGATGAA
Zeb2 (mouse)	Zeb2-02	TRCN0000070884	CCGAATGAGAAACAATATCAA
Zeb2 (mouse)	Zeb2-03	TRCN0000070887	CCCATTTAGTGCCAAGCCTTT
Zeb2 (mouse)	Zeb2-04	TRCN0000070886	CCAGTGTCAGATTTGTAAGAA
Zeb2 (mouse)	Zeb2-05	TRCN0000070861	ATGCAATTTAGCCACTAATAG
Zeb2 (mouse)	Zeb2-06	TRCN0000070883	CCACTAGACTTCAATGACTAT
Luciferase (firefly)	Luc	-	CACTCGGATATTTGATATGTG

Flow cytometry

Each experiment was performed in biological triplicates; each triplicate represents the analysis of 100,000 cells by BD LSRFortessa X-20 (BD Biosciences). BrdU incorporation was performed with the APC BrdU Flow Kit (BD Pharmingen) according to the manufacturer's instructions. Briefly, 2–3×10^5 cells were seeded in 1 ml medium and pulsed with 10 μM BrdU for 1 hour. Cells were treated with BD Cytofix/Cytoperm Buffer, BD Cytoperm Plus Buffer, and then re-fixed with Cytofix/Cytoperm Buffer. Cells were then treated with 10 μg DNase for 1 hour at 37°C, and stained with 1:50 BrdU antibody. Cells were then immediately washed with BD Cytoperm/Wash buffer and analyzed.

CD marker staining was performed using the following fluorescently conjugated antibodies: CD11b-PE-Cy7, CD13-APC, CD14-APC-Cy7, CD16-PE-Cy5, and CD66-PE (BD Biosciences). Single-channel staining was performed for all samples to determine fluorescence compensation. Briefly, 1×10^6 cells were washed twice in staining buffer (PBS, 0.2% BSA), resuspended in 80 μl staining buffer and 20 μl antibody, and incubated 20 minutes on ice in dark. Cells were then washed twice in staining buffer and analyzed.

May-Grunwald-Giemsa staining

HL-60 and THP-1 cells were virally transduced with GFP-labeled shRNA and sorted at day 4 post-transduction. At day 10 post-transduction, cells were spun onto glass slides by cytospin and fixed with methanol for 5 minutes, stained with May-Grunwald (Sigma-Aldrich MG80) for 5 minutes, and then washed with PBS for 5 minutes. Slides were then stained with 1:20 freshly made Giemsa stain (Sigma-Aldrich GS1L) for 20 minutes, and washed with ddH_2O. Images for air-dried slides were taken at 20X and 40X magnification.

AML genomic data and Gene Set Enrichment Analysis (GSEA)

Mutation, microRNA, and methylation data of TCGA AML samples were downloaded from the Broad Institute TCGA GDAC Firehose (gdac.broadinstitute.org) or UCSC Cancer Genome Browser (genome-cancer.ucsc.edu). CCLE mRNA expression data were obtained from the data portal (broadinstitute.org/ccle/home). GSEA of the 353 screen hits was performed based on methods described in Section 2.4 and Li et al. (2017).[301] Normalized microarray data from Stegmaier et al. (2004)[349] and Novershtern et al. (2011)[350] were downloaded respectively from the Broad Institute Cancer Program and the Differentiation Map Portal (broadinstitute.org/dmap/). One thousand (1,000) gene set permutations were used in GSEA.

4.5 Chapter Contributions

I had the privilege to contribute to the publication of these findings[301] thanks to Hubo Li, Ph.D. '15, who spearheaded this work during his graduate studies. Hubo Li built and validated all reagents,[301] and contributed data shown in Figure 4-1, Figure 4-2B–C, and Figure 4-6, and respective methods. The human AML cell line screen was conducted as part of Project Achilles.[338] The murine screen was primarily performed by Hubo Li and Brenton Mar in Prof. Benjamin Ebert's group (Brigham and Women's Hospital, Boston, MA). Francisca Vazquez and Barbara Weir in Prof. William Hahn's group (Broad Institute, Cambridge, MA) analyzed screen data.

My special thanks go to Brenton Mar, who offered essential guidance that enabled me to acquire and analyze the data in Figure 4-2A and Figure 4-3–Figure 4-5; collaborated with me on the analysis for Figure 4-5; and provided constructive comments on this chapter.

Chapter 5 : Conclusions and Future Directions

5.1 Conclusions

5.1.1 SPINT2 is a versatile tumor suppressor

5.1.2 Is aneuploidy tolerance an integral part of oncogenic signaling?

5.1.3 SPINT2 and ZEB2 are regulators of epithelial-mesenchymal transition (EMT)

5.2 Future Directions

5.2.1 Define the SPINT2-YAP signaling mechanism

5.2.2 Evaluate YAP's role in aneuploidy tolerance

5.2.3 Characterize SPINT2's role in tumorigenesis

5.1 Conclusions

5.1.1 SPINT2 is a versatile tumor suppressor

SPINT2 is a putative tumor suppressor that has emerged as a cell-surface factor on which multiple extracellular signals converge. It functions through three main pathways (Figure 5-1).

First, through its previously documented inhibitory effects on hepsin and HGFA,[86,190,191] SPINT2 restricts growth factor-mediated signaling and downstream activation of AKT and ERK.[178] Second, SPINT2 likely serves as a regulator of extracellular matrix remodeling via suppression of matrix-degrading proteases. For instance, matriptase, one of SPINT2's best-characterized inhibitory targets,[88,89,177,222,237] has been shown to degrade extracellular matrix proteins *in vitro*,[362] mediate matrix remodeling in prostate cancer,[363] and also promote cartilage collagenolysis in osteoarthritis.[364] Lastly, as shown in Chapter 2, SPINT2 limits YAP/TAZ transcriptional activity through inhibition of PAR1 and PAR2. Loss of SPINT2 results in the induction of YAP/TAZ and EMT gene expression signatures (Figure 2-6).

Given these discrete yet interrelated mechanisms, it is not surprising that SPINT2 loss confers cellular tolerance for multiple stresses including DNA damage, cytokinesis failure,[178] and chromosome missegregation (Chapter 3). The signaling and phenotypic interactions surrounding SPINT2 (Figure 5-1) reveals a potentially self-reinforcing mechanism of malignant transformation.

To illustrate: upon early epigenetic silencing of *SPINT2*, a premalignant cell may become capable of continued proliferation following DNA damage or chromosome missegregation, hence permitting additional oncogenic alterations to accumulate. For example, during the subsequent cell cycles, the daughter cells may lose tumor suppressors such as p53 or gain oncoproteins such as mutant KRAS.[9] Mutant KRAS, in turn, may maintain the silencing of *SPINT2* (Figure 3-5A) and other tumor suppressor genes.[257] In addition, growth factor signaling, YAP activity, and protease-

mediated migratory phenotypes potentiated by SPINT2 loss may continue to fuel cell proliferation, migration, as well as the genome instability (e.g., Figure 3-10) that initiates another round of mutagenesis, further advancing the tumorigenic process.

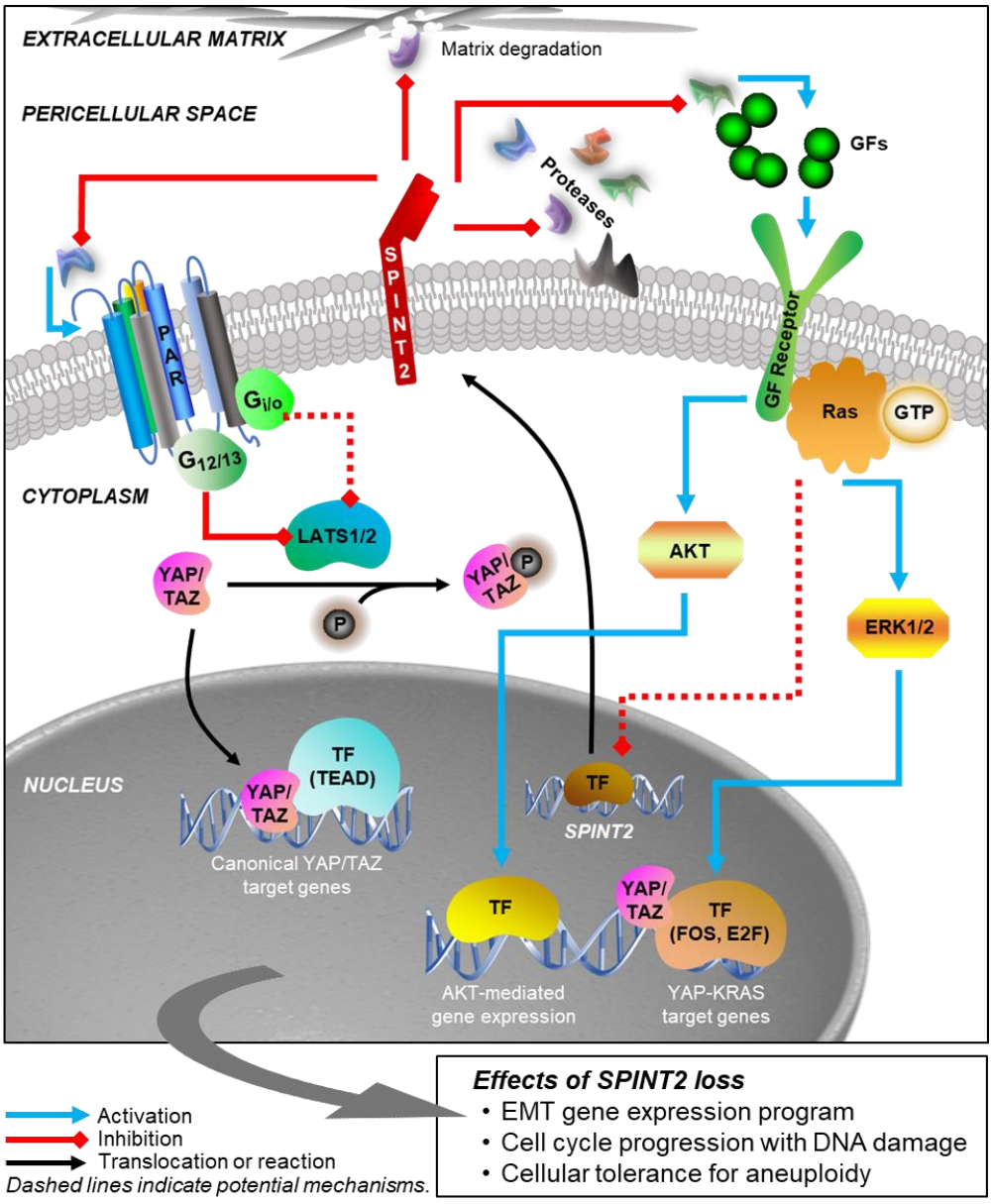

Figure 5-1. A model of the SPINT2-mediated signaling network.

Schematic representation of known and potential signaling components regulated by SPINT2. GF, growth factor; P, phosphoryl group; TF, transcription factor. Not drawn to scale.

Embodying this intriguing model of interactions between tumor microenvironment, cell signaling, and genome instability is the empirical observation of the chromosome 11q22 amplicon, a recurrent structural genome abnormality frequently seen in human tumors such as glioblastomas, oral squamous-cell carcinomas, and pancreatic, lung, ovarian, and cervical cancers.[136,365] Chromosome 11q22 harbors *YAP1*, as well as genes encoding multiple MMPs and anti-apoptotic proteins.[136] Remarkably, in murine transplantation models, mammary epithelial tumors derived from oncogenic tetraploid cells, as well as *Myc* oncogene-driven hepatocellular carcinomas, have been shown to harbor mouse chromosome 9qA1 amplicons syntenic to human 11q22.[138,139]

In summary, SPINT2 inhibits intracellular proliferative and migratory signals triggered by the extracellular environment. Specifically, I have demonstrated that SPINT2 attenuates YAP/TAZ activity by inhibiting endogenous protease-mediated activation of PAR1 and PAR2. This signaling process likely depends on the suppression of $G_{i/o}$ and the activation of LATS kinases. Phenotypically, I have shown that SPINT2 depletion induces an EMT gene expression signature and confers cellular tolerance for aneuploidy. Detailed characterization is required to dissect the intermediary factors linking SPINT2 and YAP, as well as the crosstalk between SPINT2-mediated signals in the physiological context.

5.1.2 Is aneuploidy tolerance an integral part of oncogenic signaling?

While it is currently unclear whether the aneuploidy tolerance conferred by SPINT2 depletion is a result of YAP activation (discussed in Section 3.3.2), my findings raise the possibility that instead of requiring separate cellular machineries, tolerance for aneuploidy may be a direct result of oncogenic signaling. In other words, SPINT2 depletion-induced YAP activation

may not only promote oncogenic processes such as EMT gene expression, but also allow cells to better tolerate consequences of chromosome missegregation.

Recently, Sheltzer et al. (2017)[174] showed that HCT-116 cells harboring trisomies experienced growth delays. Specifically, in a competition assay starting with equal numbers of diploid and trisomic cells, cells harboring single-chromosome trisomies dropped to or below 30% of the combined population by the sixth day.[174] These observations confirm prior findings that gaining a single chromosome causes a significant reduction in cellular fitness,[162,169] and also suggest that the endogenous oncogenic alterations such as mutant KRAS in HCT-116 cells are insufficient to equalize the differential fitness between euploids and aneuploids.[174] In contrast, within an identical time frame of six days following chromosome missegregation, SPINT2 depletion almost completely abrogated the rapid drop-out of aneuploid cells observed in the wild-type HCT-116 population (Figure 3-6 and Figure 3-7). This finding suggests that SPINT2 loss largely restores the reduced fitness associated with aneuploidy.

It is important to note that SPINT2 depletion confers aneuploidy tolerance without inducing chromosome instability; basal levels of aneuploidy in HCT-116 cells without drug treatment remained unchanged following SPINT2 knock-down (Figure 3-6 and Figure 3-7). This conclusion is corroborated by the observed *SPINT2* silencing in aneuploid but chromosomally stable RPE-1 cells (Figure 3-2–Figure 3-4). Therefore, SPINT2 represents a putative tumor suppressor that limits aneuploidy tolerance without directly regulating chromosome segregation.

It has been demonstrated that potent tumorigenic signals such as overexpression of oncogenic mutant KRAS or loss of tumor suppressor RB almost inevitably lead to aneuploidy due to the induced genome instability.[172,366,367] However, these models prevent the precise interpretation of how oncogenes may confer cellular tolerance for aneuploidy due to global cellular

defects and constant genomic changes (e.g., Figure 3-10; discussed in Section 3.2.3). Therefore, moderate and defined whole-chromosome aneuploidies are best-suited for investigating mechanisms of aneuploidy tolerance. Mechanisms by which SPINT2 suppresses aneuploidy tolerance, and whether these mechanisms are related to SPINT2's role in regulating YAP, require further investigation.

5.1.3 SPINT2 and ZEB2 are regulators of epithelial-mesenchymal transition (EMT)

A common thread that connects Chapters 2–4 is SPINT2 and ZEB2's roles in modulating EMT. ZEB2 is a well-characterized promoter of EMT (discussed in Section 4.1.2) known for its repression of epithelial markers such as E-cadherin and its activation of mesenchymal genes such as N-cadherin and MMPs.[312] Loss of ZEB2 results in aberrant differentiation of AML cells (Figure 4-5), and interestingly, also suppresses cell migration and invasion in solid tumors such as Ewing sarcoma[368] and colorectal cancer.[369]

SPINT2, on the other hand, appears to repress an EMT gene expression program (Figure 2-6). Indeed, SPINT2's canonical inhibitory target, HGF signaling, is known to induce EMT.[312] YAP and TAZ have also been shown to mediate EMT through TEAD family transcription factors.[231] Furthermore, in renal cell carcinoma and melanoma cells that epigenetically silence *SPINT2*, restoration of *SPINT2* expression suppresses cell migration.[96,100] Taken together, my results on ZEB2 and SPINT2 highlight the central role of EMT in mediating tumorigenic processes such as enhanced stem cell characteristics and migratory phenotypes.[370]

In summary, my dissertation research has elucidated a putative tumor suppressor pathway mediated by SPINT2 and an oncogenic program regulated by ZEB2. My findings expand our

understanding of mechanisms that promote cancer development and provide the basis for follow-up investigations. I outline several specific future directions in the following section.

5.2 Future Directions

5.2.1 Define the SPINT2-YAP signaling mechanism

I have established that SPINT2 limits YAP activity by inhibiting PAR1 and PAR2 activation (Figure 2-7 and Figure 2-9). Additionally, I have identified $G_{i/o}$ as a necessary component in this pathway (Figure 2-7). Furthermore, we have obtained preliminary data suggesting that SPINT2 promotes LATS phosphorylation (Figure 2-5).

$G_{i/o}$ inhibits adenylyl cyclase (AC) and AC-mediated cellular cAMP production.[66] Considering cAMP's direct activation of protein kinase A (PKA)[66] and potential PKA-mediated LATS phosphorylation,[144] we hypothesize that when SPINT2 is depleted, PAR1/2-$G_{i/o}$ signaling is activated, leading to suppression of cellular cAMP production; the lowered cAMP leads to attenuated PKA-mediated LATS phosphorylation, and consequently, activation of YAP/TAZ. The following experimental plan is geared toward addressing this hypothesis as well as informing potential alternative models.

Confirm $G_{i/o}$ dependency of SPINT2-YAP signaling by orthogonal inhibition

$G_{i/o}$ was identified using previously validated siRNAs (Table 2-2) as a dependency of YAP activation following SPINT2 depletion (Figure 2-7). Biochemical inhibition of $G_{i/o}$ can serve as an orthogonal approach to complement this finding. Pertussis toxin (PTX) is a commonly used $G_{i/o}$ inhibitor.[371-373] PTX is a bacterial protein toxin that specifically ADP-ribosylates $G_{i/o}$ subunits,

locking the G protein in an inactive state.[373] $G_{i/o}$-coupled GPCRs in cells pre-treated with PTX (on the order of 10–100 ng/ml) for 16–24 h are rendered unresponsive to ligand stimulation.[374,375]

In human colorectal carcinoma cell line HT-29, lysophosphatidic acid (LPA) induces robust ERK phosphorylation in a $G_{i/o}$-dependent manner.[375] Therefore, ERK phosphorylation status may serve as a positive control for the effectiveness of PTX treatment.

PTX treatment of RPE-1 and HCT-116 cells following SPINT2 depletion is expected to mimic the effect of $G_{i/o}$ siRNA in abolishing YAP target gene expression. Although unlikely, it is possible that PTX treatment may not yield results consistent with RNAi experiments; this would suggest that siRNAs against G_i and G_o subunits (Table 2-2) exerted off-target effects. Transgenic expression of dominant-negative mutants of G_α subunits may help resolve this potential discrepancy.[376] Notably, dominant-negative mutants of all major categories of G_α subunits have been characterized, including G_{i2}^{S48C}, G_o^{S47C}, and G_o^{G203T}.[376]

Determine whether PKA mediates SPINT2's suppression of YAP

Considering its potential role in phosphorylating LATS kinases,[144] PKA is a key link in our hypothesized pathway. PKA is a holoenzyme with multiple subunits[377] and is therefore not amenable to RNAi knock-down. Small-molecule PKA inhibitors such as H-89[378] and (R_P)-cAMPS,[379] and activators such as forskolin,[380,381] can be used to examine PKA's potential role in SPINT2-based YAP regulation. As a positive control for inhibitor or activator treatment, PKA activity can be measured by phosphorylation of CREB, a well-characterized PKA substrate.[382]

First, it would be highly informative to understand whether SPINT2 promotes PKA activity. This can be determined using SPINT2 gain-of-function by overexpressing *SPINT2* ORF and measuring CREB phosphorylation. SPINT2 overexpression is expected to increase PKA-mediated

CREB phosphorylation due to the inhibition of $G_{i/o}$. Furthermore, PKA activation or inhibition can serve as a co-treatment in SPINT2 loss- and gain-of-function experiments, respectively. In cells transfected with *SPINT2* siRNA, forskolin is expected to abrogate the observed YAP dephosphorylation, nuclear localization, and target gene expression. Conversely, in cells overexpressing *SPINT2*, H-89 or (R_P)-cAMPS is expected to negate the suppression of YAP.

Evaluate SPINT2's effect on cellular cAMP

In addition, SPINT2 is hypothesized to promote cellular cAMP production through PAR1/2 and $G_{i/o}$ inhibition. Therefore, to fully characterize the potential PKA-mediated pathway downstream of SPINT2-mediated $G_{i/o}$ signaling, cellular cAMP can be measured following SPINT2 depletion or overexpression using commercially available assays (e.g., LANCE cAMP Detection Kit, PerkinElmer AD0262). SPINT2 overexpression is expected to result in an increase in cellular cAMP. Forskolin, an activator of PKA through promotion of cAMP production, serves as a positive control for cAMP assays.

The results from the aforementioned experiments will either support our model or inform alternative hypotheses. While $G_{i/o}$ predominantly inhibits AC-cAMP signaling,[66] it has been shown to modulate a wide array of cellular effectors including ion channels (Ca^{2+}, K^+, and Na^+), diacylglycerol (DAG) kinase, and phosphatidylinositol-4-kinase (PI4K).[383] Indeed, it was recently reported that HEK-293A cells treated with 12-*O*-tetradecanoylphorbol-13-acetate (TPA), a DAG analog, exhibited YAP dephosphorylation and nuclear localization.[384] Therefore, it is possible that SPINT2 may regulate YAP through PKA-independent pathways.

5.2.2 Evaluate YAP's role in aneuploidy tolerance

As noted in Section 3.3.2, it remains to be elucidated whether YAP activity directly contributes to the increased cellular tolerance for aneuploidy conferred by SPINT2 depletion. While overexpression of phosphorylation-resistant YAP is thought to result in mitotic defects[127] that render chromosome FISH results difficult to interpret, double knock-down of LATS1 and LATS2 by shRNAs has also proved to be an ineffective method to investigate functional consequences of moderate YAP activation. Namely, *LATS1* mRNA exhibited significant compensatory expression following *LATS2* knock-down (Figure 5-2). This compensatory regulation persisted when the concentrations of viruses for infection and subsequent antibiotics for selection (*LATS1* shRNA, neomycin; *LATS2* shRNA, puromycin) were doubled, ruling out the possibility of insufficient viral titers or low shRNA expression.

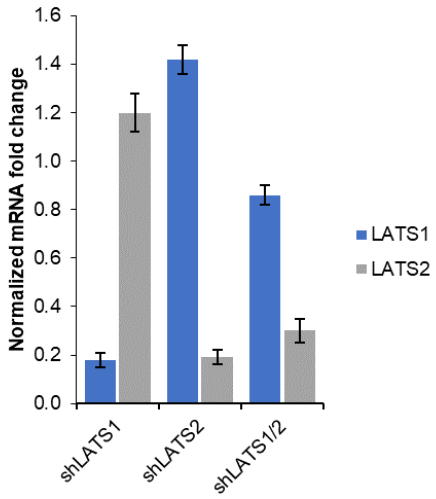

Figure 5-2. LATS1 and LATS2 are resistant to double shRNA knock-down.
LATS2 knock-down induces *LATS1* mRNA expression in HCT-116 cells. Error bars, SD (n=3).

Therefore, a more plausible method to attain mild YAP activation (similar to that resulting from SPINT2 knock-down) may be titratable expression of wild-type YAP or YAP-5SA using inducible promoters such as the cumate gene switch[385] or metallothionein promoter-based

systems.[386,387] Empty vectors will serve as negative controls, while the titratable level of YAP activation can be calibrated using gene expression (panel of target genes by qPCR or transcriptome-wide measurement by microarrays) against transcriptome data from SPINT2-depleted cells. Subsequently, cells will be treated with monastrol or AZ3146 to induce chromosome missegregation, and whether aneuploid cells persist in the population will be measured using chromosome FISH (as in Figure 3-6).

This experiment will more definitively address whether moderate YAP activation confers aneuploidy tolerance. If a moderate level of YAP activation similar to that induced by SPINT2 depletion does not lead to a heightened tolerance for aneuploidy, we hypothesize that SPINT2 depletion induces an increase in growth factor signaling that contributes to this phenotype. To test this alternative hypothesis, cells will be treated with growth factors (such as IGF for RPE-1 or EGF for HCT-116) in amounts that result in comparable levels of elevated AKT and ERK phosphorylation in a serum starvation and re-stimulation assay.[178] Chromosome FISH will be performed following monastrol- or AZ3146-induced chromosome missegregation.

5.2.3 Characterize SPINT2's role in tumorigenesis

Determine whether SPINT2 restricts cell motility via YAP/TAZ suppression

SPINT2 loss has been linked to enhanced cell migration and invasion via increased matriptase activity in prostate cancer.[177] However, the underlying mechanisms remain unclear. For example, the migratory and invasive phenotypes may be due to matriptase-mediated extracellular matrix degradation,[364] YAP/TAZ-mediated transcription (Figure 2-4), or an EMT gene expression program (Figure 2-6) potentially independent of YAP/TAZ.

To test YAP/TAZ dependency of SPINT2's suppression of cell motility, it would be worthwhile to perform transcriptome analyses on SPINT2-depleted cells treated with YAP/TAZ dual-specific siRNA (Table 2-2).[232] I expect to observe that the EMT gene expression signatures no longer enrich in the resultant transcriptome data, confirming prior reports that YAP and TAZ promote EMT[212,231,232] and establishing this regulation in the cell lines used in this dissertation.

Phenotypically, cell migration can be measured using a wound healing assay[388] in SPINT2-depleted RPE-1,[389] HCT-116,[390] and MCF-10A cells.[391] In addition to SPINT2 knock-down in otherwise unperturbed conditions, two co-treatments should be performed to provide additional insights on SPINT2's regulation of cell motility.

First, YAP/TAZ knock-down can demonstrate whether potential migratory phenotypes resulting from SPINT2 depletion are dependent on YAP or TAZ. I hypothesize that YAP/TAZ knock-down will attenuate or completely abolish cell motility induced by SPINT2 siRNA.

Second, pro-HGF can be used to as a co-treatment to increase the dynamic range of the wound healing assay. Pro-HGF, a latent precursor, is proteolytically processed to generate active HGF, a growth factor that enhances cell motility via MET signaling.[392-395] Proteolytic activation of pro-HGF is inhibited by SPINT1 and SPINT2.[191]

Therefore, SPINT2-depleted cells are expected to activate pro-HGF more efficiently and exhibit enhanced motility. If this increased motility is eliminated when cells are co-transfected with YAP/TAZ siRNA, it suggests that YAP/TAZ are downstream effectors of HGF-MET signaling and that there is crosstalk between HGF and Hippo pathways.

Alternatively, it is possible that SPINT2 may mediate cell motility predominantly through protease-mediated extracellular matrix remodeling[364] but not YAP/TAZ or HGF. A gelatin degradation assay helps address this hypothesis by measuring extracellular matrix degradation of

cells with SPINT2 depletion or overexpression. Briefly, cells will be plated on a uniform layer of fluorescently labeled gelatin, and loss of fluorescence signifies gelatin degradation.[396] Therefore, if SPINT2 restricts cell motility mainly through inhibition of extracellular matrix remodeling, I expect to observe increased gelatin degradation following SPINT2 depletion.

Determine whether SPINT2 loss promotes oncogenic transformation

SPINT2 depletion alone does not appear to initiate oncogenic transformation (Figure 2-11). However, considering *SPINT2* silencing in cancers ranging from medulloblastoma to renal cell carcinoma,[94-100] it is likely that SPINT2 loss cooperates with other signals in a multi-step process[397] to potentiate tumorigenesis. The principle of multi-step transformation of mammalian cells has been extensively documented in the literature,[397] and can be illustrated with the following two examples. First, tetraploid $p53^{-/-}$ mouse mammary epithelial cells exhibited anchorage-independent growth only after treatment with mutagen 7,12-dimethylbenz[*a*]anthacene (DMBA) followed by tumor promoter 12-*O*-tetradecanoylphorbol-13-acetate (TPA).[139] Along the same line, transformation of hTERT-immortalized human fibroblasts already harboring functional loss of p53 and overexpression of MYC requires additional loss of tumor suppressor RB.[398] Therefore, it is informative to examine the pathological role of SPINT2 loss using *in vitro* and *in vivo* models of cooperative tumorigenesis.

In vitro studies of oncogenic transformation will be carried out using soft agar assay of MCF-10A human mammary epithelial cells for anchorage-independent growth. MCF-10A is a well-characterized cell line model for oncogenic transformation and has been shown to transform upon YAP overactivation.[136] Specifically, an initiating perturbation will be introduced to cells with or without shRNA against *SPINT2*, and the course of colony formation on soft agar will be

monitored. As shown in Figure 2-11, $KRAS^{G12V}$ expression (with or without p53 suppression) induces robust colony formation and may be used as an initiating condition; however, considering the high potency of oncogenic KRAS, it may be difficult to distinguish potential additive effects of SPINT2 depletion.

Alternatively, it has been shown that HGF induces anchorage-independent growth of MCF-10A cells.[399] Given SPINT2's inhibitory effect on HGF signaling, it is especially interesting to understand whether SPINT2 suppression accelerates HGF or pro-HGF-driven colony formation on soft agar. I hypothesize that SPINT2 depletion accelerates HGF-mediated anchorage-independent growth. To complement SPINT2 loss-of-function assays, the effect of SPINT2 overexpression on HGF-induced transformation of MCF-10A cells can be examined. As described in Section 2.4, it is possible to moderately overexpress *SPINT2* ORF without compromising cell proliferation and viability (personal observations) using a cumate-inducible system. In prior studies that examined SPINT2 overexpression in long-term soft agar assays, the proliferation or viability of starting cells was significantly compromised,[94,100] presumably due to the overly strong expression of *SPINT2* ORF. Therefore, cumate-inducible *SPINT2* expression represents a more nuanced approach that enables detailed dissection of SPINT2's role as a tumor suppressor.

In vivo studies of SPINT2 function will greatly benefit from tissue-specific *Spint2* knock-out murine models using Cre-lox recombination.[400] In these models, the *Spint2* genomic sequence, when flanked by *lox* sites, would be deleted in the presence of tissue-specific Cre recombinase. In adult mice, *Spint1* and *Spint2* are frequently co-expressed in somatic tissues including colon, gallbladder, pancreas, trachea, and kidney.[89] On the other hand, *Spint2*, but not *Spint1*, has been detected in adult murine gastric parietal cells, ovary, lymph nodes, brain, and cerebellum;[89] these tissues will enable the specific investigation of Spint2's functions.

Considering Spint2's role in embryonic neural development,[80] as well as silencing of *SPINT2* in human medulloblastoma (pediatric cancers of the cerebellum),[95] the cerebellar tissue is of particular interest for understanding Spint2's role *in vivo*. Several genetically defined murine medulloblastoma models have been developed.[401] For example, when conditionally driven by cerebellar progenitor- or cerebellar-specific promoters such as *hGFAP*, *Math1*, *Olig2*, and *Tlx3*, an activating mutant of the Hedgehog pathway effector *Smo* resulted in medulloblastoma with 100% penetrance.[402] In addition to embryonically engineered transgenes, exogenous genetic perturbations can be delivered using avian retrovirus RCAS, which only infects cells engineered to express the RCAS receptor tv-a.[401] The RCAS/tv-a system provides additional flexibility in experimental design, and enables temporally controlled delivery of multiple genetic elements such as shRNAs against *Spint2* and *p53*.

Consistent with SPINT2's putative role as a tumor suppressor, high HGF and MET expression is associated with poor prognoses in human medulloblastoma cases.[401] In murine models, HGF signaling cooperates with the Hedgehog pathway to drive malignant medulloblastoma.[401] Therefore, by leveraging murine medulloblastoma models, we have the opportunity to elucidate *in vivo* functions of SPINT2 in tumorigenesis.

Determine the timing of SPINT2 silencing in human cancers

As discussed in Section 5.1.1, I hypothesize that *SPINT2* silencing is an early driver mutation in human cancers. To understand whether SPINT2 loss promotes tumorigenesis in humans and to determine whether epigenetic silencing of *SPINT2* is a driver or a passenger mutation, the mutational timing of *SPINT2* silencing can be measured.[403,404]

Tumors undergo branched evolutionary processes and often harbor high levels of genetic heterogeneity: clonal (also termed founder or truncal) mutations are detected in all cells in a given tumor and delineate the trunk of the phylogenetic tree; they represent early, and often driver, mutational events. Sub-clonal (also termed branch) mutations represent later events during tumorigenesis and are found only in subsets of tumor cells, and are often passenger mutations.[403]

Like genetic mutations, DNA methylation-mediated epigenetic silencing can serve as truncal or branch events during tumorigenesis. Recently, it has been shown that promoter hypermethylation of tumor suppressor genes such as *RASSF1* (RAS association domain family 1)[405] and *PRKCB* (protein kinase Cβ)[406] are founder mutations in prostate cancers.[407]

To infer whether *SPINT2* silencing is a founder mutation, the clonality of *SPINT2* promoter hypermethylation can be determined in primary samples of human tumors such as gastric and renal cancers as well as melanoma.[94,96,100] A common assay for DNA methylation, bisulfite sequencing, measures CpG methylation on individual DNA fragments (see 3.4 Materials and Methods),[255] and thus provides information on clonality within a cell population when the sample size is sufficient. Therefore, bisulfite sequencing serves as a robust first test to gauge whether *SPINT2* promoter hypermethylation is a common alteration in all lineages within a tumor. If hypermethylation is only observed in a small subset of *SPINT2* promoter fragments, it is likely that *SPINT2* silencing is a late-occurring event during tumorigenesis.

Further investigation can be carried out to pinpoint the timeline of *SPINT2* silencing during cancer progression. For example, genome-wide DNA methylation profiling coupled with copy number analysis enables high-resolution dissection of intratumor sub-clonal heterogeneity, and facilitates comprehensive reconstruction of tumor evolutionary history.[407] By sampling spatially

discrete regions of a tumor such as premalignant lesions, the primary tumor, and metastatic sites, it is possible to identify the specific tumorigenic processes promoted by the loss of SPINT2.

* * *

"It is almost—not quite, but almost—as hard as finding some agent that will dissolve away the left ear, say, yet leave the right ear unharmed. So slight is the difference between the cancer cell and its normal ancestor."

—William H. Woglom, 1947, at an AAAS conference on chemotherapy[408]

"The six acquired capabilities—the hallmarks of cancer—have stood the test of time as being integral components of most forms of cancer. Further refinement of these organizing principles will surely come in the foreseeable future…"

—Douglas Hanahan and Robert A. Weinberg, 2011,
in *Hallmarks of Cancer: The Next Generation*[9]

During the seven decades since Woglom's left-ear-right-ear analogy on the remarkable similarities between normal and tumor cells,[408] researchers have developed a much more refined grasp of tumorigenesis and have built theoretical frameworks—such as a unifying set of hallmarks—to understand unique cellular and molecular characteristics of cancer.[9] My dissertation has aimed to add to our current knowledge regarding cancer's salient features such as silencing of tumor suppressor genes, extra- and intra-cellular oncogenic signaling, and chromosome instability. With this goal, I have established SPINT2's roles in suppressing YAP activity and limiting cellular tolerance for aneuploidy, and have elucidated ZEB2's modulation of cellular differentiation in acute myeloid leukemia.

References

1. Virchow R. Cellular-pathologie. *Virchows Archiv*. 1855;8(1):3-39.

2. Mukherjee S. The emperor of all maladies: a biography of cancer: Simon and Schuster; 2010.

3. Mazzarello P. A unifying concept: the history of cell theory. *Nature Cell Biology*. 1999;1(1):E13-E15.

4. Farber S, Diamond LK, Mercer RD, Sylvester RFJ, Wolff JA. Temporary Remissions in Acute Leukemia in Children Produced by Folic Acid Antagonist, 4-Aminopteroyl-Glutamic Acid (Aminopterin). *New England Journal of Medicine*. 1948;238(23):787-793.

5. Beutler E. The treatment of acute leukemia: past, present, and future. *Leukemia*. 2001;15(4):658.

6. Takimoto CH. New antifolates: pharmacology and clinical applications. *The Oncologist*. 1996;1(1 & 2):68-81.

7. Li MC, Hertz R, Spencer DB. Effect of methotrexate therapy upon choriocarcinoma and chorioadenoma. *Proceedings of the Society for Experimental Biology and Medicine*. 1956;93(2):361-366.

8. Hanahan D, Weinberg RA. The hallmarks of cancer. *Cell*. 2000;100(1):57-70.

9. Hanahan D, Weinberg RA. Hallmarks of cancer: the next generation. *Cell*. 2011;144(5):646-674.

10. Shuai K, Halpern J, Ten Hoeve J, Rao X, Sawyers CL. Constitutive activation of STAT5 by the BCR-ABL oncogene in chronic myelogenous leukemia. *Oncogene*. 1996;13(2):247-254.

11. Heisterkamp N, Jenster G, Ten Hoeve J, Zovich D, Pattengale PK. Acute leukaemia in bcr/abl transgenic mice. *Nature*. 1990;344(6263):251.

12. Demetri GD, Von Mehren M, Blanke CD, et al. Efficacy and safety of imatinib mesylate in advanced gastrointestinal stromal tumors. *New England Journal of Medicine*. 2002;347(7):472-480.

13. Chapman PB, Hauschild A, Robert C, et al. Improved survival with vemurafenib in melanoma with BRAF V600E mutation. *New England Journal of Medicine*. 2011;364(26):2507-2516.

14. Brose MS, Volpe P, Feldman M, et al. BRAF and RAS mutations in human lung cancer and melanoma. *Cancer Research*. 2002;62(23):6997-7000.

15. Satyamoorthy K, Li G, Gerrero MR, Brose MS, Volpe P, Weber BL, van Belle P, Elder DE, Herlyn M. Constitutive mitogen-activated protein kinase activation in melanoma is mediated by both BRAF mutations and autocrine growth factor stimulation. *Cancer Research*. 2003;63(4):756-759.

16. Garon EB, Rizvi NA, Hui R, et al. Pembrolizumab for the treatment of non–small-cell lung cancer. *New England Journal of Medicine*. 2015;372(21):2018-2028.

17. Hirano F, Kaneko K, Tamura H, et al. Blockade of B7-H1 and PD-1 by monoclonal antibodies potentiates cancer therapeutic immunity. *Cancer Research*. 2005;65(3):1089-1096.

18. Topalian SL, Hodi FS, Brahmer JR, et al. Safety, activity, and immune correlates of anti–PD-1 antibody in cancer. *N Engl J Med*. 2012;2012(366):2443-2454.

19. Berg J. Proteases: Facilitating a Difficult Reaction. Biochemistry (5th edition): W H Freeman; 2002; Available from: www.ncbi.nlm.nih.gov/books/NBK22526/.

20. Pérez-Silva JG, Español Y, Velasco G, Quesada V. The Degradome database: expanding roles of mammalian proteases in life and disease. *Nucleic Acids Research*. 2015;44(D1):D351-D355.

21. Quesada V, Ordóñez GR, Sanchez LM, Puente XS, López-Otín C. The Degradome database: mammalian proteases and diseases of proteolysis. *Nucleic Acids Research*. 2008;37(suppl_1):D239-D243.

22. Hecht PM, Anderson KV. Extracellular proteases and embryonic pattern formation. *Trends in Cell Biology*. 1992;2(7):197-202.

23. Zhang Y, Pothakos K, Tsirka S-AS. Extracellular proteases: biological and behavioral roles in the mammalian central nervous system. *Current Topics in Developmental Biology*. 2005;66:161-188.

24. Heutinck KM, ten Berge IJ, Hack CE, Hamann J, Rowshani AT. Serine proteases of the human immune system in health and disease. *Molecular immunology*. 2010;47(11):1943-1955.

25. Moali C, Hulmes DJ. Extracellular and cell surface proteases in wound healing: new players are still emerging. *European Journal of Dermatology*. 2009;19(6):552-564.

26. Crawley J, Zanardelli S, Chion C, Lane D. The central role of thrombin in hemostasis. *Journal of thrombosis and haemostasis*. 2007;5(s1):95-101.

27. Yamazaki K, Kato Y. Sites of zona pellucida shedding by mouse embryo other than muran trophectoderm. *Journal of Experimental Zoology Part A: Ecological Genetics and Physiology*. 1989;249(3):347-349.

28. Brenner CA, Adler RR, Rappolee DA, Pedersen RA, Werb Z. Genes for extracellular-matrix-degrading metalloproteinases and their inhibitor, TIMP, are expressed during early mammalian development. *Genes & Development*. 1989;3(6):848-859.

29. Gilbert S. Early Mammalian Development. Developmental Biology (6th edition): Sinauer Associates; 2000; Available from: www.ncbi.nlm.nih.gov/books/NBK10052/.

30. Oakley C, Larjava H. Hemostasis, coagulation, and complications. *Endodontic Topics*. 2011;24(1):4-25.

31. Mackman N. The role of tissue factor and factor VIIa in hemostasis. *Anesthesia and analgesia*. 2009;108(5):1447.

32. Walsh PN, Ahmad SS. Proteases in blood clotting. *Essays in biochemistry*. 2002;38:95-111.

33. Caley MP, Martins VL, O'Toole EA. Metalloproteinases and wound healing. *Advances in wound care*. 2015;4(4):225-234.

34. Steffensen B, Häkkinen L, Larjava H. Proteolytic events of wound-healing—coordinated interactions among matrix metalloproteinases (MMPs), integrins, and extracellular matrix molecules. *Critical Reviews in Oral Biology & Medicine*. 2001;12(5):373-398.

35. LeMosy EK, Tan Y-Q, Hashimoto C. Activation of a protease cascade involved in patterning the Drosophila embryo. *Proceedings of the National Academy of Sciences*. 2001;98(9):5055-5060.

36. Cho YS, Stevens LM, Stein D. Pipe-dependent ventral processing of Easter by Snake is the defining step in Drosophila embryo DV axis formation. *Current Biology*. 2010;20(12):1133-1137.

37. DeLotto Y, DeLotto R. Proteolytic processing of the Drosophila Spätzle protein by easter generates a dimeric NGF-like molecule with ventralising activity. *Mechanisms of Development*. 1998;72(1):141-148.

38. Black RA, Kronheim SR, Cantrell M, et al. Generation of biologically active interleukin-1 beta by proteolytic cleavage of the inactive precursor. *Journal of Biological Chemistry*. 1988;263(19):9437-9442.

39. Afonina IS, Müller C, Martin SJ, Beyaert R. Proteolytic processing of interleukin-1 family cytokines: variations on a common theme. *Immunity*. 2015;42(6):991-1004.

40. Soh UJ, Dores MR, Chen B, Trejo J. Signal transduction by protease‐activated receptors. *British Journal of Pharmacology*. 2010;160(2):191-203.

41. Traynelis SF, Trejo J. Protease-activated receptor signaling: new roles and regulatory mechanisms. *Current Opinion in Hematology*. 2007;14(3):230-235.

42. Coughlin SR. Thrombin signalling and protease-activated receptors. *Nature*. 2000;407(6801):258-264.

43. Vassar R, Kovacs DM, Yan R, Wong PC. The β-secretase enzyme BACE in health and Alzheimer's disease: regulation, cell biology, function, and therapeutic potential. *Journal of Neuroscience*. 2009;29(41):12787-12794.

44. De Strooper B. Proteases and proteolysis in Alzheimer disease: a multifactorial view on the disease process. *Physiological Reviews*. 2010;90(2):465-494.

45. Kato GJ. Human genetic diseases of proteolysis. *Human Mutation*. 1999;13(2):87-98.

46. Friedl P, Alexander S. Cancer invasion and the microenvironment: plasticity and reciprocity. *Cell*. 2011;147(5):992-1009.

47. Sevenich L, Joyce JA. Pericellular proteolysis in cancer. *Genes & Development*. 2014;28(21):2331-2347.

48. Mason SD, Joyce JA. Proteolytic networks in cancer. *Trends in cell biology*. 2011;21(4):228-237.

49. Kessenbrock K, Plaks V, Werb Z. Matrix metalloproteinases: regulators of the tumor microenvironment. *Cell*. 2010;141(1):52-67.

50. Hynes NE, Lane HA. ERBB receptors and cancer: the complexity of targeted inhibitors. *Nature reviews Cancer*. 2005;5(5):341.

51. Ligoxygakis P, Roth S, Reichhart J-M. A serpin regulates dorsal-ventral axis formation in the Drosophila embryo. *Current Biology*. 2003;13(23):2097-2102.

52. Kawaguchi M, Takeda N, Hoshiko S, et al. Membrane-bound serine protease inhibitor HAI-1 is required for maintenance of intestinal epithelial integrity. *The American journal of pathology*. 2011;179(4):1815-1826.

53. Brew K, Nagase H. The tissue inhibitors of metalloproteinases (TIMPs): an ancient family with structural and functional diversity. *Biochimica et Biophysica Acta (BBA)-Molecular Cell Research*. 2010;1803(1):55-71.

54. Farady CJ, Craik CS. Mechanisms of macromolecular protease inhibitors. *Chembiochem*. 2010;11(17):2341-2346.

55. Vincenti M. The Matrix Metalloproteinase (MMP) and Tissue Inhibitor of Metalloproteinase (TIMP) Genes. In: Clark I, ed. Matrix Metalloproteinase Protocols Methods in Molecular Biology (Vol 151): Humana Press; 2001.

56. Palermo C, Joyce JA. Cysteine cathepsin proteases as pharmacological targets in cancer. *Trends in Pharmacological Sciences*. 2008;29(1):22-28.

57. Camerer E, Barker A, Duong DN, et al. Local Protease Signaling Contributes to Neural Tube Closure in the Mouse Embryo. *Developmental Cell*. 2010;18(1):25-38.

58. Coughlin SR. Protease‐activated receptors in hemostasis, thrombosis and vascular biology. *Journal of Thrombosis and Haemostasis*. 2005;3(8):1800-1814.

59. Arora P, Ricks TK, Trejo J. Protease-activated receptor signalling, endocytic sorting and dysregulation in cancer. *Journal of Cell Science*. 2007;120(6):921-928.

60. Caruso R, Pallone F, Fina D, et al. Protease-activated receptor-2 activation in gastric cancer cells promotes epidermal growth factor receptor trans-activation and proliferation. *The American journal of pathology*. 2006;169(1):268-278.

61. Morris DR, Ding Y, Ricks TK, Gullapalli A, Wolfe BL, Trejo J. Protease-activated receptor-2 is essential for factor viia and xa–induced signaling, migration, and invasion of breast cancer cells. *Cancer Research*. 2006;66(1):307-314.

62. Otsuki T, Fujimoto D, Hirono Y, Goi T, Yamaguchi A. Thrombin conducts epithelial-mesenchymal transition via protease-activated receptor-1 in human gastric cancer. *International journal of oncology*. 2014;45(6):2287-2294.

63. Oldham WM, Hamm HE. Heterotrimeric G protein activation by G-protein-coupled receptors. *Nature Reviews Molecular Cell Biology*. 2008;9(1):60.

64. Alberts B, Johnson A, Lewis J, Raff M, Roberts K, Walter P. Signaling through G-Protein-Linked Cell-Surface Receptors. Molecular Biology of the Cell: Garland Science; 2002.

65. Khan SM, Sleno R, Gora S, Zylbergold P, Laverdure J-P, Labbé J-C, Miller GJ, Hébert TE. The expanding roles of Gβγ subunits in G protein–coupled receptor signaling and drug action. *Pharmacological Reviews*. 2013;65(2):545-577.

66. Hur E-M, Kim K-T. G protein-coupled receptor signalling and cross-talk: achieving rapidity and specificity. *Cellular Signalling*. 2002;14(5):397-405.

67. HUGO Gene Nomenclature Committee. G protein subunits alpha (GNA). www.genenames.org/cgi-bin/genefamilies/set/1425; Accessed 6/28/2017.

68. Malbon CC. G proteins in development. *Nature Reviews Molecular Cell Biology*. 2005;6(9):689.

69. Offermanns S, Toombs CF, Yi-Hui H, Simon MI. Defective platelet activation in Galphaq-deficient mice. *Nature*. 1997;389(6647):183.

70. Moers A, Nieswandt B, Massberg S, et al. G13 is an essential mediator of platelet activation in hemostasis and thrombosis. *Nature medicine*. 2003;9(11):1418-1422.

71. Varga‐Szabo D, Braun A, Nieswandt B. Calcium signaling in platelets. *Journal of Thrombosis and Haemostasis*. 2009;7(7):1057-1066.

72. Aslan JE, McCarty OJ. Rho GTPases in platelet function. *Journal of Thrombosis and Haemostasis*. 2013;11(1):35-46.

73. Booden MA, Eckert LB, Der CJ, Trejo J. Persistent signaling by dysregulated thrombin receptor trafficking promotes breast carcinoma cell invasion. *Molecular and cellular biology*. 2004;24(5):1990-1999.

74. Puente XS, Sánchez LM, Overall CM, López-Otín C. Human and mouse proteases: a comparative genomic approach. *Nature Reviews Genetics*. 2003;4(7):544.

75. Rawlings ND, Barrett AJ. 2. Families of serine peptidases. *Methods in Enzymology*. 1994;244:19-61.

76. Rau J, Beaulieu L, Huntington J, Church FC. Serpins in thrombosis, hemostasis and fibrinolysis. *Journal of Thrombosis and Haemostasis*. 2007;5(s1):102-115.

77. Fan B, Brennan J, Grant D, Peale F, Rangell L, Kirchhofer D. Hepatocyte growth factor activator inhibitor-1 (HAI-1) is essential for the integrity of basement membranes in the developing placental labyrinth. *Developmental biology*. 2007;303(1):222-230.

78. Nagaike K, Kawaguchi M, Takeda N, Fukushima T, Sawaguchi A, Kohama K, Setoyama M, Kataoka H. Defect of hepatocyte growth factor activator inhibitor type 1/serine protease inhibitor, Kunitz type 1 (Hai-1/Spint1) leads to ichthyosis-like condition and abnormal hair development in mice. *The American Journal of Pathology*. 2008;173(5):1464-1475.

79. Heinz-Erian P, Müller T, Krabichler B, et al. Mutations in SPINT2 cause a syndromic form of congenital sodium diarrhea. *The American Journal of Human Genetics*. 2009;84(2):188-196.

80. Szabo R, Hobson JP, Christoph K, Kosa P, List K, Bugge TH. Regulation of cell surface protease matriptase by HAI2 is essential for placental development, neural tube closure and embryonic survival in mice. *Development*. 2009;136(15):2653-2663.

81. Szabo R, Kosa P, List K, Bugge TH. Loss of matriptase suppression underlies spint1 mutation-associated ichthyosis and postnatal lethality. *The American Journal of Pathology*. 2009;174(6):2015-2022.

82. Buchanan A, Revell JD. Chapter 8 - Novel Therapeutic Proteins and Peptides. Novel Approaches and Strategies for Biologics, Vaccines and Cancer Therapies. San Diego: Academic Press; 2015:171-197.

83. Johns Hopkins University. Online Mendelian Inheritance in Man (OMIM); www.omim.org; Accessed 6/28/2017.

84. Oberst MD, Chen L-YL, Kiyomiya K-I, Williams CA, Lee M-S, Johnson MD, Dickson RB, Lin C-Y. HAI-1 regulates activation and expression of matriptase, a membrane-bound serine protease. *American Journal of Physiology-Cell Physiology*. 2005;289(2):C462-C470.

85. Itoh H, Yamauchi M, Kataoka H, Hamasuna R, Kitamura N, Koono M. Genomic structure and chromosomal localization of the human hepatocyte growth factor activator inhibitor type 1 and 2 genes. *The FEBS Journal*. 2000;267(11):3351-3359.

86. Kawaguchi T, Qin L, Shimomura T, Kondo J, Matsumoto K, Denda K, Kitamura N. Purification and cloning of hepatocyte growth factor activator inhibitor type 2, a Kunitz-type serine protease inhibitor. *Journal of Biological Chemistry*. 1997;272(44):27558-27564.

87. Godiksen S, Selzer-Plon J, Pedersen ED, Abell K, Rasmussen HB, Szabo R, Bugge TH, Vogel LK. Hepatocyte growth factor activator inhibitor-1 has a complex subcellular itinerary. *Biochemical Journal*. 2008;413(2):251-259.

88. Lai Y-JJ, Chang H-HD, Lai H, et al. N-Glycan Branching Affects the Subcellular Distribution of and Inhibition of Matriptase by HAI-2/Placental Bikunin. *PloS One*. 2015;10(7):e0132163.

89. Szabo R, Hobson JP, List K, Molinolo A, Lin C-Y, Bugge TH. Potent inhibition and global co-localization implicate the transmembrane Kunitz-type serine protease inhibitor hepatocyte growth factor activator inhibitor-2 in the regulation of epithelial matriptase activity. *Journal of Biological Chemistry*. 2008;283(43):29495-29504.

90. Szabo R, Molinolo A, List K, Bugge T. Matriptase inhibition by hepatocyte growth factor activator inhibitor-1 is essential for placental development. *Oncogene*. 2007;26(11):1546.

91. Lonsdale J, Thomas J, Salvatore M, et al. The genotype-tissue expression (GTEx) project. *Nature Genetics*. 2013;45(6):580-585.

92. Oberst MD, Johnson MD, Dickson RB, et al. Expression of the Serine Protease Matriptase and Its Inhibitor HAI-1 in Epithelial Ovarian Cancer. *Clinical cancer research*. 2002;8(4):1101-1107.

93. Vogel LK, Sæbø M, Skjelbred CF, Abell K, Pedersen ED, Vogel U, Kure EH. The ratio of Matriptase/HAI-1 mRNA is higher in colorectal cancer adenomas and carcinomas than corresponding tissue from control individuals. *BMC cancer*. 2006;6(1):176.

94. Dong W, Chen X, Xie J, Sun P, Wu Y. Epigenetic inactivation and tumor suppressor activity of HAI‐2/SPINT2 in gastric cancer. *International journal of cancer*. 2010;127(7):1526-1534.

95. Kongkham PN, Northcott PA, Ra YS, Nakahara Y, Mainprize TG, Croul SE, Smith CA, Taylor MD, Rutka JT. An epigenetic genome-wide screen identifies SPINT2 as a novel tumor suppressor gene in pediatric medulloblastoma. *Cancer Research*. 2008;68(23):9945-9953.

96. Morris MR, Gentle D, Abdulrahman M, et al. Tumor suppressor activity and epigenetic inactivation of hepatocyte growth factor activator inhibitor type 2/SPINT2 in papillary and clear cell renal cell carcinoma. *Cancer Research*. 2005;65(11):4598-4606.

97. Roversi FM, Cury NM, Lopes MR, Pericole FV, Prax MCA, Ferro KP, Favaro P, Yunes JA, Saad STO. Methylation of HAI-2/SPINT2 in Bone Marrow Mesenchymal Stromal Cells of MDS and AML Patients Affects Hematopoietic Stem Cell Survival and Adhesion. *Blood*. 2015;126(23):2847-2847.

98. Yue D, Fan Q, Chen X, et al. Epigenetic inactivation of SPINT2 is associated with tumor suppressive function in esophageal squamous cell carcinoma. *Experimental cell research*. 2014;322(1):149-158.

99. Fukai K, Yokosuka O, Chiba T, Hirasawa Y, Tada M, Imazeki F, Kataoka H, Saisho H. Hepatocyte growth factor activator inhibitor 2/placental bikunin (HAI-2/PB) gene is frequently hypermethylated in human hepatocellular carcinoma. *Cancer Research*. 2003;63(24):8674-8679.

100. Hwang S, Kim H-E, Min M, Raghunathan R, Panova IP, Munshi R, Ryu B. Epigenetic Silencing of SPINT2 Promotes Cancer Cell Motility via HGF-MET Pathway Activation in Melanoma. *Journal of Investigative Dermatology*. 2015;135(9):2283-2291.

101. Harvey KF, Zhang X, Thomas DM. The Hippo pathway and human cancer. *Nature Reviews Cancer*. 2013;13(4):246-257.

102. Yu F-X, Zhao B, Guan K-L. Hippo pathway in organ size control, tissue homeostasis, and cancer. *Cell*. 2015;163(4):811-828.

103. Piccolo S, Dupont S, Cordenonsi M. The biology of YAP/TAZ: hippo signaling and beyond. *Physiological Reviews*. 2014;94(4):1287-1312.

104. Varelas X. The Hippo pathway effectors TAZ and YAP in development, homeostasis and disease. *Development*. 2014;141(8):1614-1626.

105. Justice RW, Zilian O, Woods DF, Noll M, Bryant PJ. The Drosophila tumor suppressor gene warts encodes a homolog of human myotonic dystrophy kinase and is required for the control of cell shape and proliferation. *Genes & Development*. 1995;9(5):534-546.

106. Xu T, Wang W, Zhang S, Stewart RA, Yu W. Identifying tumor suppressors in genetic mosaics: the Drosophila lats gene encodes a putative protein kinase. *Development*. 1995;121(4):1053-1063.

107. Harvey KF, Pfleger CM, Hariharan IK. The Drosophila Mst ortholog, hippo, restricts growth and cell proliferation and promotes apoptosis. *Cell*. 2003;114(4):457-467.

108. Jia J, Zhang W, Wang B, Trinko R, Jiang J. The Drosophila Ste20 family kinase dMST functions as a tumor suppressor by restricting cell proliferation and promoting apoptosis. *Genes & Development*. 2003;17(20):2514-2519.

109. Pantalacci S, Tapon N, Léopold P. The Salvador partner Hippo promotes apoptosis and cell-cycle exit in Drosophila. *Nature Cell Biology*. 2003;5(10):921.

110. Udan RS, Kango-Singh M, Nolo R, Tao C, Halder G. Hippo promotes proliferation arrest and apoptosis in the Salvador/Warts pathway. *Nature Cell Biology*. 2003;5(10):914.

111. Wu S, Huang J, Dong J, Pan D. Hippo encodes a Ste-20 family protein kinase that restricts cell proliferation and promotes apoptosis in conjunction with salvador and warts. *Cell*. 2003;114(4):445-456.

112. Kango-Singh M, Nolo R, Tao C, Verstreken P, Hiesinger PR, Bellen HJ, Halder G. Shar-pei mediates cell proliferation arrest during imaginal disc growth in Drosophila. *Development*. 2002;129(24):5719-5730.

113. Tapon N, Harvey KF, Bell DW, Wahrer DC, Schiripo TA, Haber DA, Hariharan IK. salvador Promotes both cell cycle exit and apoptosis in Drosophila and is mutated in human cancer cell lines. *Cell*. 2002;110(4):467-478.

114. Lai Z-C, Wei X, Shimizu T, Ramos E, Rohrbaugh M, Nikolaidis N, Ho L-L, Li Y. Control of cell proliferation and apoptosis by mob as tumor suppressor, mats. *Cell*. 2005;120(5):675-685.

115. Huang J, Wu S, Barrera J, Matthews K, Pan D. The Hippo signaling pathway coordinately regulates cell proliferation and apoptosis by inactivating Yorkie, the Drosophila Homolog of YAP. *Cell*. 2005;122(3):421-434.

116. He C, Mao D, Hua G, et al. The Hippo/YAP pathway interacts with EGFR signaling and HPV oncoproteins to regulate cervical cancer progression. *EMBO molecular medicine*. 2015;7(11):1426-1449.

117. Zhao B, Tumaneng K, Guan K-L. The Hippo pathway in organ size control, tissue regeneration and stem cell self-renewal. *Nature Cell Biology*. 2011;13(8):877-883.

118. Mhawech P. 14-3-3 proteins--an update. *Cell Research*. 2005;15(4):228.

119. Karpowicz P, Perez J, Perrimon N. The Hippo tumor suppressor pathway regulates intestinal stem cell regeneration. *Development*. 2010;137(24):4135-4145.

120. Bai H, Zhang N, Xu Y, et al. Yes‐associated protein regulates the hepatic response after bile duct ligation. *Hepatology*. 2012;56(3):1097-1107.

121. Su T, Bondar T, Zhou X, Zhang C, He H, Medzhitov R. Two-signal requirement for growth-promoting function of Yap in hepatocytes. *Elife*. 2015;4:e02948.

122. Mohseni M, Sun J, Lau A, et al. A genetic screen identifies an LKB1/PAR1 signaling axis controlling the Hippo/YAP pathway. *Nature cell biology*. 2014;16(1):108.

123. Yin F, Yu J, Zheng Y, Chen Q, Zhang N, Pan D. Spatial organization of Hippo signaling at the plasma membrane mediated by the tumor suppressor Merlin/NF2. *Cell*. 2013;154(6):1342-1355.

124. Zhang N, Bai H, David KK, et al. The Merlin/NF2 tumor suppressor functions through the YAP oncoprotein to regulate tissue homeostasis in mammals. *Developmental cell*. 2010;19(1):27-38.

125. Meng Z, Moroishi T, Mottier-Pavie V, et al. MAP4K family kinases act in parallel to MST1/2 to activate LATS1/2 in the Hippo pathway. *Nature Communications*. 2015;6.

126. Levy D, Adamovich Y, Reuven N, Shaul Y. Yap1 phosphorylation by c-Abl is a critical step in selective activation of proapoptotic genes in response to DNA damage. *Molecular Cell*. 2008;29(3):350-361.

127. Yang S, Zhang L, Liu M, Chong R, Ding S-J, Chen Y, Dong J. CDK1 phosphorylation of YAP promotes mitotic defects and cell motility and is essential for neoplastic transformation. *Cancer Research*. 2013.

128. Meng Z, Moroishi T, Guan K-L. Mechanisms of Hippo pathway regulation. *Genes & Development*. 2016;30(1):1-17.

129. Ota M, Sasaki H. Mammalian Tead proteins regulate cell proliferation and contact inhibition as transcriptional mediators of Hippo signaling. *Development*. 2008;135(24):4059-4069.

130. Nishioka N, Inoue K-i, Adachi K, et al. The Hippo signaling pathway components Lats and Yap pattern Tead4 activity to distinguish mouse trophectoderm from inner cell mass. *Developmental cell*. 2009;16(3):398-410.

131. Zhao B, Wei X, Li W, et al. Inactivation of YAP oncoprotein by the Hippo pathway is involved in cell contact inhibition and tissue growth control. *Genes & Development*. 2007;21(21):2747-2761.

132. Zhao B, Li L, Wang L, Wang C-Y, Yu J, Guan K-L. Cell detachment activates the Hippo pathway via cytoskeleton reorganization to induce anoikis. *Genes & Development*. 2012;26(1):54-68.

133. Dupont S, Morsut L, Aragona M, et al. Role of YAP/TAZ in mechanotransduction. *Nature*. 2011;474(7350):179.

134. DeRan M, Yang J, Shen C-H, et al. Energy stress regulates hippo-YAP signaling involving AMPK-mediated regulation of angiomotin-like 1 protein. *Cell Reports*. 2014;9(2):495-503.

135. Mo J-S, Meng Z, Kim YC, Park HW, Hansen CG, Kim S, Lim D-S, Guan K-L. Cellular energy stress induces AMPK-mediated regulation of YAP and the Hippo pathway. *Nature Cell Biology*. 2015;17(4):500.

136. Overholtzer M, Zhang J, Smolen GA, Muir B, Li W, Sgroi DC, Deng C-X, Brugge JS, Haber DA. Transforming properties of YAP, a candidate oncogene on the chromosome 11q22 amplicon. *Proceedings of the National Academy of Sciences*. 2006;103(33):12405-12410.

137. Murakami H, Mizuno T, Taniguchi T, et al. LATS2 is a tumor suppressor gene of malignant mesothelioma. *Cancer Research*. 2011;71(3):873-883.

138. Zender L, Spector MS, Xue W, et al. Identification and validation of oncogenes in liver cancer using an integrative oncogenomic approach. *Cell*. 2006;125(7):1253-1267.

139. Fujiwara T, Bandi M, Nitta M, Ivanova EV, Bronson RT, Pellman D. Cytokinesis failure generating tetraploids promotes tumorigenesis in p53-null cells. *Nature*. 2005;437(7061):1043-1047.

140. Wennmann D, Vollenbröker B, Eckart A, et al. The Hippo pathway is controlled by Angiotensin II signaling and its reactivation induces apoptosis in podocytes. *Cell death & disease*. 2014;5(11):e1519.

141. Zhou X, Wang S, Wang Z, et al. Estrogen regulates Hippo signaling via GPER in breast cancer. *The Journal of Clinical Investigation*. 2015;125(5):2123-2135.

142. Yu F-X, Zhao B, Panupinthu N, et al. Regulation of the Hippo-YAP pathway by G-protein-coupled receptor signaling. *Cell*. 2012;150(4):780-791.

143. Mo J-S, Yu F-X, Gong R, Brown JH, Guan K-L. Regulation of the Hippo–YAP pathway by protease-activated receptors (PARs). *Genes & Development*. 2012;26(19):2138-2143.

144. Kim M, Kim M, Lee S, Kuninaka S, Saya H, Lee H, Lee S, Lim DS. cAMP/PKA signalling reinforces the LATS–YAP pathway to fully suppress YAP in response to actin cytoskeletal changes. *The EMBO journal*. 2013;32(11):1543-1555.

145. Boveri TH. Zur Frage der Entstehung maligner Tumoren (The Origin of Malignant Tumors)(Jena: Gustav Fischer). 1914.

146. Gordon DJ, Resio B, Pellman D. Causes and consequences of aneuploidy in cancer. *Nature Reviews Genetics*. 2012;13(3):189-203.

147. Naylor RM, Van Deursen JM. Aneuploidy in Cancer and Aging. *Annual review of genetics*. 2016;50:45-66.

148. Sheltzer JM, Amon A. The aneuploidy paradox: costs and benefits of an incorrect karyotype. *Trends in Genetics*. 2011;27(11):446-453.

149. Mitelman F, Johansson B, Mertens F. Mitelman database of chromosome aberrations and gene fusions in cancer. 2017. http://cgap.nci.nih.gov/Chromosomes/Mitelman; Accessed 7/8/2017.

150. Beroukhim R, Mermel CH, Porter D, et al. The landscape of somatic copy-number alteration across human cancers. *Nature*. 2010;463(7283):899-905.

151. Weaver BA, Cleveland DW. Does aneuploidy cause cancer? *Curr Opin Cell Biol*. 2006;18(6):658-667.

152. Holland AJ, Cleveland DW. Boveri revisited: chromosomal instability, aneuploidy and tumorigenesis. *Nat Rev Mol Cell Biol*. 2009;10(7):478-487.

153. Ganem NJ, Godinho SA, Pellman D. A mechanism linking extra centrosomes to chromosomal instability. *Nature*. 2009;460(7252):278.

154. Solomon DA, Kim T, Diaz-Martinez LA, et al. Mutational Inactivation of STAG2 Causes Aneuploidy in Human Cancer. *Science*. 2011;333(6045):1039-1043.

155. Brownlee PM, Chambers AL, Cloney R, Bianchi A, Downs JA. BAF180 promotes cohesion and prevents genome instability and aneuploidy. *Cell Reports*. 2014;6(6):973-981.

156. Losada A. Cohesin in cancer: chromosome segregation and beyond. *Nature reviews Cancer*. 2014;14(6):389-393.

157. Brown S. Miscarriage and its associations. Seminars in reproductive medicine: © Thieme Medical Publishers; 2008:391-400.

158. Rehen SK, McConnell MJ, Kaushal D, Kingsbury MA, Yang AH, Chun J. Chromosomal variation in neurons of the developing and adult mammalian nervous system. *Proceedings of the National Academy of Sciences*. 2001;98(23):13361-13366.

159. Yurov YB, Iourov IY, Vorsanova SG, et al. Aneuploidy and confined chromosomal mosaicism in the developing human brain. *PloS One*. 2007;2(6):e558.

160. Gupta S. Hepatic polyploidy and liver growth control. Seminars in cancer biology: Elsevier; 2000:161-171.

161. Duncan AW, Taylor MH, Hickey RD, Newell AEH, Lenzi ML, Olson SB, Finegold MJ, Grompe M. The ploidy conveyor of mature hepatocytes as a source of genetic variation. *Nature*. 2010;467(7316):707-710.

162. Torres EM, Sokolsky T, Tucker CM, Chan LY, Boselli M, Dunham MJ, Amon A. Effects of aneuploidy on cellular physiology and cell division in haploid yeast. *Science*. 2007;317(5840):916-924.

163. Mao R, Zielke CL, Zielke HR, Pevsner J. Global up-regulation of chromosome 21 gene expression in the developing Down syndrome brain. *Genomics*. 2003;81(5):457-467.

164. FitzPatrick DR, Ramsay J, McGill NI, Shade M, Carothers AD, Hastie ND. Transcriptome analysis of human autosomal trisomy. *Human Molecular Genetics*. 2002;11(26):3249-3256.

165. Pavelka N, Rancati G, Zhu J, Bradford WD, Saraf A, Florens L, Sanderson BW, Hattem GL, Li R. Aneuploidy confers quantitative proteome changes and phenotypic variation in budding yeast. *Nature*. 2010;468(7321):321.

166. Huettel B, Kreil DP, Matzke M, Matzke AJ. Effects of aneuploidy on genome structure, expression, and interphase organization in Arabidopsis thaliana. *PLoS Genetics*. 2008;4(10):e1000226.

167. Williams BR, Prabhu VR, Hunter KE, Glazier CM, Whittaker CA, Housman DE, Amon A. Aneuploidy affects proliferation and spontaneous immortalization in mammalian cells. *Science*. 2008;322(5902):703-709.

168. Santaguida S, Amon A. Short-and long-term effects of chromosome mis-segregation and aneuploidy. *Nature Reviews Molecular Cell Biology*. 2015;16(8):473-485.

169. Oromendia AB, Dodgson SE, Amon A. Aneuploidy causes proteotoxic stress in yeast. *Genes & Development*. 2012;26(24):2696-2708.

170. Donnelly N, Passerini V, Dürrbaum M, Stingele S, Storchová Z. HSF1 deficiency and impaired HSP90‐dependent protein folding are hallmarks of aneuploid human cells. *The EMBO Journal*. 2014;33(20):2374-2387.

171. Santaguida S, Vasile E, White E, Amon A. Aneuploidy-induced cellular stresses limit autophagic degradation. *Genes & development*. 2015;29(19):2010-2021.

172. Manning AL, Longworth MS, Dyson NJ. Loss of pRB causes centromere dysfunction and chromosomal instability. *Genes & Development*. 2010;24(13):1364-1376.

173. Sotillo R, Schvartzman J-M, Socci ND, Benezra R. Mad2-induced chromosome instability leads to lung tumour relapse after oncogene withdrawal. *Nature*. 2010;464(7287):436-440.

174. Sheltzer JM, Ko JH, Replogle JM, et al. Single-chromosome gains commonly function as tumor suppressors. *Cancer Cell*. 2017;31(2):240-255.

175. Blank HM, Sheltzer JM, Meehl CM, Amon A. Mitotic entry in the presence of DNA damage is a widespread property of aneuploidy in yeast. *Molecular Biology of the Cell*. 2015;26(8):1440-1451.

176. Passerini V, Ozeri-Galai E, De Pagter MS, Donnelly N, Schmalbrock S, Kloosterman WP, Kerem B, Storchová Z. The presence of extra chromosomes leads to genomic instability. *Nature Communications*. 2016;7:10754.

177. Tsai C-H, Teng C-H, Tu Y-T, et al. HAI-2 suppresses the invasive growth and metastasis of prostate cancer through regulation of matriptase. *Oncogene*. 2014;33(38):4643-4652.

178. Ganem NJ, Cornils H, Chiu S-Y, O'Rourke KP, Arnaud J, Yimlamai D, Théry M, Camargo FD, Pellman D. Cytokinesis failure triggers hippo tumor suppressor pathway activation. *Cell*. 2014;158(4):833-848.

179. Johnson R, Halder G. The two faces of Hippo: targeting the Hippo pathway for regenerative medicine and cancer treatment. *Nature reviews Drug discovery*. 2014;13(1):63-79.

180. Hwang S-M, Jin M, Shin YH, Choi SK, Namkoong E, Kim M, Park M-Y, Park K. Role of LPA and the Hippo pathway on apoptosis in salivary gland epithelial cells. *Experimental & molecular medicine*. 2014;46(12):e125.

181. Liu C-Y, Zha Z-Y, Zhou X, et al. The hippo tumor pathway promotes TAZ degradation by phosphorylating a phosphodegron and recruiting the SCFβ-TrCP E3 ligase. *Journal of Biological Chemistry*. 2010;285(48):37159-37169.

182. Moroishi T, Park HW, Qin B, et al. A YAP/TAZ-induced feedback mechanism regulates Hippo pathway homeostasis. *Genes & development*. 2015;29(12):1271-1284.

183. Lin X, Ruan X, Anderson MG, McDowell JA, Kroeger PE, Fesik SW, Shen Y. siRNA-mediated off-target gene silencing triggered by a 7 nt complementation. *Nucleic Acids Res*. 2005;33(14):4527-4535.

184. Gehlenborg N, Wong B. Points of view: Heat maps. *Nature Methods*. 2012;9(3):213.

185. Broad Institute. Morpheus: versatile matrix visualization and analysis software; https://software.broadinstitute.org/morpheus/.

186. Zhang J, Smolen GA, Haber DA. Negative regulation of YAP by LATS1 underscores evolutionary conservation of the Drosophila Hippo pathway. *Cancer research*. 2008;68(8):2789-2794.

187. Dong J, Feldmann G, Huang J, et al. Elucidation of a universal size-control mechanism in Drosophila and mammals. *Cell*. 2007;130(6):1120-1133.

188. Subramanian A, Tamayo P, Mootha VK, et al. Gene set enrichment analysis: a knowledge-based approach for interpreting genome-wide expression profiles. *Proc Natl Acad Sci U S A*. 2005;102(43):15545-15550.

189. Liberzon A, Birger C, Thorvaldsdóttir H, Ghandi M, Mesirov JP, Tamayo P. The molecular signatures database hallmark gene set collection. *Cell systems*. 2015;1(6):417-425.

190. Kirchhofer D, Peek M, Lipari MT, Billeci K, Fan B, Moran P. Hepsin activates pro‐hepatocyte growth factor and is inhibited by hepatocyte growth factor activator inhibitor‐1B (HAI‐1B) and HAI‐2. *FEBS letters*. 2005;579(9):1945-1950.

191. Parr C, Jiang WG. Hepatocyte growth factor activation inhibitors (HAI‐1 and HAI‐2) regulate HGF‐induced invasion of human breast cancer cells. *International journal of cancer*. 2006;119(5):1176-1183.

192. Fujimoto D, Hirono Y, Goi T, Katayama K, Matsukawa S, Yamaguchi A. The activation of Proteinase-Activated Receptor-1 (PAR1) mediates gastric cancer cell proliferation and invasion. *BMC cancer*. 2010;10(1):443.

193. Gherardi E, Birchmeier W, Birchmeier C, Woude GV. Targeting MET in cancer: rationale and progress. *Nature Reviews Cancer*. 2012;12(2):89-103.

194. Kauskot A, Hoylaerts MF. Platelet receptors. Antiplatelet Agents: Springer; 2012:23-57.

195. Ludeman MJ, Zheng YW, Ishii K, Coughlin SR. Regulated shedding of PAR1 N-terminal exodomain from endothelial cells. *Journal of Biological Chemistry*. 2004;279(18):18592-18599.

196. Reginato M, Mills K, Paulus J, Lynch D, Sgroi D, Debnath J, Muthuswamy S, Brugge J. Integrins and EGFR coordinately regulate the pro-apoptotic protein Bim to prevent anoikis. *Nature Cell Biology*. 2003;5(8):733.

197. Thompson KN, Whipple RA, Yoon JR, et al. The combinatorial activation of the PI3K and Ras/MAPK pathways is sufficient for aggressive tumor formation, while individual pathway activation supports cell persistence. *Oncotarget*. 2015;6(34):35231.

198. Godinho SA, Picone R, Burute M, et al. Oncogene-like induction of cellular invasion from centrosome amplification. *Nature*. 2014;510(7503):167-171.

199. Bashyam MD, Bair R, Kim YH, Wang P, Hernandez-Boussard T, Karikari CA, Tibshirani R, Maitra A, Pollack JR. Array-based comparative genomic hybridization identifies localized DNA amplifications and homozygous deletions in pancreatic cancer. *Neoplasia*. 2005;7(6):556IN551-562IN516.

200. Snijders AM, Schmidt BL, Fridlyand J, Dekker N, Pinkel D, Jordan RC, Albertson DG. Rare amplicons implicate frequent deregulation of cell fate specification pathways in oral squamous cell carcinoma. *Oncogene*. 2005;24(26):4232-4242.

201. Dai Z, Zhu W-G, Morrison CD, et al. A comprehensive search for DNA amplification in lung cancer identifies inhibitors of apoptosis cIAP1 and cIAP2 as candidate oncogenes. *Human molecular genetics*. 2003;12(7):791-801.

202. Basu S, Totty NF, Irwin MS, Sudol M, Downward J. Akt phosphorylates the Yes-associated protein, YAP, to induce interaction with 14-3-3 and attenuation of p73-mediated apoptosis. *Molecular cell*. 2003;11(1):11-23.

203. Straßburger K, Tiebe M, Pinna F, Breuhahn K, Teleman AA. Insulin/IGF signaling drives cell proliferation in part via Yorkie/YAP. *Developmental Biology*. 2012;367(2):187-196.

204. Xin M, Kim Y, Sutherland LB, Qi X, McAnally J, Schwartz RJ, Richardson JA, Bassel-Duby R, Olson EN. Regulation of insulin-like growth factor signaling by Yap governs cardiomyocyte proliferation and embryonic heart size. *Science signaling*. 2011;4(196):ra70.

205. Reddy B, Irvine KD. Regulation of Hippo signaling by EGFR-MAPK signaling through Ajuba family proteins. *Developmental Cell*. 2013;24(5):459-471.

206. van Adelsberg J, Sehgal S, Kukes A, Brady C, Barasch J, Yang J, Huan Y. Activation of hepatocyte growth factor (HGF) by endogenous HGF activator is required for metanephric kidney morphogenesis in vitro. *Journal of Biological Chemistry*. 2001;276(18):15099-15106.

207. Yamauchi M, Kataoka H, Itoh H, Seguchi T, Hasui Y, Osada Y. Hepatocyte growth factor activator inhibitor types 1 and 2 are expressed by tubular epithelium in kidney and down-regulated in renal cell carcinoma. *The Journal of urology*. 2004;171(2):890-896.

208. Morris MR, Latif F. The epigenetic landscape of renal cancer. *Nature Reviews Nephrology*. 2016.

209. Adjei AA. Blocking oncogenic Ras signaling for cancer therapy. *Journal of the National Cancer Institute*. 2001;93(14):1062-1074.

210. Engelman JA, Chen L, Tan X, et al. Effective use of PI3K and MEK inhibitors to treat mutant Kras G12D and PIK3CA H1047R murine lung cancers. *Nature medicine*. 2008;14(12):1351-1356.

211. Kapoor A, Yao W, Ying H, et al. Yap1 activation enables bypass of oncogenic Kras addiction in pancreatic cancer. *Cell*. 2014;158(1):185-197.

212. Shao DD, Xue W, Krall EB, et al. KRAS and YAP1 converge to regulate EMT and tumor survival. *Cell*. 2014;158(1):171-184.

213. Suen J, Cotterell A, Lohman R, et al. Pathway‐selective antagonism of proteinase activated receptor 2. *British journal of pharmacology*. 2014;171(17):4112-4124.

214. Ellis CA, Tiruppathi C, Sandoval R, Niles WD, Malik AB. Time course of recovery of endothelial cell surface thrombin receptor (PAR-1) expression. *American Journal of Physiology-Cell Physiology*. 1999;276(1):C38-C45.

215. Lappano R, Maggiolini M. G protein-coupled receptors: novel targets for drug discovery in cancer. *Nature reviews Drug discovery*. 2011;10(1):47-60.

216. Hall A. Rho GTPases and the actin cytoskeleton. *Science*. 1998;279(5350):509-514.

217. Park HW, Guan K-L. Regulation of the Hippo pathway and implications for anticancer drug development. *Trends in Pharmacological Sciences*. 2013;34(10):581-589.

218. Das R, Esposito V, Abu-Abed M, Anand GS, Taylor SS, Melacini G. cAMP activation of PKA defines an ancient signaling mechanism. *Proceedings of the National Academy of Sciences*. 2007;104(1):93-98.

219. Lijnen H. Plasmin and matrix metalloproteinases in vascular remodeling. *Thrombosis and haemostasis*. 2001;86(1):324-333.

220. Pendurthi UR, Ngyuen M, Andrade-Gordon P, Petersen LC, Rao LVM. Plasmin induces Cyr61 gene expression in fibroblasts via protease-activated receptor-1 and p44/42 mitogen-activated protein kinase–dependent signaling pathway. *Arteriosclerosis, thrombosis, and vascular biology*. 2002;22(9):1421-1426.

221. Dano K, Behrendt N, Hoyer-Hansen G, Johnsen M, Lund LR, Ploug M, Romer J. Plasminogen activation and cancer. *Thromb Haemost*. 2005;93(4):676-681.

222. Uhland K. Matriptase and its putative role in cancer. *Cellular and molecular life sciences*. 2006;63(24):2968-2978.

223. Zoratti GL, Tanabe LM, Varela FA, et al. Targeting matriptase in breast cancer abrogates tumor progression via impairment of stromal-epithelial growth factor signaling. *Nature communications*. 2015;6:6776.

224. Bocheva G, Rattenholl A, Kempkes C, Goerge T, Lin C-Y, D'andrea MR, Ständer S, Steinhoff M. Role of matriptase and proteinase-activated receptor-2 in nonmelanoma skin cancer. *Journal of Investigative Dermatology*. 2009;129(7):1816-1823.

225. Sales KU, Friis S, Konkel JE, et al. Non-hematopoietic PAR-2 is essential for matriptase-driven pre-malignant progression and potentiation of ras-mediated squamous cell carcinogenesis. *Oncogene*. 2015;34(3):346-356.

226. Duffy MJ, McGowan PM, Harbeck N, Thomssen C, Schmitt M. uPA and PAI-1 as biomarkers in breast cancer: validated for clinical use in level-of-evidence-1 studies. *Breast Cancer Research*. 2014;16(4):428.

227. Majumdar M, Tarui T, Shi B, Akakura N, Ruf W, Takada Y. Plasmin-induced migration requires signaling through protease-activated receptor 1 and integrin α9β1. *Journal of Biological Chemistry*. 2004;279(36):37528-37534.

228. Vihinen P, Kähäri VM. Matrix metalloproteinases in cancer: prognostic markers and therapeutic targets. *International Journal of Cancer*. 2002;99(2):157-166.

229. Heerboth S, Housman G, Leary M, Longacre M, Byler S, Lapinska K, Willbanks A, Sarkar S. EMT and tumor metastasis. *Clinical and Translational Medicine*. 2015;4(1):6.

230. Varelas X, Sakuma R, Samavarchi-Tehrani P, Peerani R, Rao BM, Dembowy J, Yaffe MB, Zandstra PW, Wrana JL. TAZ controls Smad nucleocytoplasmic shuttling and regulates human embryonic stem-cell self-renewal. *Nature cell biology*. 2008;10(7):837-848.

231. Diepenbruck M, Waldmeier L, Ivanek R, Berninger P, Arnold P, van Nimwegen E, Christofori G. Tead2 expression levels control the subcellular distribution of Yap and Taz, zyxin expression and epithelial–mesenchymal transition. *J Cell Sci*. 2014;127(7):1523-1536.

232. Hiemer SE, Szymaniak AD, Varelas X. The transcriptional regulators TAZ and YAP direct transforming growth factor β-induced tumorigenic phenotypes in breast cancer cells. *Journal of Biological Chemistry*. 2014;289(19):13461-13474.

233. Rozario T, DeSimone DW. The extracellular matrix in development and morphogenesis: a dynamic view. *Developmental biology*. 2010;341(1):126-140.

234. Krumins AM, Gilman AG. Targeted knockdown of G protein subunits selectively prevents receptor-mediated modulation of effectors and reveals complex changes in non-targeted signaling proteins. *Journal of Biological Chemistry*. 2006;281(15):10250-10262.

235. Moffat J, Grueneberg DA, Yang X, et al. A lentiviral RNAi library for human and mouse genes applied to an arrayed viral high-content screen. *Cell*. 2006;124(6):1283-1298.

236. Sanjana NE, Shalem O, Zhang F. Improved vectors and genome-wide libraries for CRISPR screening. *Nature methods*. 2014;11(8):783-784.

237. Le Gall SM, Szabo R, Lee M, Kirchhofer D, Craik CS, Bugge TH, Camerer E. Matriptase activation connects tissue factor–dependent coagulation initiation to epithelial proteolysis and signaling. *Blood*. 2016;127(25):3260-3269.

238. Negrini S, Gorgoulis VG, Halazonetis TD. Genomic instability—an evolving hallmark of cancer. *Nature reviews Molecular cell biology*. 2010;11(3):220-228.

239. Torres EM, Williams BR, Amon A. Aneuploidy: cells losing their balance. *Genetics*. 2008;179(2):737-746.

240. Williams BR, Amon A. Aneuploidy: cancer's fatal flaw? *Cancer Res*. 2009;69(13):5289-5291.

241. Chandhok NS, Pellman D. A little CIN may cost a lot: revisiting aneuploidy and cancer. *Curr Opin Genet Dev*. 2009;19(1):74-81.

242. Storchova Z, Pellman D. From polyploidy to aneuploidy, genome instability and cancer. *Nature reviews Molecular cell biology*. 2004;5(1):45-54.

243. Zack TI, Schumacher SE, Carter SL, et al. Pan-cancer patterns of somatic copy number alteration. *Nature genetics*. 2013;45(10):1134-1140.

244. Sheltzer JM. A transcriptional and metabolic signature of primary aneuploidy is present in chromosomally unstable cancer cells and informs clinical prognosis. *Cancer research*. 2013;73(21):6401-6412.

245. Ohashi A, Ohori M, Iwai K, et al. Aneuploidy generates proteotoxic stress and DNA damage concurrently with p53-mediated post-mitotic apoptosis in SAC-impaired cells. *Nature Communications*. 2015;6:7668.

246. Dodgson SE, Santaguida S, Kim S, Sheltzer J, Amon A. The pleiotropic deubiquitinase Ubp3 confers aneuploidy tolerance. *Genes & development*. 2016;30(20):2259-2271.

247. Santaguida S, Richardson A, Iyer DR, et al. Chromosome Mis-segregation Generates Cell-Cycle-Arrested Cells with Complex Karyotypes that Are Eliminated by the Immune System. *Developmental Cell*. 2017;41(6):638-651.e635.

248. Davoli T, Uno H, Wooten EC, Elledge SJ. Tumor aneuploidy correlates with markers of immune evasion and with reduced response to immunotherapy. *Science*. 2017;355(6322):eaaf8399.

249. Potapova TA, Seidel CW, Box AC, Rancati G, Li R. Transcriptome analysis of tetraploid cells identifies cyclin D2 as a facilitator of adaptation to genome doubling in the presence of p53. *Molecular Biology of the Cell*. 2016;27(20):3065-3084.

250. Zhang C-Z, Spektor A, Cornils H, Francis JM, Jackson EK, Liu S, Meyerson M, Pellman D. Chromothripsis from DNA damage in micronuclei. *Nature*. 2015;522(7555):179-184.

251. Di Nicolantonio F, Arena S, Gallicchio M, et al. Replacement of normal with mutant alleles in the genome of normal human cells unveils mutation-specific drug responses. *Proceedings of the National Academy of Sciences*. 2008;105(52):20864-20869.

252. Tomizuka K, Yoshida H, Uejima H, et al. Functional expression and germline transmission of a human chromosome fragment in chimaeric mice. *Nat Genet*. 1997;16(2):133-143.

253. Doherty AM, Fisher EM. Microcell-mediated chromosome transfer (MMCT): small cells with huge potential. *Mamm Genome*. 2003;14(9):583-592.

254. Dephoure N, Hwang S, O'Sullivan C, Dodgson SE, Gygi SP, Amon A, Torres EM. Quantitative proteomic analysis reveals posttranslational responses to aneuploidy in yeast. *Elife*. 2014;3:e03023.

255. Li Y, Tollefsbol TO. DNA methylation detection: bisulfite genomic sequencing analysis. *Epigenetics Protocols*. 2011:11-21.

256. Jeltsch A, Jurkowska RZ. New concepts in DNA methylation. *Trends in biochemical sciences*. 2014;39(7):310-318.

257. Serra RW, Fang M, Park SM, Hutchinson L, Green MR. A KRAS-directed transcriptional silencing pathway that mediates the CpG island methylator phenotype. *Elife*. 2014;3:e02313.

258. Thompson SL, Compton DA. Proliferation of aneuploid human cells is limited by a p53-dependent mechanism. *The Journal of Cell Biology*. 2010:jcb. 200905057.

259. Uetake Y, Sluder G. Prolonged prometaphase blocks daughter cell proliferation despite normal completion of mitosis. *Current Biology*. 2010;20(18):1666-1671.

260. Kapoor TM, Mayer TU, Coughlin ML, Mitchison TJ. Probing spindle assembly mechanisms with monastrol, a small molecule inhibitor of the mitotic kinesin, Eg5. *The Journal of cell biology*. 2000;150(5):975-988.

261. Ertych N, Stolz A, Stenzinger A, Weichert W, Kaulfuß S, Burfeind P, Aigner A, Wordeman L, Bastians H. Increased microtubule assembly rates influence chromosomal instability in colorectal cancer cells. *Nature cell biology*. 2014;16(8):779-791.

262. Malumbres M, Barbacid M. Cell cycle, CDKs and cancer: a changing paradigm. *Nat Rev Cancer*. 2009;9(3):153-166.

263. Sakaue-Sawano A, Kurokawa H, Morimura T, et al. Visualizing spatiotemporal dynamics of multicellular cell-cycle progression. *Cell*. 2008;132(3):487-498.

264. Ryan J, Letai A. BH3 profiling in whole cells by fluorimeter or FACS. *Methods*. 2013;61(2):156-164.

265. Kelekar A, Chang BS, Harlan JE, Fesik SW, Thompson CB. Bad is a BH3 domain-containing protein that forms an inactivating dimer with Bcl-XL. *Molecular and cellular biology*. 1997;17(12):7040-7046.

266. Shibue T, Takeda K, Oda E, et al. Integral role of Noxa in p53-mediated apoptotic response. *Genes & development*. 2003;17(18):2233-2238.

267. Inohara N, Ding L, Chen S, Núñez G. harakiri, a novel regulator of cell death, encodes a protein that activates apoptosis and interacts selectively with survival‐promoting proteins Bcl‐2 and Bcl‐X L. *The EMBO journal*. 1997;16(7):1686-1694.

268. Schuler M, Green DR. Transcription, apoptosis and p53: catch-22. *Trends in genetics*. 2005;21(3):182-187.

269. Speidel D. Transcription-independent p53 apoptosis: an alternative route to death. *Trends in cell biology*. 2010;20(1):14-24.

270. Yang X, Li D-m, Chen W, Xu T. Human homologue of Drosophila lats, LATS 1, negatively regulate growth by inducing G 2/M arrest or apoptosis. *Oncogene*. 2001;20(45):6516-6523.

271. Ke H, Pei J, Ni Z, Xia H, Qi H, Woods T, Kelekar A, Tao W. Putative tumor suppressor Lats2 induces apoptosis through downregulation of Bcl-2 and Bcl-x L. *Experimental cell research*. 2004;298(2):329-338.

272. McPherson JP, Tamblyn L, Elia A, et al. Lats2/Kpm is required for embryonic development, proliferation control and genomic integrity. *The EMBO journal*. 2004;23(18):3677-3688.

273. Lee D-H, Park JO, Kim T-S, et al. LATS-YAP/TAZ controls lineage specification by regulating TGF [beta] signaling and Hnf4 [alpha] expression during liver development. *Nature communications*. 2016;7.

274. Hébrant A, Dom G, Dewaele M, Andry G, Trésallet C, Leteurtre E, Dumont JE, Maenhaut C. mRNA expression in papillary and anaplastic thyroid carcinoma: molecular anatomy of a killing switch. *PLoS One*. 2012;7(10):e37807.

275. Espinal-Enríquez J, Muñoz-Montero S, Imaz-Rosshandler I, Huerta-Verde A, Mejía C, Hernández-Lemus E. Genome-wide expression analysis suggests a crucial role of dysregulation of matrix metalloproteinases pathway in undifferentiated thyroid carcinoma. *BMC genomics*. 2015;16(1):207.

276. Quiros RM, Ding HG, Gattuso P, Prinz RA, Xu X. Evidence that one subset of anaplastic thyroid carcinomas are derived from papillary carcinomas due to BRAF and p53 mutations. *Cancer*. 2005;103(11):2261-2268.

277. Hemmer S, Wasenius V-M, Knuutila S, Franssila K, Joensuu H. DNA copy number changes in thyroid carcinoma. *The American journal of pathology*. 1999;154(5):1539-1547.

278. Herrmann MA, Hay ID, Bartelt Jr D, Ritland SR, Dahl RJ, Grant CS, Jenkins RB. Cytogenetic and molecular genetic studies of follicular and papillary thyroid cancers. *Journal of Clinical Investigation*. 1991;88(5):1596.

279. Mark J, Ekedahl C, Dahlenfors R, Wester-Mark B. Cytogenetical observations in five human anaplastic thyroid carcinomas. *Hereditas*. 1987;107(2):163-174.

280. Cancer Genome Atlas Research Network. Integrated genomic characterization of papillary thyroid carcinoma. *Cell*. 2014;159(3):676-690.

281. Carter SL, Cibulskis K, Helman E, et al. Absolute quantification of somatic DNA alterations in human cancer. *Nature biotechnology*. 2012;30(5):413-421.

282. López-García C, Sansregret L, Domingo E, et al. BCL9L dysfunction impairs caspase-2 expression permitting aneuploidy tolerance in colorectal cancer. *Cancer cell*. 2017;31(1):79-93.

283. Brembeck FH, Schwarz-Romond T, Bakkers J, Wilhelm S, Hammerschmidt M, Birchmeier W. Essential role of BCL9-2 in the switch between β-catenin's adhesive and transcriptional functions. *Genes & development*. 2004;18(18):2225-2230.

284. Lum JJ, Bauer DE, Kong M, Harris MH, Li C, Lindsten T, Thompson CB. Growth factor regulation of autophagy and cell survival in the absence of apoptosis. *Cell*. 2005;120(2):237-248.

285. Li TY, Lin S-Y, Lin S-C. Mechanism and physiological significance of growth factor-related autophagy. *Physiology*. 2013;28(6):423-431.

286. Manning BD, Toker A. AKT/PKB Signaling: Navigating the Network. *Cell*. 2017;169(3):381-405.

287. Gao X, Pan D. TSC1 and TSC2 tumor suppressors antagonize insulin signaling in cell growth. *Genes & development*. 2001;15(11):1383-1392.

288. Goncharova EA, Goncharov DA, Eszterhas A, et al. Tuberin regulates p70 S6 kinase activation and ribosomal protein S6 phosphorylation A role for the TSC2 tumor suppressor gene in pulmonary lymphangioleiomyomatosis (LAM). *Journal of Biological Chemistry*. 2002;277(34):30958-30967.

289. Manning BD, Tee AR, Logsdon MN, Blenis J, Cantley LC. Identification of the tuberous sclerosis complex-2 tumor suppressor gene product tuberin as a target of the phosphoinositide 3-kinase/akt pathway. *Molecular cell*. 2002;10(1):151-162.

290. Potter CJ, Pedraza LG, Xu T. Akt regulates growth by directly phosphorylating Tsc2. *Nature cell biology*. 2002;4(9):658-665.

291. Ganley IG, Lam dH, Wang J, Ding X, Chen S, Jiang X. ULK1· ATG13· FIP200 complex mediates mTOR signaling and is essential for autophagy. *Journal of Biological Chemistry*. 2009;284(18):12297-12305.

292. Hosokawa N, Hara T, Kaizuka T, et al. Nutrient-dependent mTORC1 association with the ULK1–Atg13–FIP200 complex required for autophagy. *Molecular biology of the cell*. 2009;20(7):1981-1991.

293. del Peso L, González-García M, Page C, Herrera R, Nuñez G. Interleukin-3-induced phosphorylation of BAD through the protein kinase Akt. *Science*. 1997;278(5338):687-689.

294. Datta SR, Dudek H, Tao X, Masters S, Fu H, Gotoh Y, Greenberg ME. Akt phosphorylation of BAD couples survival signals to the cell-intrinsic death machinery. *Cell*. 1997;91(2):231-241.

295. Brazil DP, Hemmings BA. Ten years of protein kinase B signalling: a hard Akt to follow. *Trends in biochemical sciences*. 2001;26(11):657-664.

296. Tumaneng K, Schlegelmilch K, Russell RC, et al. YAP mediates crosstalk between the Hippo and PI (3) K–TOR pathways by suppressing PTEN via miR-29. *Nature Cell Biology*. 2012;14(12):1322-1329.

297. Park G-S, Oh H, Kim M, Kim T, Johnson RL, Irvine KD, Lim D-S. An evolutionarily conserved negative feedback mechanism in the Hippo pathway reflects functional difference between LATS1 and LATS2. *Oncotarget*. 2016;7(17):24063.

298. He C, Lv X, Hua G, Lele SM, Remmenga S, Dong J, Davis JS, Wang C. YAP forms autocrine loops with the ERBB pathway to regulate ovarian cancer initiation and progression. *Oncogene*. 2015;34(50):6040-6054.

299. Schneider A, Klingmüller U, Schilling M. Short‐term information processing, long‐term responses: Insights by mathematical modeling of signal transduction. *BioEssays*. 2012;34(7):542-550.

300. Gaudet S, Janes KA, Albeck JG, Pace EA, Lauffenburger DA, Sorger PK. A compendium of signals and responses triggered by prodeath and prosurvival cytokines. *Molecular & Cellular Proteomics*. 2005;4(10):1569-1590.

301. Li H, Mar BG, Zhang H, Puram RV, Vazquez F, Weir BA, Hahn WC, Ebert B, Pellman D. The EMT regulator ZEB2 is a novel dependency of human and murine acute myeloid leukemia. *Blood*. 2017;129(4):497-508.

302. American Society of Hematology. Rights and Permissions; www.bloodjournal.org/page/rights-permissions; Accessed 6/9/2017.

303. Greaves M. Leukaemia 'firsts' in cancer research and treatment. *Nature Reviews Cancer*. 2016;16(3):163-172.

304. Ema H, Morita Y, Suda T. Heterogeneity and hierarchy of hematopoietic stem cells. *Exp Hematol*. 2014;42(2):74-82 e72.

305. Bozzone DM. 3: Blood Cell Development and Function; and 4: Leukemias Are Not All the Same. Leukemia: Chelsea House; 2009:38-70.

306. American Cancer Society. Cancer Facts & Figures 2017; www.cancer.org/research/cancer-facts-statistics/all-cancer-facts-figures/cancer-facts-figures-2017.html; Accessed 6/15/2017.

307. National Cancer Institute. SEER (Surveillance, Epidemiology and End Results) Cancer Statistics Review, 1975-2010; 2013.

308. Ferrara F, Schiffer CA. Acute myeloid leukaemia in adults. *Lancet*. 2013;381(9865):484-495.

309. Bennett JM, Catovsky D, Daniel MT, Flandrin G, Galton DA, Gralnick HR, Sultan C. Proposals for the classification of the acute leukaemias. French-American-British (FAB) co-operative group. *Br J Haematol*. 1976;33(4):451-458.

310. Swerdlow SH, Campo E, Pileri SA, et al. The 2016 revision of the World Health Organization classification of lymphoid neoplasms. *Blood*. 2016;127(20):2375-2390.

311. Sanchez M, Levine RL, Rampal R. Integrating Genomics Into Prognostic Models for AML. *Semin Hematol*. 2014;51(4):298-305.

312. Lamouille S, Xu J, Derynck R. Molecular mechanisms of epithelial–mesenchymal transition. *Nature reviews Molecular cell biology*. 2014;15(3):178-196.

313. Sánchez-Tilló E, Siles L, De Barrios O, Cuatrecasas M, Vaquero EC, Castells A, Postigo A. Expanding roles of ZEB factors in tumorigenesis and tumor progression. *Am J Cancer Res*. 2011;1(7):897-912.

314. Hegarty SV, Sullivan AM, O'Keeffe GW. Zeb2: A multifunctional regulator of nervous system development. *Progress in neurobiology*. 2015;132:81-95.

315. Vandewalle C, Van Roy F, Berx G. The role of the ZEB family of transcription factors in development and disease. *Cellular and molecular life sciences*. 2009;66(5):773-787.

316. Van de Putte T, Maruhashi M, Francis A, Nelles L, Kondoh H, Huylebroeck D, Higashi Y. Mice lacking ZFHX1B, the gene that codes for Smad-interacting protein-1, reveal a role for multiple neural crest cell defects in the etiology of Hirschsprung disease-mental retardation syndrome. *Am J Hum Genet*. 2003;72(2):465-470.

317. Van de Putte T, Francis A, Nelles L, van Grunsven LA, Huylebroeck D. Neural crest-specific removal of Zfhx1b in mouse leads to a wide range of neurocristopathies reminiscent of Mowat–Wilson syndrome. *Human molecular genetics*. 2007;16(12):1423-1436.

318. Goossens S, Janzen V, Bartunkova S, et al. The EMT regulator Zeb2/Sip1 is essential for murine embryonic hematopoietic stem/progenitor cell differentiation and mobilization. *Blood*. 2011;117(21):5620-5630.

319. Scott CL, Soen B, Martens L, et al. The transcription factor Zeb2 regulates development of conventional and plasmacytoid DCs by repressing Id2. *Journal of Experimental Medicine*. 2016;213(6):897-911.

320. Wu X, Briseño CG, Grajales-Reyes GE, et al. Transcription factor Zeb2 regulates commitment to plasmacytoid dendritic cell and monocyte fate. *Proceedings of the National Academy of Sciences*. 2016;113(51):14775-14780.

321. Goossens S, Radaelli E, Blanchet O, et al. ZEB2 drives immature T-cell lymphoblastic leukaemia development via enhanced tumour-initiating potential and IL-7 receptor signalling. *Nat Commun*. 2015;6:5794.

322. Caudell D, Harper DP, Novak RL, Pierce RM, Slape C, Wolff L, Aplan PD. Retroviral insertional mutagenesis identifies Zeb2 activation as a novel leukemogenic collaborating event in CALM-AF10 transgenic mice. *Blood*. 2010;115(6):1194-1203.

323. Tenen DG. Disruption of differentiation in human cancer: AML shows the way. *Nature reviews cancer*. 2003;3(2):89-101.

324. Engel P, Boumsell L, Balderas R, et al. CD Nomenclature 2015: human leukocyte differentiation antigen workshops as a driving force in immunology. *The Journal of Immunology*. 2015;195(10):4555-4563.

325. Shipp MA, Stefano GB, Scharrer B, Reinherz EL. CD 10 (CALLA, common acute lymphoblastic leukemia antigen)/neutral endopeptidase 24.11 (NEP,“nkephalinase”): molecular structure and role in regulating met-enkephalin mediated inflammatory responses. *Advances in Neuroimmunology*. 1991;1(2):139-149.

326. Seita J, Weissman IL. Hematopoietic stem cell: self‐renewal versus differentiation. *Wiley Interdisciplinary Reviews: Systems Biology and Medicine*. 2010;2(6):640-653.

327. Nakase K, Bradstock K, Sartor M, Gottlieb D, Byth K, Kita K, Shiku H, Kamada N. Geographic heterogeneity of cellular characteristics of acute myeloid leukemia: a comparative study of Australian and Japanese adult cases. *Leukemia*. 2000;14(1):163.

328. Elghetany MT. Surface antigen changes during normal neutrophilic development: a critical review. *Blood Cells, Molecules, and Diseases*. 2002;28(2):260-274.

329. Attar A. Changes in the cell surface markers during normal hematopoiesis: a guide to cell isolation. *Global J Hematol Blood Transfu*. 2014;1:20-28.

330. BD Biosciences. Human and Mouse CD Marker Handbook; www.bdbiosciences.com/us/s/cdmarkers. Accessed 6/15/2017.

331. Saultz JN, Garzon R. Acute Myeloid Leukemia: A Concise Review. *Journal of Clinical Medicine*. 2016;5(3):33.

332. Dos Santos GA, Kats L, Pandolfi PP. Synergy against PML-RARa: targeting transcription, proteolysis, differentiation, and self-renewal in acute promyelocytic leukemia. *J Exp Med*. 2013;210(13):2793-2802.

333. Marchwicka A, Cebrat M, Sampath P, Śnieżewski Ł, Marcinkowska E. Perspectives of differentiation therapies of acute myeloid leukemia: the search for the molecular basis of patients' variable responses to 1, 25-dihydroxyvitamin D and vitamin D analogs. *Frontiers in Oncology*. 2014;4.

334. Shah MV, Barochia A, Loughran TP, Jr. Impact of genetic targets on cancer therapy in acute myelogenous leukemia. *Adv Exp Med Biol*. 2013;779:405-437.

335. Barretina J, Caponigro G, Stransky N, et al. The Cancer Cell Line Encyclopedia enables predictive modelling of anticancer drug sensitivity. *Nature*. 2012;483(7391):603-607.

336. Cancer Genome Atlas Research N. Genomic and epigenomic landscapes of adult de novo acute myeloid leukemia. *N Engl J Med*. 2013;368(22):2059-2074.

337. Hill L, Browne G, Tulchinsky E. ZEB/miR-200 feedback loop: at the crossroads of signal transduction in cancer. *Int J Cancer*. 2013;132(4):745-754.

338. Cowley GS, Weir BA, Vazquez F, Tamayo P, Scott JA, Rusin S, East-Seletsky A, Ali LD, Gerath WF. Parallel genome-scale loss of function screens in 216 cancer cell lines for the identification of context-specific genetic dependencies. *Sci Data*. 2014;1(140035).

339. Shao DD, Tsherniak A, Gopal S, et al. ATARiS: computational quantification of gene suppression phenotypes from multisample RNAi screens. *Genome Res*. 2013;23(4):665-678.

340. Miller PG, Al-Shahrour F, Hartwell KA, et al. In vivo RNAi screening identifies a leukemia-specific dependence on integrin beta 3 signaling. *Cancer Cell*. 2013;24(1):45-58.

341. Krivtsov AV, Twomey D, Feng Z, et al. Transformation from committed progenitor to leukaemia stem cell initiated by MLL-AF9. *Nature*. 2006;442(7104):818-822.

342. Lindsley RC, Mar BG, Mazzola E, et al. Acute myeloid leukemia ontogeny is defined by distinct somatic mutations. *Blood*. 2015;125(9):1367-1376.

343. Rapin N, Bagger FO, Jendholm J, et al. Comparing cancer vs normal gene expression profiles identifies new disease entities and common transcriptional programs in AML patients. *Blood*. 2014;123(6):894-904.

344. Jackson AL, Burchard J, Schelter J, Chau BN, Cleary M, Lim L, Linsley PS. Widespread siRNA "off-target" transcript silencing mediated by seed region sequence complementarity. *RNA*. 2006;12(7):1179-1187.

345. Buehler E, Chen YC, Martin S. C911: A bench-level control for sequence specific siRNA off-target effects. *PLoS One*. 2012;7(12):e51942.

346. Sinha J, Bhattacharya S. Laboratory Techniques. A Text Book of Immunology: Academic Publishers; 2006:429-445.

347. Kee N, Sivalingam S, Boonstra R, Wojtowicz J. The utility of Ki-67 and BrdU as proliferative markers of adult neurogenesis. *Journal of Neuroscience Methods*. 2002;115(1):97-105.

348. Daigneault M, Preston JA, Marriott HM, Whyte MK, Dockrell DH. The identification of markers of macrophage differentiation in PMA-stimulated THP-1 cells and monocyte-derived macrophages. *PloS One*. 2010;5(1):e8668.

349. Stegmaier K, Ross KN, Colavito SA, O'Malley S, Stockwell BR, Golub TR. Gene expression-based high-throughput screening(GE-HTS) and application to leukemia differentiation. *Nat Genet*. 2004;36(3):257-263.

350. Novershtern N, Subramanian A, Lawton LN, et al. Densely interconnected transcriptional circuits control cell states in human hematopoiesis. *Cell*. 2011;144(2):296-309.

351. Li J, Riedt T, Goossens S, et al. The EMT transcription factor Zeb2 controls adult murine hematopoietic differentiation by regulating cytokine signaling. *Blood*. 2017;129(4):460-472.

352. Lu G, Middleton RE, Sun H, Naniong M, Ott CJ, Mitsiades CS, Wong K-K, Bradner JE, Kaelin WG. The myeloma drug lenalidomide promotes the cereblon-dependent destruction of Ikaros proteins. *Science*. 2014;343(6168):305-309.

353. Krönke J, Udeshi ND, Narla A, et al. Lenalidomide causes selective degradation of IKZF1 and IKZF3 in multiple myeloma cells. *Science*. 2014;343(6168):301-305.

354. Winter GE, Buckley DL, Paulk J, Roberts JM, Souza A, Dhe-Paganon S, Bradner JE. Phthalimide conjugation as a strategy for in vivo target protein degradation. *Science*. 2015;348(6241):1376-1381.

355. Perez-Mancera PA, Perez-Caro M, Gonzalez-Herrero I, et al. Cancer development induced by graded expression of Snail in mice. *Hum Mol Genet*. 2005;14(22):3449-3461.

356. Perez-Mancera PA, Gonzalez-Herrero I, Perez-Caro M, Gutierrez-Cianca N, Flores T, Gutierrez-Adan A, Pintado B, Sanchez-Martin M, Sanchez-Garcia I. SLUG in cancer development. *Oncogene*. 2005;24(19):3073-3082.

357. Hamabe A, Konno M, Tanuma N, et al. Role of pyruvate kinase M2 in transcriptional regulation leading to epithelial–mesenchymal transition. *Proceedings of the National Academy of Sciences*. 2014;111(43):15526-15531.

358. Byers LA, Diao L, Wang J, et al. An epithelial–mesenchymal transition gene signature predicts resistance to EGFR and PI3K inhibitors and identifies Axl as a therapeutic target for overcoming EGFR inhibitor resistance. *Clinical Cancer Research*. 2013;19(1):279-290.

359. Roversi FM, Lopes MR, Machado-Neto JA, et al. Serine protease inhibitor kunitz-type 2 is downregulated in myelodysplastic syndromes and modulates cell–cell adhesion. *Stem Cells and Development*. 2014;23(10):1109-1120.

360. Mani SA, Guo W, Liao MJ, et al. The epithelial-mesenchymal transition generates cells with properties of stem cells. *Cell*. 2008;133(4):704-715.

361. Stijf-Bultsma Y, Sommer L, Tauber M, et al. The basal transcription complex component TAF3 transduces changes in nuclear phosphoinositides into transcriptional output. *Molecular Cell*. 2015;58(3):453-467.

362. Velasco G, Cal S, Quesada V, Sánchez LM, López-Otín C. Matriptase-2, a membrane-bound mosaic serine proteinase predominantly expressed in human liver and showing degrading activity against extracellular matrix proteins. *Journal of Biological Chemistry*. 2002;277(40):37637-37646.

363. Ko C-J, Huang C-C, Lin H-Y, et al. Androgen-induced TMPRSS2 activates matriptase and promotes extracellular matrix degradation, prostate cancer cell invasion, tumor growth, and metastasis. *Cancer research*. 2015;75(14):2949-2960.

364. Milner JM, Patel A, Davidson RK, et al. Matriptase is a novel initiator of cartilage matrix degradation in osteoarthritis. *Arthritis & Rheumatology*. 2010;62(7):1955-1966.

365. Imoto I, Yang Z-Q, Pimkhaokham A, Tsuda H, Shimada Y, Imamura M, Ohki M, Inazawa J. Identification of cIAP1 as a candidate target gene within an amplicon at 11q22 in esophageal squamous cell carcinomas. *Cancer Research*. 2001;61(18):6629-6634.

366. Drost J, Van Jaarsveld RH, Ponsioen B, et al. Sequential cancer mutations in cultured human intestinal stem cells. *Nature*. 2015;521(7550):43.

367. Perera D, Venkitaraman AR. Oncogenic KRAS triggers MAPK-dependent errors in mitosis and MYC-dependent sensitivity to anti-mitotic agents. *Scientific Reports*. 2016;6:29741.

368. Wiles ET, Bell R, Thomas D, Beckerle M, Lessnick SL. ZEB2 represses the epithelial phenotype and facilitates metastasis in Ewing sarcoma. *Genes & Cancer*. 2013;4(11-12):486-500.

369. Kahlert C, Lahes S, Radhakrishnan P, et al. Overexpression of ZEB2 at the invasion front of colorectal cancer is an independent prognostic marker and regulates tumor invasion in vitro. *Clinical Cancer Research*. 2011;17(24):7654-7663.

370. De Craene B, Berx G. Regulatory networks defining EMT during cancer initiation and progression. *Nature Reviews Cancer*. 2013;13(2):97.

371. Leaney JL, Tinker A. The role of members of the pertussis toxin-sensitive family of G proteins in coupling receptors to the activation of the G protein-gated inwardly rectifying potassium channel. *Proceedings of the National Academy of Sciences*. 2000;97(10):5651-5656.

372. Lee M-H, Appleton KM, Strungs EG, Kwon JY, Morinelli TA, Peterson YK, Laporte SA, Luttrell LM. The conformational signature of arrestin3 predicts its trafficking and signaling functions. *Nature*. 2016;531(7596):665.

373. Locht C, Coutte L, Mielcarek N. The ins and outs of pertussis toxin. *The FEBS journal*. 2011;278(23):4668-4682.

374. Okamoto H, Takuwa N, Gonda K, Okazaki H, Chang K, Yatomi Y, Shigematsu H, Takuwa Y. EDG1 is a functional sphingosine-1-phosphate receptor that is linked via a Gi/o to multiple signaling pathways, including phospholipase C activation, Ca2+ mobilization, Ras-mitogen-activated protein kinase activation, and adenylate cyclase inhibition. *Journal of Biological Chemistry*. 1998;273(42):27104-27110.

375. Massa F, Tormo A, Béraud-Dufour S, Coppola T, Mazella J. Neurotensin-induced Erk1/2 phosphorylation and growth of human colonic cancer cells are independent from growth factors receptors activation. *Biochemical and Biophysical Research Communications*. 2011;414(1):118-122.

376. Barren B, Artemyev NO. Mechanisms of dominant negative G‐protein α subunits. *Journal of Neuroscience Research*. 2007;85(16):3505-3514.

377. Taylor S, Yang J, Wu J, Haste N, Radzio-Andzelm E, Anand G. PKA: a portrait of protein kinase dynamics. *Biochimica et Biophysica Acta (BBA)-Proteins and Proteomics*. 2004;1697(1):259-269.

378. Lochner A, Moolman J. The many faces of H89: a review. *Cardiovascular Therapeutics*. 2006;24(3‐4):261-274.

379. Dostmann WR. (RP)-cAMPS inhibits the cAMP-dependent protein kinase by blocking the cAMP-induced conformational transition. *FEBS letters*. 1995;375(3):231-234.

380. Misra UK, Pizzo SV. Coordinate Regulation of Forskolin-induced Cellular Proliferation in Macrophages by Protein Kinase A/cAMP-response Element-binding Protein (CREB) and Epac1-Rap1 Signaling: effects of silencing CREB gene expression on Akt activation. *Journal of Biological Chemistry*. 2005;280(46):38276-38289.

381. Alasbahi R, Melzig M. Forskolin and derivatives as tools for studying the role of cAMP. *Die Pharmazie-An International Journal of Pharmaceutical Sciences*. 2012;67(1):5-13.

382. Chen AE, Ginty DD, Chen-Ming F. Protein kinase A signalling via CREB controls myogenesis induced by Wnt proteins. *Nature*. 2005;433(7023):317.

383. Jiang M, Bajpayee NS. Molecular mechanisms of Go signaling. *Neurosignals*. 2009;17(1):23-41.

384. Gong R, Hong AW, Plouffe SW, Zhao B, Liu G, Yu F-X, Xu Y, Guan K-L. Opposing roles of conventional and novel PKC isoforms in Hippo-YAP pathway regulation. *Cell Research*. 2015;25(8):985.

385. Mullick A, Xu Y, Warren R, et al. The cumate gene-switch: a system for regulated expression in mammalian cells. *BMC Biotechnology*. 2006;6(1):43.

386. Dickerson I, Peden K, Mains R. Metallothionein-I promoter-directed expression of foreign proteins in a mouse pituitary corticotrope tumor cell line. *Molecular and Cellular Endocrinology*. 1989;64(2):205-212.

387. Santos AK, Parreira RC, Resende RR. Expression system based on an MTIIa promoter to produce hPSA in mammalian cell cultures. *Frontiers in Microbiology*. 2016;7.

388. Rodriguez LG, Wu X, Guan J-L. Wound-healing assay. *Cell Migration: Developmental Methods and Protocols*. 2005:23-29.

389. Shafaq-Zadah M, Gomes-Santos CS, Bardin S, et al. Persistent cell migration and adhesion rely on retrograde transport of [beta] 1 integrin. *Nature Cell Biology*. 2016;18(1):54.

390. Qazi AK, Hussain A, Aga MA, Ali S, Taneja SC, Sharma PR, Saxena AK, Mondhe DM, Hamid A. Cell specific apoptosis by RLX is mediated by NFκB in human colon carcinoma HCT-116 cells. *BMC Cell Biology*. 2014;15(1):36.

391. Botlagunta M, Winnard PT, Raman V. Neoplastic transformation of breast epithelial cells by genotoxic stress. *BMC Cancer*. 2010;10(1):343.

392. Matsumoto K, Nakamura T. Emerging multipotent aspects of hepatocyte growth factor. *The Journal of Biochemistry*. 1996;119(4):591-600.

393. Seton-Rogers SE, Lu Y, Hines LM, Koundinya M, LaBaer J, Muthuswamy SK, Brugge JS. Cooperation of the ErbB2 receptor and transforming growth factor ß in induction of migration and invasion in mammary epithelial cells. *PNAS*. 2004;101(5):1257-1262.

394. Bradley CA, Dunne PD, Bingham V, et al. Transcriptional upregulation of c-MET is associated with invasion and tumor budding in colorectal cancer. *Oncotarget*. 2016;7(48):78932.

395. Liou GI, Matragoon S, Samuel S, et al. MAP kinase and beta-catenin signaling in HGF induced RPE migration. *Molecular Vision*. 2002;8:483-493.

396. Anderl J, Ma J, Armstrong L, Millipore E. Fluorescent Gelatin Degradation Assays for Investigating Invadopodia Formation. *Nature Methods*. 2012;121007:1-5.

397. Hahn WC, Weinberg RA. Rules for making human tumor cells. *New England Journal of Medicine*. 2002;347(20):1593-1603.

398. Boehm JS, Hession MT, Bulmer SE, Hahn WC. Transformation of human and murine fibroblasts without viral oncoproteins. *Molecular and Cellular Biology*. 2005;25(15):6464-6474.

399. Zoltan-Jones A, Huang L, Ghatak S, Toole BP. Elevated hyaluronan production induces mesenchymal and transformed properties in epithelial cells. *Journal of Biological Chemistry*. 2003;278(46):45801-45810.

400. Hardy S, Kitamura M, Harris-Stansil T, Dai Y, Phipps ML. Construction of adenovirus vectors through Cre-lox recombination. *Journal of Virology*. 1997;71(3):1842-1849.

401. Lau J, Schmidt C, Markant SL, Taylor MD, Wechsler-Reya RJ, Weiss WA. Matching mice to malignancy: molecular subgroups and models of medulloblastoma. *Child's Nervous System*. 2012;28(4):521-532.

402. Schüller U, Heine VM, Mao J, et al. Acquisition of granule neuron precursor identity is a critical determinant of progenitor cell competence to form Shh-induced medulloblastoma. *Cancer Cell*. 2008;14(2):123-134.

403. Turajlic S, McGranahan N, Swanton C. Inferring mutational timing and reconstructing tumour evolutionary histories. *Biochimica et Biophysica Acta (BBA)-Reviews on Cancer*. 2015;1855(2):264-275.

404. Vogelstein B, Papadopoulos N, Velculescu VE, Zhou S, Diaz LA, Kinzler KW. Cancer genome landscapes. *Science*. 2013;339(6127):1546-1558.

405. Donninger H, Vos MD, Clark GJ. The RASSF1A tumor suppressor. *Journal of Cell Science*. 2007;120(18):3163-3172.

406. Antal CE, Hudson AM, Kang E, et al. Cancer-associated protein kinase C mutations reveal kinase's role as tumor suppressor. *Cell*. 2015;160(3):489-502.

407. Brocks D, Assenov Y, Minner S, et al. Intratumor DNA methylation heterogeneity reflects clonal evolution in aggressive prostate cancer. *Cell Reports*. 2014;8(3):798-806.

408. Elson L. Experimental approaches to the chemotherapy of leukaemia: SAGE Publications; 1963.